

Space Sciences Laboratory
University of California
Berkeley, California 94720

THE GENERATION OF ELECTRON
CYCLOTRON WAVES IN THE
MAGNETOSPHERE AND THE TURBULENCE
DIFFUSION OF OUTER BELT ELECTRONS

by

Richard I. Miller

Technical Report on

NsG 243

Series No. 6, Issue No. 33

August 20, 1965

CONTENTS

ABSTRACT	iii
I. INTRODUCTION	1
II. ELECTRON CYCLOTRON WAVE DISPERSION RELATION	5
III. MAGNETOSPHERIC MODELS AND WAVE GROWTH RATES	22
IV. ELECTROMAGNETIC TURBULENCE AND ELECTRON VELOCITY DIFFUSION	54
V. APPLICATION TO OBSERVED PHENOMENA	90
VI. DISCUSSION	115

APPENDICES

APPENDIX I. Dispersion Relation for Complex k	118
APPENDIX II. Solution to Fokker-Planck Diffusion Equation.	126
REFERENCES	130

THE GENERATION OF ELECTRON CYCLOTRON
WAVES IN THE MAGNETOSPHERE AND
THE TURBULENCE DIFFUSION OF
OUTER BELT ELECTRONS

Richard I. Miller

Space Sciences Laboratory
University of California
Berkeley, California

August 20, 1965

ABSTRACT

14637

The velocity distribution of energetic electrons trapped on geomagnetic field lines in the magnetosphere is found to be unstable with respect to the generation of electron cyclotron (whistler mode) waves. The growth of these waves results from the excess of transverse over parallel energy inherent in any loss cone type of velocity distribution. As a result, a spectrum of electromagnetic electron cyclotron wave turbulence is set up in the magnetosphere. This turbulence field then reacts on the electrons to diffuse them in pitch angle, resulting in the scattering of electrons into the atmospheric loss cone and their precipitation from the outer radiation belt. A Fokker-Planck type of diffusion equation is set up to describe this scattering process and the pitch angle distributions it predicts are in agreement with satellite observations. The low level electron precipitation background termed "drizzle" is found to require a root mean square turbulence field of magnitude $4.0 \times 10^{-3} \left(\frac{6}{L}\right)^{3.5}$ gamma at the geomagnetic equator, while the frequent but short lived precipitation bursts termed

"splash" require a momentary order of magnitude increase in this turbulence field strength. Such sporadic increases in the level of the turbulence field can readily be triggered by small (order of gammas) geomagnetic field compressions which will adiabatically increase the electron magnetic moment and hence the degree of velocity anisotropy required for significant instability growth rates. It is proposed that the pitch angle diffusion resulting from electron cyclotron turbulence is the dominant electron scattering mechanism in the outer radiation belt and determines trapped electron precipitation rates and lifetimes.

Author

I. INTRODUCTION

This paper presents a theory of electron cyclotron wave generation in the magnetosphere and considers the effect of these waves upon magnetically trapped electrons in the outer radiation belt. The interaction between particles and waves in a magnetic field requires the particles and waves to be in gyroresonance, so that the particles "see" the wave at a doppler shifted frequency which equals their gyrofrequency. Dragt (1961) and Wentzel (1961 a, b) have considered this gyroresonance in the case of protons in the magnetosphere interacting with hydromagnetic waves. They find that when there is gyroresonance between the protons and the waves the magnetic moment of the protons is no longer conserved, and the random walk scattering of the proton's magnetic moment upon encounters with successive hydromagnetic waves results in pitch angle diffusion and particle loss from the trapped radiation belts. Cornwall (1964) and Dungey (1963 a, b) have considered in a similar fashion the interaction between whistlers and gyroresonant electrons. The resultant diffusion of the electron pitch angle and consequent scattering loss into the atmospheric loss cone is able to account for the short lifetimes of artificially injected fission electrons in the "slot" at $2 \leq L \leq 3.5$. The process that we shall treat involves the electrons in the outer radiation belt generating the very same electromagnetic waves which then in turn interact with the electrons to diffuse them in pitch angle and scatter them into the atmospheric loss cone.

The electromagnetic waves are generated by an instability driven by the excess of transverse over parallel energy in the electrons themselves mirroring along magnetic field lines. Such an energy anisotropy is inherent in any loss cone type of velocity distribution as would apply to geomagnetically

trapped particles. A spectrum of electromagnetic electron cyclotron turbulence is set up which then acts to diffuse the electrons in pitch angle, resulting in electron precipitation and determining the trapped electron lifetime.

In a recent paper, Piddington (1965) has comprehensively reviewed the morphology of auroral electron precipitation. Three separate but occasionally overlapping auroral precipitation zones are distinguished: a) Zone I, a ring lying between parallels of geomagnetic latitude 63° and 73° ; b) Zone II, lying within Zone I and also ring shaped, but skewed so that its centerline reaches 80° lat. at noon and falls to 68° at midnight; c) Zone III, a circular zone lying within Zone II and covering the polar cap. Zone I connects with the field lines of the outer radiation belt and its phenomena include auroral-zone X-ray events, resulting from the bremsstrahlung radiation emitted by precipitated electrons slowing down in the upper atmosphere; auroral absorption, caused by the increased ionization resulting from precipitated electrons; and mantle auroras, which are widespread glows not immediately visible to the naked eye because of their low intensity and lack of discrete structure. Zone II connects with the outer part of the geomagnetic tail and is the region of discrete visual auroras observable to the naked eye and having relatively small scale structure, while Zone III is the region of polar glow auroras produced by solar protons. In the following we shall be concerned only with Zone I phenomena, since only Zone I connects with field lines linking the northern and southern hemispheres and having the ordered structure required for particle trapping and the generation of electron cyclotron waves.

Two major types of Zone I electron precipitation phenomena have been observed on the polar orbited satellites Injun I and III (O'Brien (1962), (1964)). The first is a relatively low level of electron precipitation which provides a constant precipitation background unvarying over a time scale on the order of minutes. Superimposed upon this low level "drizzle" are sporadic and short lived (order of seconds) "splashes", in which the precipitation rate increases by one or two orders of magnitude. Electron cyclotron turbulence diffusion is able to account reasonably for both these precipitation phenomena, the "drizzle" being driven by a constant low level of electromagnetic turbulence in the magnetosphere, the "splashes" by sporadic increases in the magnitude of the turbulence field triggered by small solar wind driven geomagnetic compressions. The existence and magnitude of these turbulence fields is consistent with VLF measurements made on Injun III (Gurnett and O'Brien (1964)).

The above theory does not include an injection and acceleration mechanism, but only a means of precipitating electrons once they have been somehow injected into the outer belt and then accelerated by some suitable mechanism as drift motions in the asymmetric magnetic field of the solar wind deformed magnetosphere, magnetic compressions driven by the fluctuating solar wind, or possibly a mechanism involving the recently discovered neutral sheet in the magnetospheric tail. In addition, as with many magnetospheric problems, a number of approximations have to be made because of the complexity of the magnetosphere, the lack of complete knowledge of many of its properties, and the variability of those properties for which experimental knowledge does exist. We shall try to choose models

and work out their implications in such a way as to minimize the model dependence of our results and to include the wide range of variability found in magnetospheric properties.

In section II, the dispersion relation for electron cyclotron waves propagating along magnetic field lines in the magnetosphere is derived. An instability is found due to the effect of a pressure or mean square velocity anisotropy and its growth rates are derived in both the complex ω and the complex k planes. In section III, various models to describe the electron distribution in the magnetosphere are derived from the available experimental data. A suitably representative model is chosen and the growth rates for the instability derived in part II are solved for. In section IV, estimates are made for the spectral shape of the turbulence in the magnetosphere resulting from the above instability. We then derive and solve a velocity diffusion equation of the Fokker-Planck type, which represents the effects of electromagnetic electron cyclotron turbulence on the electrons in the outer radiation belt. In section V, results are derived for the form of the electron precipitation resulting from the velocity diffusion theory presented in part IV. The characteristics of this precipitation are then compared with the properties of electron precipitation observed on the Injun I and III satellites and in auroral balloon experiments. Reasonable agreement between theory and experiment is found, although the basic problems of a suitable acceleration mechanism and the exact process by which electrons are injected into the magnetosphere remain unanswered. These matters are discussed further in section VI, and a final evaluation is made of the role of turbulence diffusion in determining the properties of outer belt electrons.

II. ELECTRON CYCLOTRON WAVE DISPERSION RELATION

The magnetosphere is capable of supporting the whole wealth of wave phenomena known to exist in plasmas. In the following we shall concern ourselves only with the transverse electron cyclotron wave propagating along the direction of the geomagnetic field. This wave is identical with the whistler mode waves well known to exist in the magnetosphere (Helliwell (1965)).

In a recent series of papers, Scarf (1962) and Liemohn and Scarf (1964) have investigated the effects of Landau damping upon whistler propagation in the exosphere. Their results are in good agreement with the observed whistler cutoff frequency of approximately one-half the local electron gyro-frequency at that point at which the field line guided whistler crosses the geomagnetic equator, and it can reasonable be assumed that Landau damping plays a significant role in exospheric whistler propagation.

In the following, we shall consider the additional effects of a velocity anisotropy in the magnetospheric electron plasma. Such an anisotropy is inherent in any loss cone type of velocity distribution and so anisotropy effects must necessarily occur when considering waves supported by magnetospheric electrons trapped on geomagnetic field lines. Bell and Buneman (1964) have already considered the case of a cold electron stream with a transverse velocity spread and a longitudinal streaming velocity. They find an instability in the electron cyclotron mode, but their analysis holds only if there is no longitudinal velocity spread. Such electron streams, however, are unstable with respect to the growth of the electrostatic two stream instability, and, because of its large growth rate, this instability will completely dominate the future behavior of such a plasma. In the following we shall consider a more realistic model for the magnetospheric

electron velocity distribution which is stable with respect to the two stream instability and has both transverse and longitudinal velocity spreads.

Velocity or pressure anisotropies are well known to lead to transverse instability, and work along these lines has been done by various investigators (Harris (1961), Sudan (1963), and Noerdlinger (1963)). We shall investigate this instability under reasonable magnetospheric conditions. The physical mechanism for these instabilities is the coherent phase bunching in velocity space which results when the doppler shifted wave frequency equals the electron gyrofrequency, as described by Furth (1963) and separately by Brice (1963). This instability is most probably in some way responsible for various types of VLF emissions, but we shall not go into this point in this paper. This same instability, when applied to the ion cyclotron wave rather than the electron cyclotron wave as shall be done here, is most probably associated with hydromagnetic whistlers or micropulsations of the pearl variety or pc 1 class (Cornwall (1965)).

The basis for our derivation of the dispersion relation is in Maxwell's equations and the first order Boltzmann equation. The solution for the roots of the dispersion relation is usually carried out in the complex ω plane. These roots are then given by the position of poles in the complex ω plane which come in when making the inverse transformation from frequency to time. The problem was first properly treated by Landau (1946) in terms of a Laplace transform in time, which essentially solves the initial value problem in terms of $t = 0$ initial value parameters. We, however, are concerned also with the boundary value problem which solves for complex wave number k in terms of

$x = 0$ boundary value parameters. This is so since we shall want to find the damping or growth that a wave undergoes in traversing a given region of space. Thus we shall also solve the boundary value problem for complex k which involves a Laplace transformation in space and a Fourier transformation in time. We shall now solve the dispersion equation for complex ω , leaving the solution for complex k to Appendix I.

The three equations to be solved are the collisionless Boltzmann equation for the electrons

$$\frac{\partial f}{\partial t} + \underline{v} \cdot \frac{\partial f}{\partial \underline{r}} - \frac{e}{m} \left(\underline{E} + \frac{\underline{v}}{c} \times \underline{B} \right) \cdot \frac{\partial f}{\partial \underline{v}} = 0 \quad \text{II-1}$$

and the two Maxwell equations (cgs)

$$\underline{\nabla} \times \underline{E} = -\frac{1}{c} \frac{\partial \underline{B}}{\partial t} \quad \text{II-2}$$

$$\underline{\nabla} \times \underline{B} = \frac{4\pi}{c} \underline{j} + \frac{1}{c} \frac{\partial \underline{E}}{\partial t} \quad \text{II-3}$$

where f is the distribution function for the electrons, \underline{E} and \underline{B} are the self-consistent electromagnetic fields, and \underline{j} the current density given by

$$\underline{j} = -eN_0 \int \underline{v} f d^3 v \quad \text{II-4}$$

where N_0 is the charge density of electrons and the positive ions are considered to constitute a stationary positive charge background.

This set of equations, often termed the Vlasov equations, is now linearized by considering $f = f_0 + f_1$, where $f_0 = f_0(\underline{v})$ is the unperturbed velocity distribution normalized to a single particle per unit volume and $f_1 = f_1(\underline{r}, \underline{v}, t)$ is a small perturbation. The magnetic field is considered

to have a zero order component \underline{B}_0 along the z direction. The zero order equation

$$-\frac{e}{mc} (\underline{v} \times \underline{B}_0) \cdot \frac{\partial f_0}{\partial \underline{v}} = 0 \quad \text{II-5}$$

has the solution $f_0 = f_0(v_z, v_\perp)$, where $v_\perp^2 = v_x^2 + v_y^2$.

The first order Boltzmann equation is then given by

$$\frac{\partial f_1}{\partial t} + \underline{v} \cdot \frac{\partial f_1}{\partial \underline{r}} - \frac{e}{mc} (\underline{v} \times \underline{B}_0) \cdot \frac{\partial f_1}{\partial \underline{v}} = \frac{e}{m} (\underline{E} + \frac{\underline{v}}{c} \times \underline{B}) \cdot \frac{\partial f_0}{\partial \underline{v}} \quad \text{II-6}$$

In order to solve the set II-6, II-2, II-3 for f_1 , we Fourier analyze in space and Laplace analyze in time according to the transformation pair

$$P(\omega, k) = \int_0^t dt \int_{-\infty}^{\infty} dz e^{-i(kz - \omega t)} P(t, z) \quad \text{II-7a}$$

$$P(t, z) = \frac{1}{(2\pi)^2} \int_W d\omega \int_{-\infty}^{\infty} dk e^{+i(kz - \omega t)} P(\omega, k) \quad \text{II-7b}$$

where W is chosen in the upper half ω plane, above any singularities of $P(\omega, k)$. This insures that $P(\omega, k)$ exists and that $P(z, t) = 0$ for $t < 0$.

We have also limited ourselves to propagation along the magnetic field,

for which $\underline{k} = (0, 0, k)$. Introducing the velocity vector $\underline{v} = (v_\perp \cos \theta,$

$v_\perp \sin \theta, v_z)$, II-6 and II-2 become

$$-i\omega f_1(\omega, k) + ik v_z f_1(\omega, k) + \frac{eB_0}{mc} \frac{\partial f_1(\omega, k)}{\partial \theta} = \frac{e}{m} (\underline{E}(\omega, k) + \frac{\underline{v}}{c} \times \underline{B}(\omega, k)) \cdot \frac{\partial f_0}{\partial \underline{v}} - \int_{-\infty}^{\infty} dz \left[f_1(\underline{v}, \underline{r}, t) e^{-i(kz - \omega t)} \right]_{t=0}^{t=\infty} \quad \text{II-8}$$

$$i\mathbf{k} \times \mathbf{E}(\omega, \mathbf{k}) = \frac{i\omega}{c} \mathbf{B}(\omega, \mathbf{k}) - \frac{1}{c} \int_{-\infty}^{\infty} dz \left[\mathbf{B}(\mathbf{v}, \mathbf{r}, t) e^{-i(\mathbf{kz} - \omega t)} \right]_{t=0}^{t=\infty} \quad \text{II-9}$$

Because of the assumption that ω is in the upper half plane, the limits at $t = \infty$ of the last terms in Eqs. II-8 and II-9 may be neglected. Using II-9 for $\mathbf{B}(\omega, \mathbf{k})$ in II-8, the equation for $f_1(\omega, \mathbf{k})$ becomes

$$(-i\omega + ikv_z + \omega_c \frac{\partial}{\partial \theta}) f_1 = \frac{e}{m} \left[\mathbf{E} + \frac{1}{\omega} \mathbf{v} \times (\mathbf{k} \times \mathbf{E}) \right] \cdot \frac{\partial f_0}{\partial \mathbf{v}} + f_1^i + \frac{ei}{mc\omega} (\mathbf{v} \times \mathbf{B}^i) \cdot \frac{\partial f_0}{\partial \mathbf{v}} \quad \text{II-10}$$

where f_1^i and \mathbf{B}^i are the Fourier transforms of the initial disturbances at $t = 0$ and $\omega_c = eB_0/mc$ is the electron gyrofrequency.

If f_0 were isotropic, $\partial f_0 / \partial \mathbf{v}$ would be along \mathbf{v} and $(\mathbf{v} \times (\mathbf{k} \times \mathbf{E}))$. $\partial f_0 / \partial \mathbf{v} = 0$. The terms that are responsible for the instability will be shown to come from just this term, however, since the $\mathbf{E} \cdot \partial f_0 / \partial \mathbf{v}$ gives only the usual Landau damping and so is not able to contribute to instability. The $(\mathbf{v} \times \mathbf{B}) \cdot \partial f_0 / \partial \mathbf{v}$ term represents the effect of the wave perturbation magnetic field on the zero order distribution, and so bears out the contention made above that the physical mechanism for the instability is the velocity phase bunching which results from the interaction of the gyroresonant particles ($\omega - kv_z = \omega_c$) in the zero-order velocity distribution with the wave magnetic field. This is readily seen by referring to figure 1, which shows the gyroresonant wave magnetic field in the rest frame of the electrons, namely in the rest frame of the electrons which "see" the magnetic field rotating at their own gyrofrequency, so that the angle between the wave magnetic field vector and the rotating electron velocity vector remains constant. The net force on a given electron is such as to bunch the

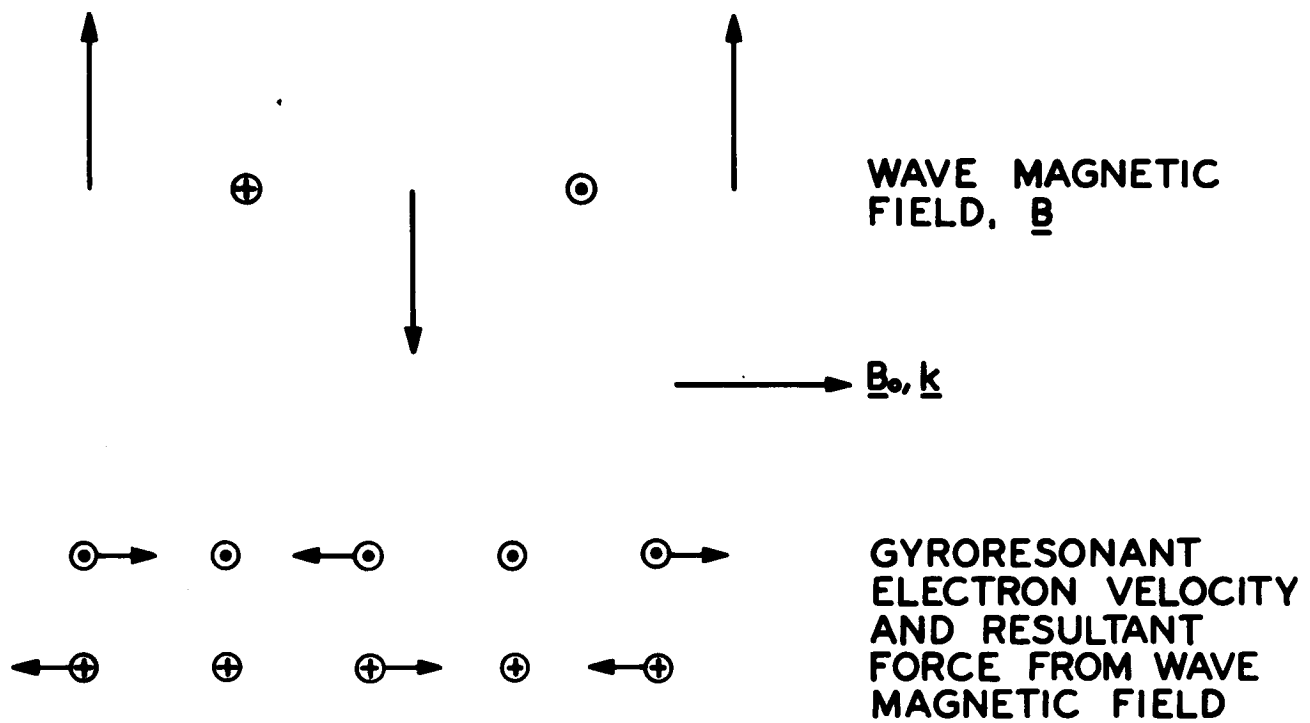


Figure 1. The resultant force of the wave magnetic field on the gyroresonant electrons.

electrons in such a way that the magnetic field that the electrons set up by their motion will tend to add coherently to the wave magnetic field. It is deceptive, however, to think of this instability only in these terms, for only if special conditions on the frequency and the initial velocity distribution are met will the Landau damping from the $\underline{E} \cdot \partial f_0 / \partial \underline{v}$ then be overcome and instability result.

Using the identities

$$\frac{E_x + iE_y}{2} e^{-i\theta} + \frac{E_x - iE_y}{2} e^{i\theta} = \frac{\underline{v}_\perp \cdot \underline{E}_\perp}{v_\perp} \quad \text{II-11a}$$

$$\frac{\partial f_0}{\partial \underline{v}_\perp} = \frac{\underline{v}_\perp}{v_\perp} \frac{\partial f_0}{\partial v_\perp} \quad \text{II-11b}$$

$$\frac{\partial f_0}{\partial v_z} = \hat{z} \frac{\partial f_0}{\partial v_z} \quad \text{II-11c}$$

II-10 becomes

$$\begin{aligned} & (-i\omega + ikv_z + \omega_c \frac{\partial}{\partial \theta}) f_1 = \\ & \frac{e}{m} \left\{ E_z \frac{\partial f_0}{\partial v_z} + \left[\left(1 - \frac{kv_z}{\omega}\right) \frac{\partial f_0}{\partial v_\perp} + \frac{kv_\perp}{\omega} \frac{\partial f_0}{\partial v_z} \right] \left(\frac{E_x + iE_y}{2} e^{-i\theta} + \frac{E_x - iE_y}{2} e^{i\theta} \right) \right\} \\ & + f_1^i - \frac{e}{mc\omega} \left(v_\perp \frac{\partial f_0}{\partial v_z} - v_z \frac{\partial f_0}{\partial v_\perp} \right) \left(\frac{B_x^i + iB_y^i}{2} e^{-i\theta} - \frac{B_x^i - iB_y^i}{2} e^{i\theta} \right) \end{aligned} \quad \text{II-12}$$

Transforming II-3 and II-2 according to II-7a, b there follows

$$\left(-k^2 + \frac{\omega^2}{c^2}\right) \underline{E} = -\frac{4\pi i\omega}{c^2} \underline{j}(\underline{k}, \omega) - \frac{4\pi}{c^2} \underline{j}^i - \frac{1}{c^2} \frac{\partial \underline{E}^i}{\partial t} + \frac{i\omega}{c} \underline{E}^i \quad \text{II-13}$$

If we now consider that the perturbation wave field at $t=0$ is such that $E_z = E_x + iE_y = 0$, so that only $E_x - iE_y = E_-$ is unequal to zero, corresponding to the right circularly polarized electron cyclotron mode, then

$$j_x - ij_y = j_- = -eN_0 \int v_{\perp} e^{-i\theta} f_1 d\theta v_{\perp} dv_{\perp} dv_z \quad \text{II-14}$$

$$f_1 = \frac{e}{2m} E_- e^{i\theta} \frac{\left\{ \left(1 - \frac{kv_z}{\omega}\right) \frac{\partial f_0}{\partial v_{\perp}} + \frac{kv_{\perp}}{\omega} \frac{\partial f_0}{\partial v_z} \right\}}{-i(\omega - kv_z - \omega_c)} + \{\text{Initial Value Terms}\} \quad \text{II-15}$$

Now using II-15 in II-14 and II-14 in II-13 we obtain the equation

$$\left(-k^2 + \frac{\omega^2}{c^2}\right) E_- = - \frac{4\pi^2 N_0 e^2 \omega}{mc^2} E_- \int \frac{\left[\left(1 - \frac{kv_z}{\omega}\right) \frac{\partial f_0}{\partial v_{\perp}} + \frac{kv_{\perp}}{\omega} \frac{\partial f_0}{\partial v_z} \right]}{\omega - kv_z - \omega_c} v_{\perp}^2 dv_{\perp} dv_z + \{\text{Initial Value Terms}\} \quad \text{II-16}$$

which has the solution

$$E_- = \frac{\{\text{Initial Value Terms}\}}{-k^2 + \frac{\omega^2}{c^2} + \frac{\pi\omega_p^2 \omega}{c^2} \int \frac{\left[\left(1 - \frac{kv_z}{\omega}\right) \frac{\partial f_0}{\partial v_{\perp}} + \frac{kv_{\perp}}{\omega} \frac{\partial f_0}{\partial v_z} \right]}{\omega - kv_z - \omega_c} v_{\perp}^2 dv_{\perp} dv_z} \quad \text{II-17}$$

where $\omega_p^2 = 4\pi N_0 e^2/m$ denotes the electron plasma frequency.

To solve for $E_-(k, t)$, E_- of II-17 is used in II-7b. The contour W in the ω plane is to go above all zeroes of the denominator in II-17. This contour is then closed in the lower half ω plane (where $e^{-i\omega t}$ will give convergence) and the integral can ideally be expressed as a sum of the residues of the enclosed poles, the n th enclosed pole giving an $e^{-i\omega_n t}$

contribution to $E_-(k, t)$. The roots $\omega_n = \omega_n(k)$ of the dispersion relation

$$k^2 c^2 = \omega^2 + \omega_p^2 \pi \int \frac{[(\omega - kv_z)(\partial f_0 / \partial v_\perp) + kv_\perp (\partial f_0 / \partial v_z)]}{\omega - kv_z - \omega_c} v_\perp^2 dv_\perp dv_z \quad \text{II-18}$$

thus give the positions of the residues contributing to $E_-(k, t)$ and so determine the time dependence of the final solution. The definition of the integral in II-18, however, is only valid for ω in the upper half plane, since only then do the boundary terms at $t = \infty$ go to zero. Thus ω in II-18 must be assumed to have a small positive imaginary part and the v_z integration in II-18 must be carried out under this assumption. In order to solve II-18 for ω in the lower half plane, analytic continuation must be made of the integral over v_z from its value in the upper half ω plane. This is the famous Landau prescription for interpreting the resonance denominator in II-18. Thus in treating the resonance denominator $1/(\omega - kv_z - \omega_c)$, $\omega = \omega_r + i\omega_i$ is to be considered to be in the upper half plane, so that the v_z integration will pass below the pole at $v_z = (\omega - \omega_c)/k$ when $k > 0$ and above the pole when $k < 0$. This prescription can be summarized by writing

$$\frac{1}{\omega - kv_z - \omega_c} = -\frac{1}{k} \left[P \frac{1}{v_z + \frac{\omega_c - \omega}{k}} + \pi i \frac{k}{|k|} \delta(v_z + \frac{\omega_c - \omega}{k}) \right] \quad \text{II-19}$$

where P denotes the Cauchy principal value obtained by averaging the two integrals which pass just above and just below the singular point at $v_z = (\omega - \omega_c)/k$. As mentioned above, the imaginary terms in II-19 and hence

in II-18, which are just the ones responsible for wave damping or growth, result from the wave interaction with those particles obeying the gyroresonant condition $\omega - kv_z - \omega_c = 0$ or $v_z = (\omega - \omega_c)/k$.

If II-19 is substituted into II-18 and terms of second order or higher in ω_i are neglected, the dispersion relation for ω becomes

$$\begin{aligned} \omega_r^2 + 2i\omega_r\omega_i = c^2k^2 + \\ \frac{\pi\omega_p^2}{k} P \int \frac{\left[(\omega_r + i\omega_i - kv_z) \frac{\partial f_o}{\partial v_z} + kv_z \frac{\partial f_o}{\partial v_z} \right]}{v_z + \frac{\omega_c - \omega_r - i\omega_i}{k}} v_z^2 dv_z \\ + \frac{\pi^2 i \omega_p^2}{|k|} \int \left[(\omega_r + i\omega_i - kv_z) \frac{\partial f_o}{\partial v_z} + kv_z \frac{\partial f_o}{\partial v_z} \right]_{v_z = \frac{\omega - \omega_c}{k}} v_z^2 dv_z \quad \text{II-20} \end{aligned}$$

In evaluating the principal value integral, we can assume that $|v_z| \ll |(\omega_r - \omega_c)/k|$, or in other words that $(\omega_r - \omega_c)/k$ is in the tail of the $f_o(v)$ velocity distribution. For the frequencies we shall be interested in, this condition will be well satisfied. It then follows that

$$\frac{1}{v_z + \frac{\omega_c - \omega_r - i\omega_i}{k}} \approx \frac{1}{\frac{\omega_c - \omega_r}{k}} - \frac{(v_z - \frac{i\omega_i}{k})}{\left(\frac{\omega_c - \omega_r}{k}\right)^2} + \frac{v_z^2}{\left(\frac{\omega_c - \omega_r}{k}\right)^3} \dots \quad \text{II-21}$$

The principal value integral can then be done by partial integration, using the fact that f_o is even in v_z and the temperature defining relations

$$2\pi \int v_z^2 f_o dv_z v_z^2 dv_z = \frac{KT_z}{m} \quad \text{II-22a}$$

$$2\pi \int v_z^2 f_o dv_z v_z^2 dv_z = \frac{2KT_\perp}{m} \quad \text{I-22b}$$

where K is Boltzmann's constant. The result is

$$\begin{aligned}
 & -\pi P \int \frac{[(\omega_r + i\omega_i - kv_z)(\partial f_o / \partial v_\perp) + kv_\perp (\partial f_o / \partial v_z)]}{v_z + \frac{\omega_c - \omega_r - i\omega_i}{k}} v_\perp^2 dv_\perp dv_z \\
 & = \frac{k\omega_r}{\omega_c - \omega_r} \left[1 + \left(\frac{k}{\omega_c - \omega_r} \right)^2 \frac{KT_\perp}{m} \left[1 - \frac{\omega_c}{\omega} \left(1 - \frac{T_z}{T_\perp} \right) \right] \right] + \frac{i\omega_i k \omega_c}{(\omega_c - \omega_r)^2} \quad \text{II-23}
 \end{aligned}$$

II-20 can then be solved for

$$c^2 k^2 = \omega_r^2 + \frac{\omega_p^2 \omega_r}{\omega_c - \omega_r} \left[1 + \left(\frac{k}{\omega_c - \omega_r} \right)^2 \cdot \frac{KT_\perp}{m} \left[1 - \frac{\omega_c}{\omega} \left(\frac{T_\perp - T_z}{T_\perp} \right) \right] \right] \quad \text{II-24}$$

which is the usual whistler dispersion relation with additional temperature corrections, and

$$\omega_i = \frac{\frac{\pi^2 \omega_p^2 \omega_r}{|k|} F_e \left(\frac{\omega_r - \omega_c}{k} \right)}{2\omega_r + \frac{(\omega_p^2 \omega_c)}{(\omega_c - \omega_r)^2}} \quad \text{II-25}$$

where

$$F_e(v_z) = \int_0^\infty \left[\left(1 - \frac{kv_z}{\omega_r} \right) \frac{\partial f_o}{\partial v_\perp} + \frac{kv_\perp}{\omega_r} \frac{\partial f_o}{\partial v_z} \right] v_\perp^2 dv_\perp \quad \text{II-26}$$

If $\omega_i > 0$, then there will be wave growth and instability, while for $\omega_i < 0$ there will be wave damping.

It is immediately seen that if f_o is isotropic, then $v_z (\partial f_o / \partial v_\perp) = v_\perp (\partial f_o / \partial v_z)$, and $F_e(v_z) = -2 \int_0^\infty v_\perp dv_\perp f_o(v_\perp, v_z) < 0$ so that an isotropic distribution only shows Landau damping and is stable with respect to the growth of electron cyclotron waves. The electron cyclotron mode will be unstable if for a given anisotropic initial velocity distribution, f_o ,

there exist values of ω for which $F_e(v_z = (\omega_r - \omega_c)/k) > 0$.

For conditions pertaining to the electron cyclotron mode in the magnetosphere, namely $\omega_p^2 > \omega_c^2 > \omega^2$, II-24 and II-25 can be reasonably well approximated by

$$c^2 k^2 \approx \omega_r^2 + \frac{\omega_p^2 \omega_r}{\omega_c - \omega_r} \approx \frac{\omega_p^2 \omega}{\omega_c - \omega} \quad \text{II-27}$$

$$\omega_i \approx \frac{\pi^2 (\omega_c - \omega)^2 \omega}{|k| \omega_c} F_e \left(\frac{\omega - \omega_c}{k} \right) \quad \text{II-28}$$

where we have dropped the subscripts on ω_r .

The solution of the boundary value problem for k_i , the imaginary part of k , with ω assumed real follows along similarly to the above, but is complicated essentially by the $k/|k|$ factor in II-19. This factor cannot be reproduced by simply assuming, analogously to the complex ω case and the Landau prescription, that k has a small imaginary part to assure convergence of the Laplace transformation in space and that the v_z integrals are to be analytically continued in this light into the whole k plane. If this is done, the imaginary part of k will be found to have the wrong sign when $\omega < \omega_c$ for $k_r > 0$ or when $\omega > \omega_c$ for $k_r < 0$! The physical requirements of causality and the symmetry of space must be introduced to determine properly the sign of k_i , and it is these requirements and not those of the Landau prescription that are able to produce the proper sign for k_i . The $k/|k|$ factor in II-19 assures that the same damping (or growth) occurs irrespective of whether the wave is travelling in the $+z$ or $-z$ direction. The prescription that in the v_z integration in

II-18 the pole at $v_z = (\omega - \omega_c)/k$ must be passed from below when $k_r > 0$ and from above when $k_r < 0$ introduces a branch cut in the k plane along the imaginary k axis which can possibly give a contribution to the inverse k transformation in addition to the pole contributions at the roots $k_n = k_n(\omega)$ of II-18. These matters are discussed in detail in Appendix I.

For those conditions that we shall be concerned with in the magnetosphere, k_i can be simply given by

$$k_i = - \frac{\omega_i}{\frac{d\omega}{dk}} = - \frac{\pi^2 \omega_p^2 \omega}{2c^2 k_r^2} \cdot \frac{k_r}{|k_r|} F_e \left(\frac{\omega - \omega_c}{k_r} \right) \\ \approx - \frac{\pi^2}{2} (\omega_c - \omega) \frac{k_r}{|k_r|} F_e \left(\frac{\omega - \omega_c}{k_r} \right) \quad \text{II-29}$$

This is, of course, physically reasonable, since $d\omega/dk$, the group velocity of the electron cyclotron wave II-27, is the velocity of wave energy transport (Stix (1962)).

In order to illustrate the type of results that follow from II-25 and II-29, we shall solve for $F_e(v_z)$ with various assumptions as to the form of the initial velocity distribution $f_o(v_z, v_\perp)$. If f_o is taken to have a Gaussian form with different temperatures perpendicular and parallel to the magnetic field

$$f_o^G(v_z, v_\perp) = \frac{1}{\pi^{3/2}} \left(\frac{m}{2KT} \right) \left(\frac{m}{2KT_z} \right)^{1/2} \exp \left[- \frac{mv_\perp^2}{2KT_\perp} - \frac{mv_z^2}{2KT_z} \right] \quad \text{II-30}$$

then

$$F_e^G(v_z) = - \frac{1}{\pi^{3/2}} \left(\frac{m}{2KT_z} \right)^{1/2} \cdot \left[1 + \frac{kv_z}{\omega} \left(\frac{T_\perp - T_z}{T_z} \right) \right] \exp - \frac{mv_z^2}{2KT_z} \quad \text{II-31}$$

$$F_e^G(v_z = \frac{\omega - \omega_c}{k}) = - \frac{1}{\pi^{3/2}} \left(\frac{m}{2KT_z} \right)^{1/2} \cdot \left[1 - \frac{\omega_c}{\omega} \left(\frac{T_\perp - T_z}{T_\perp} \right) \right] \exp - \frac{m}{2KT_z} \left(\frac{\omega - \omega_c}{k} \right)^2 \quad \text{II-32}$$

This is essentially the normalized number of particles at $v_z = (\omega - \omega_c)/k$ times a factor of order unity which can become negative and so give instability when $\omega < \omega_c \left(\frac{T_\perp - T_z}{T_\perp} \right)$.

If $f_0(v_z, v_\perp)$ is now taken to have a skewed Cauchy form

$$f_0^c(v_z, v_\perp) = \frac{(2\Delta^2)^a \Delta(a+1)!}{\pi^2 \sqrt{1-x} (2a-1)!!} \cdot \frac{1}{(v_\perp^2 + \frac{v_z^2}{1-x} + \Delta^2)^{a+2}} \quad \text{II-33}$$

which has the properties

$$\int f_0^c d^3 v = 1 \quad \text{II-34a}$$

$$\int f_0^c \frac{v_\perp^2}{2} d^3 v = \Delta^2 = \frac{KT_\perp}{m} \quad \text{II-34b}$$

$$\int f_0^c v_z^2 d^3 v = \Delta^2(1-x) = \frac{KT_z}{m} \quad \text{II-34c}$$

$$\frac{T_\perp - T_z}{T_\perp} = x \quad \text{II-34d}$$

then

$$F_e \left(\frac{\omega - \omega_c}{k} \right) = - \frac{(2\Delta^2)^a \Delta a!}{\pi^2 (1-x)^{3/2} (2a-1)!!} \cdot \frac{(1-x \frac{\omega_c}{\omega})}{2 \left[\left(\frac{\omega - \omega_c}{k} \right) / (1-x) + \Delta^2 \right]^{a+1}} \quad \text{II-35}$$

As a final example, we consider an initial velocity distribution which is a function only of the magnitude of the total velocity, v , and the magnetic moment, v_\perp^2 / B_0 , both of which are conserved by a particle's motion in a magnetic field:

$$f_0(v_z, v_\perp) = F_0(v^2) G(v_\perp^2 / B_0) \quad \text{II-36}$$

$F_0(v^2)$ is assumed normalized to unity over the whole of velocity space and for $G(v_\perp^2 / B_0)$ we take

$$G(v_\perp^2 / B_0) = \sqrt{\frac{B_{\max}}{B_{\max} - B_0}} \Theta\left(\frac{B_{\max}}{B_0} - \frac{v_\perp^2}{v^2}\right) \quad \text{II-37}$$

where $\Theta(y) = 1$ for $y > 0$, $\Theta(y) = 0$ for $y < 0$, and B_{\max} essentially represents that value of B_0 at which particles travelling along a given field line are lost to the ionosphere. Thus $G(v_\perp^2 / B_0)$ represents a pitch angle distribution which is uniform for $v_\perp^2 / v^2 \geq B_0 / B_{\max}$, and has no particles with $v_\perp^2 / v^2 < B_0 / B_{\max}$, namely a loss cone type of distribution.

$F_e(v_z)$ can now be written

$$F_e(v_z) = -2 \int v_\perp F_0(v^2) G\left(\frac{B_{\max}}{B_0} - \frac{v_\perp^2}{v^2}\right) dv_\perp - 2 \frac{kv_z}{\omega} \int \frac{v_\perp^3}{v^2} F_0(v^2) \frac{B_{\max}}{B_0} \delta\left(\frac{B_{\max}}{B_0} - \frac{v_\perp^2}{v^2}\right) dv_\perp \quad \text{II-38}$$

To work out II-38 for a particular case, we take $F_0(v^2)$ as given by II-33 with $x = 0$ and $a = 1$, namely

$$F_0(v^2) = \frac{4\Delta^3}{\pi^2} \cdot \frac{1}{(v^2 + \Delta^2)^3} \quad \text{II-39}$$

and we obtain for $F_e(v_z = \frac{\omega - \omega_c}{k})$

$$F_e\left(\frac{\omega - \omega_c}{k}\right) = -\frac{2\Delta^2}{\pi^2} \cdot \frac{\left(\frac{\omega - \omega_c}{k}\right)^2}{\left[\left(\frac{\omega - \omega_c}{k}\right)^2 \frac{B_{\max}}{B_{\max} - B_0} + \Delta^2\right]^3} \cdot \left(\frac{B_{\max}}{B_{\max} - B_0}\right)^{\frac{5}{2}} \cdot \left[\left(1 + \frac{B_0}{B_{\max}}\right) - 2 \frac{B_0}{B_{\max}} \frac{\omega_c}{\omega}\right]$$

$$\approx -\frac{2\Delta^2}{\pi^2} \cdot \frac{1}{\left[\frac{\omega - \omega_c}{k}\right]^4} \cdot \left(\frac{B_{\max} - B_0}{B_{\max}}\right)^{\frac{1}{2}} \cdot \left[\left(1 + \frac{B_0}{B_{\max}}\right) - 2 \frac{B_0}{B_{\max}} \frac{\omega_c}{\omega}\right] \quad \text{II-40}$$

Instability for each of the three types of distribution considered requires $F_e((\omega - \omega_c)/k) > 0$, which occurs only when ω is less than a given fraction of ω_c which increases with the degree of velocity anisotropy or excess of perpendicular over parallel energy. Thus between $\omega = 0$ and $\omega = \omega_{\max} < \omega_c$ the electron velocity distributions considered are unstable with respect to the growth of electron cyclotron waves. For the Gaussian distribution II-30

$$\omega_{\max} = \omega_c \left(\frac{T_{\perp} - T_z}{T_{\perp}} \right), \quad \text{II-41a}$$

for the Cauchy distribution II-33

$$\omega_{\max} = \omega_c^x = \omega_c \left(\frac{T_{\perp} - T_z}{T_{\perp}} \right) \quad \text{II-41b}$$

and for the loss cone distribution II-36

$$\omega_{\max} = \omega_c \cdot \frac{2B_0}{B_{\max} + B_0} \quad \text{II-41c}$$

It should be noted that since in the magnetosphere $B_0/B_{\max} \ll 1$, the loss cone distribution can only produce instability over a comparatively small range of frequencies. That this should be the case can be seen by rewriting Eq. II-26 for $F_e(v_z)$ in terms of v and θ , the magnitude of the total velocity and the pitch angle, rather than in terms of v_z and v_{\perp} .

II-26 then becomes

$$F_e\left(v_z = \frac{\omega - \omega_c}{k}\right) = - \int_0^{\infty} v_{\perp} \left[f_0 + \tan \theta \frac{\partial f_0}{\partial \theta} \cdot \frac{\omega - \omega_c}{\omega} \right]_{v_z = (\omega - \omega_c)/k} dv_{\perp} \quad \text{II-42}$$

So that the instability condition $F_e((\omega - \omega_c)/k) > 0$ becomes

$$\int v_{\perp} \tan \theta \frac{\partial f_0}{\partial \theta} \Big|_{v_z = (\omega - \omega_c)/k} dv_{\perp} > \frac{\omega}{\omega_c - \omega} 2 \int v_{\perp} f_0 \Big|_{v_z = (\omega - \omega_c)/k} dv_{\perp} \quad \text{II-43}$$

Because of the $\tan \theta$ factor, positive values of $\partial f_0 / \partial \theta$, which are necessary for instability, are less effective at small values of the pitch angle than they are at values of θ closer to 90° . The value of θ at the equator required for a particle to strike the earth is roughly $\theta^2 \lesssim 1/2L^3$, which is in general quite small. Thus the very steep angular dependence of the loss cone factor is masked by the $\tan \theta$ factor, which in turn enhances those values of $\partial f_0 / \partial \theta$ which come from a term as II-33.

A characteristic of this electron cyclotron velocity anisotropy instability is that it occurs only when $T_\perp > T_z$, since in the case $T_z > T_\perp$ it has been shown (Sudan (1963), Noerdlinger (1963)) that the resonant particles responsible for damping or growth must travel faster than the speed of light, with the result that in the case $T_z > T_\perp$ the potentially unstable waves are actually marginally stable, exhibiting neither damping nor growth.

In the next section we shall further investigate the above and other models for the electron velocity distribution and attempt to choose from among them one that best represents the actual situation that pertains in the magnetosphere.

III. MAGNETOSPHERIC MODELS AND WAVE GROWTH RATES

A sizeable amount of observational evidence exists for the form of the electron velocity distribution in the magnetosphere at energies $E > 40$ kev (Frank, VanAllen and Hills (1964), Frank (1965), Anderson, Harris and Paoli (1965)). Whistler determination of the total electron density in the outer belt has also been made (Liemohn and Scarf (1964), and theoretical arguments can be made for the temperature of electrons at the outer boundary of the magnetosphere. Lastly, a comparison of the electron fluxes observed, for a given L value, at the magnetic equator and just above the atmosphere (O'Brien (1962), (1964)) can be used to give an estimate of the anisotropy in the velocity distribution of geomagnetically trapped electrons. Although the velocity distribution at energies between 1 and 40 kev remains less well determined, while that below 1 kev is essentially unknown, nonetheless by a piecing together of the available experimental information we shall be able to derive a distribution function for magnetospheric electrons which is able to represent sufficiently well those properties that we shall require for a proper evaluation of Π -26.

The parameter L referred to above, introduced originally by McIlwain (1961), is constant along a magnetic line of force and labels the magnetic shell on which an electron bounces in latitude and drifts in longitude. L essentially corrects for the fact that even in the absence of the distorting solar wind the earth's magnetic field is not that of a perfect dipole. If the earth's magnetic field were that of a perfect dipole, L would be the equatorial radial distance to a magnetic

shell, expressed in units of earth radii. The invariant latitude Λ is defined by

$$L \cos^2 \Lambda = 1 \quad \text{III-1}$$

and for a perfect dipole field is equal to the magnetic latitude at which a magnetic shell intersects the earth. For the actual magnetic field of the earth, the magnetic latitude, λ , and the invariant latitude, Λ , can be considered essentially equal to within a degree. Beyond $L = 6$, the distortion of the earth's magnetic field by the solar wind makes the ordering of magnetospheric phenomena according to L increasingly difficult (O'Brien (1963)). The day side of the magnetosphere is compressed so that the high-latitude boundary of trapping is at $\Lambda \approx 75^\circ$ ($L \approx 16$), while the night side boundary of trapping is at $\Lambda \approx 69^\circ$ ($L \approx 8$). Fig. 2, taken from O'Brien (1963), illustrates this above deformation of the magnetosphere.

Information about energetic electrons in the magnetosphere is characteristically given in terms of $j(E, \theta)$ and $J(E)$, the directional and omnidirectional, respectively, number flux of electrons with energy greater than a given energy E . In the outer belt ($L \gtrsim 3$) $J(40 \text{ kev})$ is characteristically about $10^7 / \text{cm}^2\text{-sec}$, reaching a slight maximum about $L = 4$, becoming increasingly fluctuating and time dependent beyond $L = 6$, and dropping off steeply beyond $L = 8$. Beyond 10 earth radii, the magnetospheric boundary is encountered and hence the boundary of trapped particle fluxes. If the energy dependence of this omnidirectional flux is represented by the simple form

$$J(E) / J(E_0) = (E/E_0)^{-a} \quad \text{III-2}$$

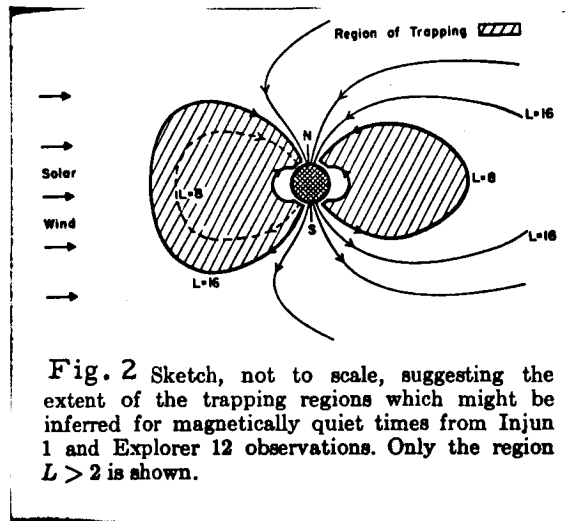


Fig. 2 Sketch, not to scale, suggesting the extent of the trapping regions which might be inferred for magnetically quiet times from Injun 1 and Explorer 12 observations. Only the region $L > 2$ is shown.

then for energies E greater than 40 keV a is found to be approximately 1 in the range $3 < L < 6$, and increases to about 2 - 2.5 in the range $6 < L < 8$ (Frank (1965)). The spectral parameter a is found to increase during periods of high magnetic index, K_p , indicating a spectral softening during periods of geomagnetic disturbance.

In the process of relating $J(E)$ to an electron velocity distribution, we first consider the omnidirectional spectral flux $I(E)$ (number/cm²-sec-keV), the spectral number density $\rho(E)$ (number/cm³-keV), the integral density $\xi(E)$ (ergs/cm³), and the integral energy flux $\epsilon(E)$ (ergs/cm²-sec). The omnidirectional spectral flux $I(E)$ is defined by the relation

$$J(E_1) = \int_{E_1}^{\infty} I(E) dE \quad / \text{cm}^2\text{-sec} \quad \text{III-3}$$

Using III-2, $I(E)$ is solved for in the form

$$I(E) = aJ(E_0) E_0^a / E^{a+1} \quad / \text{cm}^2\text{-sec-keV} \quad \text{III-4}$$

where E is understood to be in keV. The spectral number density is given by

$$\begin{aligned} \rho(E) &= I(E)/v \quad / \text{cm}^3\text{-keV} \\ &= 6.25 \times 10^8 I(E)/v \quad / \text{cm}^3\text{-erg} \end{aligned} \quad \text{III-5}$$

where v is given nonrelativistically in terms of E by

$$v = \sqrt{E/255} \quad c \quad \text{III-6}$$

The integral energy density is given by

$$\begin{aligned} \xi(E_1) &= \int_{E_1}^{\infty} E \rho(E) dE \quad \text{kev/cm}^3 \\ &= 8.5 \times 10^{19} \frac{J(E_0)E_0^a}{1 - \frac{1}{2a}} \cdot \frac{1}{E_1^{a-1/2}} \quad \text{ergs/cm}^3 \end{aligned} \quad \text{III-7}$$

and the integral energy flux by

$$\begin{aligned} \epsilon(E_1) &= \int_{E_1}^{\infty} E I(E) dE \quad \text{kev/cm}^2\text{-sec} \\ &= 1.6 \times 10^{-9} \frac{J(E_0)E_0^a}{1 - \frac{1}{a}} \cdot \frac{1}{E_1^{a-1}} \quad \text{ergs/cm}^2\text{-sec} \\ & \quad (a > 1) \end{aligned} \quad \text{III-8}$$

If we assume an isotropic velocity distribution $N_0 f_0(v)$, then the spectral number density is related to f_0 by

$$\rho dE = \rho m v dv = N_0 f_0 \cdot 4\pi v^2 dv \quad \text{III-9a}$$

or

$$\begin{aligned} N_0 f_0 &= 6.2 \times 10^8 \frac{aJ(E_0)E_0^a}{4\pi} \frac{m}{v^2} \frac{1}{E^{a+1}} \quad /(\frac{\text{cm}}{\text{sec}})^3\text{-cm}^3 \\ &= (1.6 \times 10^{-9})^a \cdot \frac{a2^{a+1}}{4\pi m^a} \cdot \frac{J(E_0)E_0^a}{(v^2)^{a+2}} \end{aligned} \quad \text{III-9b}$$

If this is now related to the Cauchy distribution given in Eq. II-33 with $x = 0$, it follows that

$$N_0 = (1.6 \times 10^{-9})^a \cdot \frac{\pi J(E_0)E_0^a}{2m^a} \cdot \frac{(2a-1)!! a}{\Delta^{2a+1} (a+1)!} \quad /\text{cm}^3 \quad \text{III-10}$$

The assumption that Eq. III-10 actually is valid in the magnetosphere assumes that a as given by Eq. III-2 does not depend on energy and so holds over the complete velocity spectrum. To see if this is a reasonable assumption, we solve III-10 for Δ , the root mean square velocity of the assumed distribution (II-33), and see if this mean square velocity is in reasonable agreement with what one would expect to be the temperature of electrons in the magnetosphere. Solving for Δ , the result is

$$\Delta^{2a+1} = \frac{(1.6 \times 10^{-9})^a}{m^a} \cdot \frac{\pi(2a-1)!! a}{2(a+1)!} \cdot \frac{J(E_0)E_0^a}{N_0} \quad \text{III-11}$$

For N_0 we take the equatorial value found by Liemohn and Scarf (1964) from whistler data in the range $2 < L < 5$

$$N_0 = 1.41 \times 10^4 / L^3 \quad \text{particles/cm}^3 \quad \text{III-12}$$

It is reasonable to expect that this form holds even for $L > 5$, since it predicts a density on the order of $10 \text{ particles/cm}^3$ at the boundary of the magnetosphere ($L \approx 10$), consistent with the densities of approximately $60 \text{ particles/cm}^3$ found by the MIT plasma probe experiment on Imp 1 for protons at the subsolar point in the magnetosheath, just outside the magnetosphere boundary (Olbert (1965)). For $J(E_0)$ we take $J(40 \text{ keV}) \approx 10^7 / \text{cm}^2 \text{-sec}$, which holds within an order of magnitude for $3 < L < 8$ and is also experimentally found to be relatively independent of the spectral parameter a . With these choices for $J(E_0)$ and N_0 , only the values $a \approx 1$ give a mean square electron velocity consistent with our approximate knowledge of the temperature of electrons in the magnetosphere, namely temperatures on the order of $10^4 \text{ }^\circ\text{K}$ at the base of the

exosphere at say a couple of thousand kilometers, and on the order of 10^6 °K at the outer boundary of the magnetosphere, consistent with temperatures on the order of 3×10^6 °K found by the MIT plasma probe in the magnetosheath.

To see this agreement, we solve III-11 with $a = 1$ to obtain

$$\Delta = 3.8 \times 10^7 \text{ L cm/sec} \quad \text{III-13a}$$

$$T = (m\Delta^2)/K = 9.6 \times 10^3 \text{ L}^2 \text{ °K} \quad \text{III-13b}$$

$$\bar{E} = \frac{3}{2} \text{ KT} = 1.25 \times 10^{-3} \text{ L}^2 \text{ kev} \quad \text{III-13c}$$

Granted that the agreement found with the spectral parameter a set equal to 1 can only be termed fortuitous, nevertheless the fact that this model so well represents the properties of magnetospheric electrons to the extent that they are either known or can be reasonably surmised justifies our use of this model as a basis for our calculations. The fact that $a > 1$ for electron energies greater than 40 kev and $L > 6$ can be reasonably explained as a softening of the electron spectrum at higher energies in that region of the magnetosphere which is subject to large fluctuations, and that at some lower energy, probably above 1 kev, the energy spectrum will most likely turn over and become harder. Because of the large temporal and spatial variations that occur in the region $L > 6$, in addition to the difficulty in ordering magnetospheric phenomena according to L at these higher L values, our results in this region can represent only a very general interpretation of the phenomena we shall attempt to explain, and in such a sense our results will be presented.

It is interesting to compare the energy density of electrons as obtained from our model with the energy density in the earth's equatorial magnetic field.

$$\beta = \frac{B_0^2 / 8\pi}{N_0 kT} = 2.0 \times 10^5 / L^5 \quad \text{III-14}$$

where we have taken $B_0 = 0.31/L^3$ gauss. At the boundary of the magnetosphere, the compressed magnetic field will rise to twice the value predicted by the above, so that the energy density of magnetospheric electrons approaches from below the energy density of the magnetic field at the magnetospheric boundary at $L \approx 10$. Were $\beta < 1$, the magnetic field would not be able to contain the plasma mirroring along magnetic field lines, so that the electron plasma density at the magnetospheric boundary is close to the maximum that can be contained by the magnetic field.

It is also instructive to compare the bounce times of magnetospheric electrons with their angular diffusion times calculated on the basis of coulomb scattering theory. The bounce time of an electron on the field line characterized by its equatorial crossing at LR_0 is approximated by Hamlin et al. (1961) as

$$\begin{aligned} \tau_0 &= \frac{4LR_0}{v} (1.30 - .56 \sin \theta_0) \\ &= 1.35 \frac{L}{E^{1/2}} (1.30 - .56 \sin \theta_0) \\ &\approx 1.35 \frac{L}{E^{1/2}} \text{ sec} \end{aligned} \quad \text{III-15}$$

where θ_0 is the pitch angle of the electron as it crosses the equator and E is in kev. The time for a coulomb deflection through 90° for an electron moving in an essentially stationary background of heavier positive ions is given by Spitzer (1962) as

$$\tau_D = \frac{m^2 v^3}{8\pi N_0 e^4 \log_e \Lambda} \quad \text{III-16a}$$

where $\log_e \Lambda$ is a relatively insensitive function of T and N_0 and is typically 25 under magnetospheric conditions. It then follows that

$$\tau_D = 1.65 \times 10^{11} \frac{E^{3/2}}{N_0} = 1.17 \times 10^7 E^{3/2} L^3 \text{ sec} , \quad \text{III-16b}$$

so that the ratio of the coulomb diffusion time to the bounce time become s

$$\tau_D / \tau_B = 8.7 \times 10^6 E^2 L^2 \quad \text{III-17}$$

Thus particles with the mean thermal energy, $E = 1.25 \times 10^{-3} L^2$ kev have

$$\tau_D / \tau_B = 1.35 \times 10 L^6 \quad \text{III-18}$$

and can be considered to be mirroring along magnetic field lines undisturbed by coulomb collisions. Because of this, these particles can be energized by magnetic fluctuations and particle drifts in the anisotropic magnetosphere without exchanging energy with one another through coulomb interaction. Thus there is no intrinsic reason to expect magnetospheric electrons to have a collision dominated Maxwellian distribution.

The final required property of the electron velocity distribution is

the degree of velocity anisotropy. This property can be estimated by comparing the measured directional and omnidirectional intensities, $j(E, \theta)$ and $J(E)$, respectively, at different points along a given field line. We must first determine, therefore, the relation between the directional and omnidirectional intensities at two different points along a given field line for a given directional intensity at one of the two points

Consider a particle with a given pitch angle θ and the contribution it will make to the particle intensity at two different points, labelled a and b, along a given field line. The cross sectional area of the flux tube that the particle will be found in goes as the inverse of the magnetic field. This follows from the adiabatic invariance of the particle's magnetic moment, which requires that

$$\frac{R_a^2}{R_b^2} = \frac{B_b}{B_a} = \frac{\sin^2 \theta_b}{\sin^2 \theta_a} = \frac{v_{\perp b}^2}{v_{\perp a}^2} \quad \text{III-19}$$

where R is the particle's radius of gyration. Taking derivatives, III-19 states that

$$\frac{R_a dR_a}{R_b dR_b} = \frac{B_b}{B_a} = \frac{\sin \theta_b \cos \theta_b d\theta_b}{\sin \theta_a \cos \theta_a d\theta_a} \quad \text{III-20}$$

so that those particles in $R_b dR_b$ at point b will be found in $(B_b/B_a) R_b dR_b$ at point a, and similarly the particles in pitch angle range $\sin \theta_b d\theta_b$ at b will be found in $(\cos \theta_b / \cos \theta_a)(B_a/B_b) \sin \theta_b d\theta_b$ at a.

The time that a particle spends in any given unit of length, Δz , along the field line goes as $1/v \cos \theta$, since $\Delta t = \Delta z / v_z$. Thus the contribution

that a particle makes to the particle flux intensity at a given point will be given by

$$j_a(\theta_a) \sin \theta_a d\theta_a \frac{R_a dR_a}{\Delta t_a} = j_b(\theta_b) \sin \theta_b d\theta_b \frac{R_b dR_b}{\Delta t_b} \quad \text{III-21}$$

or, using III-20

$$j_a(\theta_a) = j_b(\theta_b) \quad \text{III-22}$$

where $j(\theta)$ is the particle intensity within unit solid angle in velocity space about θ .

III-22 is essentially a statement of Liouville's theorem, which states that the density of particles in phase space remains constant in time, or, in other words, that if we follow a given test particle in its orbit through position space, then the directional flux of particles in the direction of the test particle remains constant.

Thus if the directional velocity distribution of a group of particles is known at one given point b , then the omnidirectional intensity of particles at any other point a along the same field line can be expressed as

$$\begin{aligned} J_a &= \int_0^\pi j_a(\theta_a) 2\pi \sin \theta_a d\theta_a \\ &= \int_0^\pi j_b(\theta_b) 2\pi \sin \theta_a d\theta_a \\ &= \int_0^{\theta_{\max}} j_b(\theta_b) 2\pi \frac{\cos \theta_b}{\cos \theta_a} \frac{B_a}{B_b} \sin \theta_b d\theta_b \quad \text{III-23} \end{aligned}$$

where θ_{\max} is determined so that the θ_b integration extends only over those particles that do not mirror before reaching point a , namely

$$\sin^2 \theta_{\max} = \frac{v_{\perp b}^2}{v^2} = \frac{B_b}{B_a} \quad (B_b < B_a)$$

$$= 1 \quad (B_b > B_a) \quad \text{III-24}$$

With the substitution $\mu = \cos \theta$, III-23 becomes

$$J_a = 4\pi \frac{B_a}{B_b} \int_{\frac{B_b}{B_a}}^1 j_b(\mu_b) \frac{\mu_b d\mu_b}{\left[1 - \frac{B_a}{B_b} (1 - \mu_b^2)\right]^{1/2}} \quad \text{III-25}$$

It is readily seen that if at a given point along a field line the distribution in pitch angle is isotropic, then the omnidirectional particle flux will remain a constant at all other points with higher magnetic field along the same field line and the directional flux will also remain isotropic. It is not possible to make this statement for points along the field line with a weaker magnetic field, since the flux at such a point has contributions from particles which mirror before they reach the original reference point at which the velocity distribution is assumed known.

We now consider a velocity distribution of the form II-33 with $a = 1$.

This can be written

$$f_o(v_z, v) = \frac{4\Delta^3}{\pi^2 \sqrt{1-x}} \cdot \frac{1}{\left(v_{\perp}^2 + \frac{v_z^2}{1-x} + \Delta^2\right)^3} \quad \text{III-26a}$$

or

$$f_o(v, \mu) = \frac{4\Delta^3}{\pi^2 \sqrt{1-x}} \cdot \frac{(1-x)^3}{\left(v^2 + \Delta^2 (1-x) - v^2 x (1-\mu^2)\right)^3} \quad \text{III-26b}$$

Since for the velocities we shall be concerned with $v^2 \gg \Delta^2$, this can finally be written

$$f_o(v, \mu) \propto \frac{1}{(1-x+x\mu^2)^3} \quad \text{III-26c}$$

If this is now substituted into III-25, the subscript a is dropped and for the reference position b we take the equatorial crossing of the given field line, at which point the relevant quantities will be denoted by B_o , μ_o , J_o , then

$$\begin{aligned} J &\propto \frac{B}{B_o} \int_{\frac{B_o}{(1-B)}}^1 \frac{\mu_o d\mu_o}{\left(1 - \frac{B}{B_o} (1 - \mu_o^2)\right)^{1/2}} \cdot \frac{1}{(1-x+x\mu_o^2)^3} \\ &= \frac{1}{2} \int_{\gamma-1}^{\gamma} \frac{dt}{(1-\gamma+t)^{1/2}} \cdot \frac{1}{\left(1-x+\frac{xt}{\gamma}\right)^3} \end{aligned} \quad \text{III-27}$$

where $\gamma = B/B_o$, $t = \gamma\mu_o^2$. Using the fact that $\gamma \geq 1$, $x \leq 1$, J finally becomes

$$J \propto \frac{1}{(1-x/\gamma)} + \frac{3}{2(1-x/\gamma)^2} + \frac{3 \tan^{-1} \left[\frac{1}{\left(\frac{\gamma}{x}-1\right)^{1/2}} \right]}{2(1-x/\gamma)^{5/2} (x/\gamma)^{1/2}} \quad \text{III-28}$$

In figure 3, $J(B_o)/J(2B_o)$ and $J(B_o)/J(\infty)$ are plotted as functions of x , where $J(B)$ denotes J evaluated at the point where the magnetic field has the value B .

Frank, Van Allen and Hills (1964) give $J(B_o)/J(2B_o) \leq 2$ for the middle of the outer radiation belt at $L \approx 4$. Roughly simultaneous measurements by Explorer 12 at the equator and Injun I at 1000 km (O'Brien (1962)) give $J(B_o)/J(\infty) \approx 5$. Similar measurements taken on

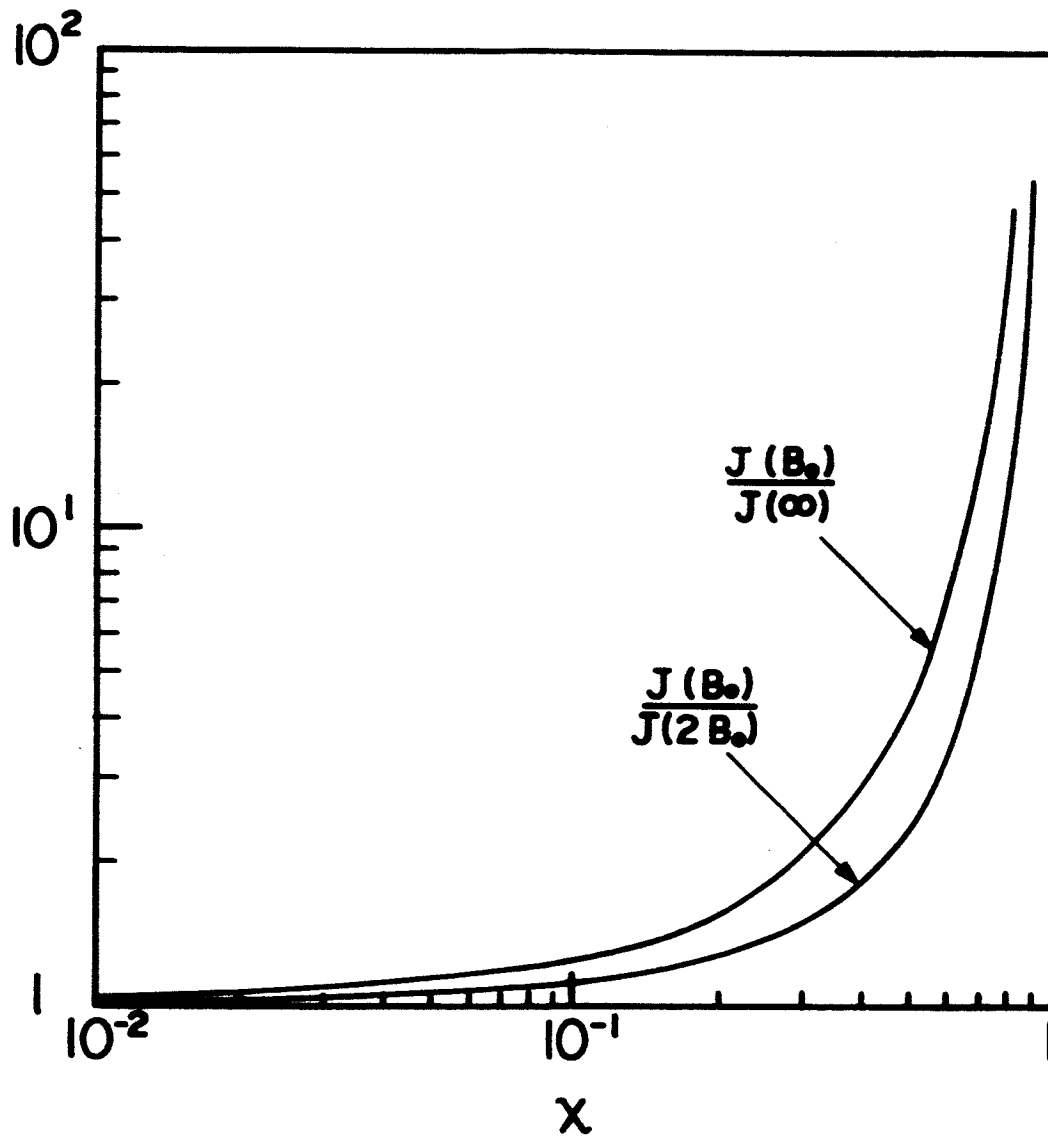


Figure 3. The relative magnitude of the omnidirectional particle flux at various points along a magnetic field line as a function of the electron velocity anisotropy parameter x .

Explorer 14 compared with those taken during the same period on Injun III give $J(B_0)/J(\infty) \approx 6$. Referring to figure 3 and with the assumption that the magnetic latitude variation in J is due solely to a term of the form III-26c, these ratios are consistent with a value of x on the order of 0.4.

Very recent data taken on Injun III (Armstrong (1965)) gives $j(40 \text{ kev}, 90^\circ)$ as a function of the value of the magnetic field, B, at the satellite altitude (237 - 2785 km) for different values of L. The results for $0.2 < B < 0.5$ and $3.5 < L < 7.5$ can be extremely well represented by the functional form $j(40 \text{ kev}, 90^\circ) = j_0 e^{-\alpha B}$ where in Table 1 j_0 and α are given as a function of L.

Table 1

L	j_0 (/cm ² -sec-sterad.)	α (/gauss)
3.5	2.7×10^6	11.8
4	1.6×10^6	10.4
4.5	5.0×10^6	11.0
5	3.3×10^6	9.5
5.5	2.1×10^6	7.7
6	1.4×10^6	7.4
6.5	1.7×10^6	8.6
7	0.85×10^6	7.2
7.5	1.6×10^6	10.0

The values of j_0 are about a factor of two higher than the equatorial values for j_0 measured during the same period by Explorer 14 (Frank (1965)).

This slight discrepancy can be accounted for by assuming that α has a value of approximately 3 for $B < 0.2$ gauss. In the following α will be considered to be given by Table 1, but at the same time we shall keep in mind that the effective value of α might be a factor of 3 or so smaller than this.

From III-22 and III-19 we are then able to express the directional intensity at the equator,

$$j_o(40 \text{ kev}, \theta_o) = j_o e^{-\alpha B} = j_o e^{-\alpha B_o / \sin^2 \theta_o} \quad \text{III-29}$$

which, being expressed in terms of the magnetic moment, is invariant along a field line. The actual pitch angle distribution must contain not only a term as $e^{-\alpha B_o / \sin^2 \theta_o}$, but also some sort of multiplicative loss cone factor as that of Eq. II-37. The $e^{-\alpha B_o / \sin^2 \theta_o}$ term can be thought of as representing a gradual diffusion of particles consistent with the fact that once the particles diffuse into the atmospheric loss cone they are removed from the distribution.

For the electron velocity distribution in the magnetosphere we therefore adopt the form

$$f_o(v, \sin^2 \theta/B) = \frac{1.6 \times 10^{-9}}{\pi m} \frac{J(E_o)E_o}{N_o} \frac{e^{-\alpha B / \sin^2 \theta}}{(v^2 + \Delta^2)^3} \left(\frac{B_{\max}}{B} \sin^2 \theta \right) \quad \text{III-30}$$

which is normalized at E_o to an omnidirectional intensity $J(E_o)$ at the equator and Δ can be fixed for a given $J(E_o)E_o$ by constraining the equatorial density of particles to be given by $N_o = 1.41 \times 10^4 / L^3$. This distribution has the advantage of being invariant in form along a field line. In figure 4, $j_o(40 \text{ kev}, \theta_o)$, the angular dependent part of III-30 evaluated at the equator and normalized to $j_o(40 \text{ kev}, 90^\circ) = 1.4 \times 10^6 / \text{cm}^2 \text{-sec-sterad.}$, is plotted vs θ_o for $L = 4$ and $L = 6$, $B_{\max}/B_o \approx 2L^3$,

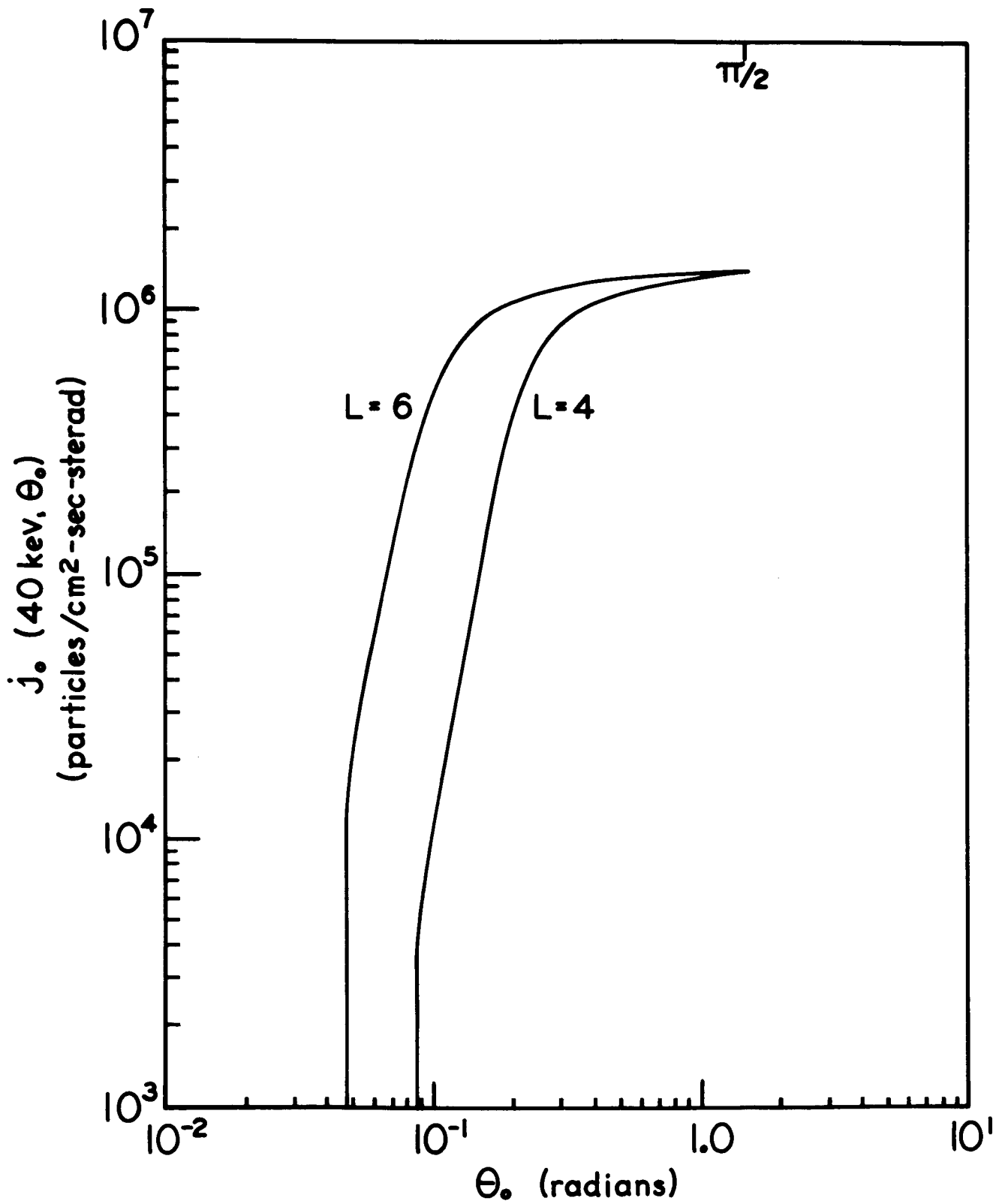


Figure 4. The equatorial directional particle flux at $L = 4$ and $L = 6$ as obtained from the assumed model, Eq. III-30, for the electron velocity distribution and plotted versus the equatorial electron pitch angle.

$B_0 = .31/L^3$ gauss and α as given in Table 1.

With the above choice for f_0 , $F_e(v_z)$ becomes

$$F_e(v_z) = -2 \frac{1.6 \times 10^{-9}}{\pi m} \frac{J(E_0) E_0}{N_0} \left\{ \int_0^{\infty} v_{\perp} \frac{e^{-\alpha B / \sin^2 \theta} \Theta\left(\frac{B_{\max}}{B} \sin^2 \theta\right)}{(v^2 + \Delta^2)^3} dv_{\perp} \right. \\ \left. + \frac{kv_z}{\omega} \int_0^{\infty} v_{\perp}^3 \frac{e^{-\alpha B / \sin^2 \theta}}{(v^2 + \Delta^2)^3} \left[\Theta\left(\frac{B_{\max}}{B} \sin^2 \theta\right) \frac{\alpha B v^2}{v_{\perp}^4} + 6 \left(\frac{B_{\max}}{B} \sin^2 \theta\right) \frac{B_{\max}}{B} \frac{1}{v^2} \right] dv_{\perp} \right\}$$

III-31

The exponential factor $e^{-\alpha B / \sin^2 \theta}$ acts as a cutoff factor at values of $v^2 < \alpha B v_z^2$. Since $1/2L^3 \lesssim \alpha B < 1$ in the magnetosphere, the integrals in III-31 can be reasonably well approximated by assuming a lower limit for v_{\perp} of $\sqrt{\alpha B v_z^2}$. The only difficulty arises in the integrals

$$\int_0^{\infty} v_{\perp}^3 \frac{e^{-\alpha B / \sin^2 \theta}}{(v^2 + \Delta^2)^3} \Theta\left(\frac{B_{\max}}{B} \sin^2 \theta\right) \frac{\alpha B v^2}{v_{\perp}^4} dv_{\perp} = \\ \int_{\left(\frac{v_z^2 B}{B_{\max} - B}\right)^{1/2}}^{\infty} \alpha B \frac{e^{-\alpha B(1 + v_z^2/v_{\perp}^2)}}{(v_z^2 + v_{\perp}^2 + \Delta^2)^3} \cdot \left(v_{\perp} + \frac{v_z^2}{v_{\perp}}\right) dv_{\perp}$$

III-32

The first of these two integrals is easily approximated by

$$\frac{\alpha B}{4(v_z^2(1 + \alpha B) + \Delta^2)^2} \approx \frac{\alpha B}{4v_z^4}$$

The second is approximated by being considered broken up into two intervals at $v_{\perp} = |v_z|$, so that

$$\int_{\left(\frac{v_z^2 B}{B_{\max} - B}\right)^{1/2}}^{\infty} \frac{e^{-\alpha B(1+v_z^2/v_{\perp}^2)}}{(v_z^2 + v_{\perp}^2 + \Delta^2)^3} \frac{dv_{\perp}}{v_{\perp}} \approx$$

$$e^{-\alpha B} \int_{|v_z|}^{\infty} \frac{dv_{\perp}}{v_{\perp}} + e^{-\alpha B} \int_{\left(v_z^2 \frac{B}{B_{\max}}\right)^{1/2}}^{|v_z|} \frac{e^{-\alpha B v_z^2/v_{\perp}^2}}{v_z^6 v_{\perp}} dv_{\perp} \quad \text{III-33}$$

The first of these integrals is trivial, and the second becomes

$$\int_{\left(v_z^2 \frac{B}{B_{\max}}\right)^{1/2}}^{v_z} \frac{e^{-\alpha B v_z^2/v_{\perp}^2}}{v_z^6 v_{\perp}} dv_{\perp} = 1/v_z^6 \cdot \frac{1}{2} \int_{1/v_z^2}^{B_{\max}/B v_z^2} \frac{e^{-\alpha B v_z^2 t}}{t} dt \approx$$

$$\frac{1}{2v_z^6} \left[\log_e(B_{\max}/B) + \sum_{n=1}^{\infty} \frac{(-\alpha B_{\max})^n}{n \cdot n!} \right] = \frac{1}{2v_z^6} Z(L, B) \quad \text{III-34}$$

Using α as given by Table 1 to solve for the L dependence of $Z(L, B_0)$, the quantity in brackets in Eq. III-34 as evaluated at the magnetic equator, we see from figure 5 that it is well approximated by $5/8 L$. If α in the vicinity of the geomagnetic equator is indeed overestimated by Table 1, then $Z(L, B_0)$ will be slightly underestimated by this assumed $5/8 L$ behavior and will tend to approach $\log_e(B_{\max}/B)$.

$F_e(v_z)$ then becomes in the vicinity of the magnetic equator

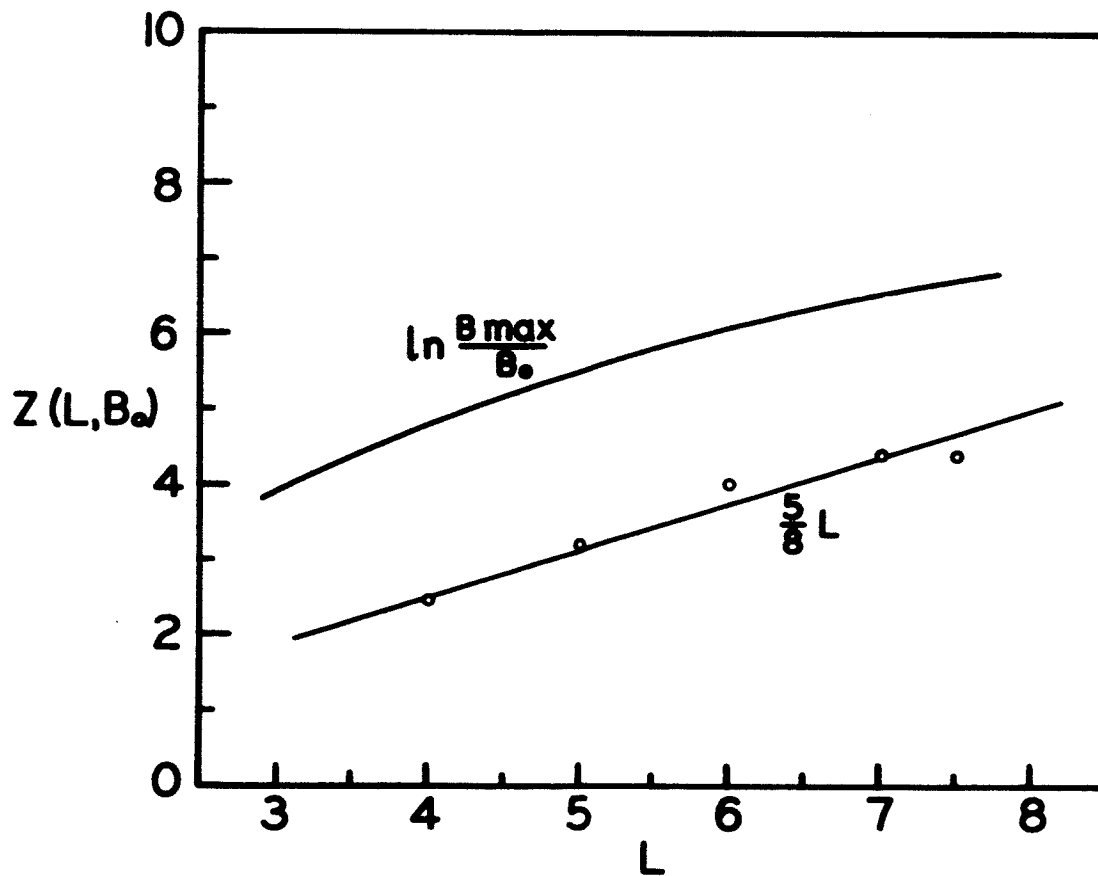


Figure 5. The L dependence of $Z(L, B_0)$ evaluated at the geomagnetic equator. The calculated values as follow from Table 1 are seen to be well approximated by the straight line $5/8 L$.

$$F_e(v_z) \approx - \frac{1.6 \times 10^{-9}}{2\pi m} \frac{J(E_o)E_o}{N_o v_z^4} \left\{ 1 + \frac{kv_z}{\omega} \left[2 \frac{B}{B_{\max}} e^{-\alpha B_{\max}} + \alpha B \left(1 + \frac{2}{3} + \frac{5L}{4} \right) \right] \right\}$$

$$\approx - \frac{1.6 \times 10^{-9}}{2\pi m} \frac{J(E_o)E_o}{N_o v_z^4} \left\{ 1 + \frac{kv_z}{\omega} \alpha B (1.67 + 1.25 L) \right\} \quad \text{III-35}$$

where it has been assumed that $B_{\max} \gg B$, $\alpha B \ll 1$, $\alpha B_{\max} > 1$.

Finally, the result for $F_e\left(\frac{\omega - \omega_c}{k}\right)$ can be given as

$$F_e\left(\frac{\omega - \omega_c}{k}\right) = - \frac{1.6 \times 10^{-9}}{2\pi m} \cdot \frac{J(E_o)E_o}{N_o} \cdot \frac{k^4}{(\omega - \omega_c)^4} \left\{ 1 + \alpha B (1.67 + 1.25L) \left(1 - \frac{\omega_c}{\omega} \right) \right\} \quad \text{III-36a}$$

$$\approx - \frac{1.6 \times 10^{-9}}{2\pi m} \cdot \frac{J(E_o)E_o}{N_o} \cdot \frac{k^4}{(\omega - \omega_c)^4} \left\{ 1 - 1.25 \alpha B L \frac{\omega_c}{\omega} \right\} \quad \text{III-36b}$$

The condition $F_e\left(\frac{\omega - \omega_c}{k}\right) > 0$ for instability becomes

$$\frac{\omega}{\omega_c} < \frac{\omega_{\max}}{\omega_c} \approx 2Z(L, B) \alpha B \quad \text{III-37a}$$

$$\left(\frac{\omega}{\omega_c}\right)_{\text{equator}} < \frac{\omega_{\max}^o}{\omega_c^o} \approx 2Z(L, B_o) \alpha B_o \approx 0.4 \alpha / L^2 \quad \text{III-37b}$$

$\omega_{\max}^o / \omega_c^o = 0.4 \alpha / L^2$ is plotted vs L in figure 6 under the assumption α is given by Table 1. This assumption will tend possibly to overestimate ω_{\max}^o by a factor of about two. Referring to Eq. II-41b, the anisotropy factor x is essentially given by $0.4 \alpha / L^2$, which is slightly less than the value $x \approx 0.4$ inferred from the arguments following Eq. III-28. Nonetheless, the two results are in reasonable agreement considering the approximations involved, showing that the result for $F_e(v_z)$ is reasonably model independent.

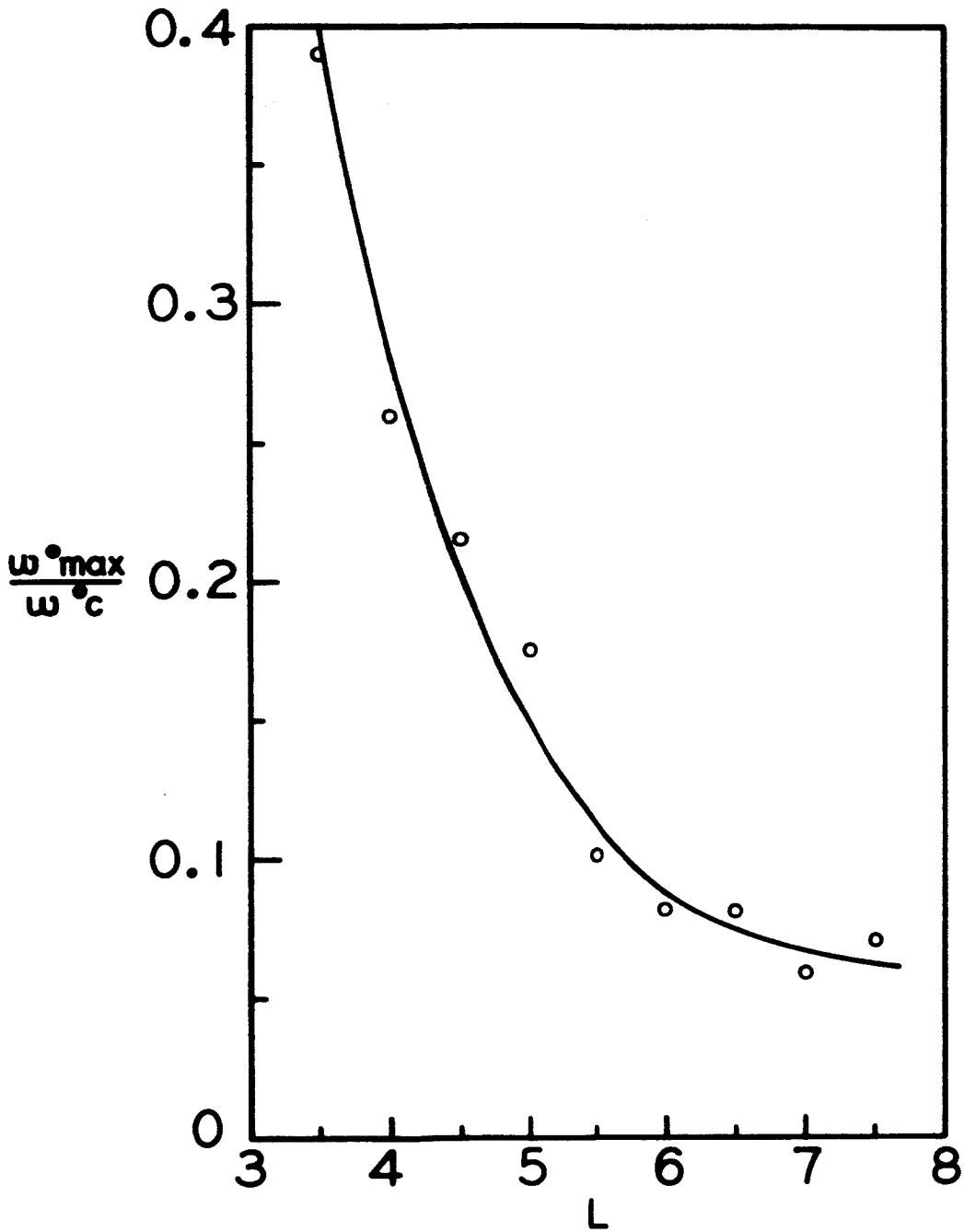


Figure 6. The L dependence of the maximum wave frequency for equatorial wave growth. The solid line represents a rough fit to the values calculated from Table 1 and goes roughly as $1/L^2$.

The imaginary wave number II-29 can now be written, using II-27, III-36 and III-37, as

$$k_i = \frac{1.6 \times 10^{-9} \pi^2 e^2}{m^2 c^4} J(E_o) E_o \frac{k_r}{|k_r|} \frac{\omega_p^2 \omega^2}{(\omega_c - \omega)^5} \left[1 - \frac{\omega_{\max}}{\omega} \right] \quad \text{III-38a}$$

$$= 5.41 \times 10^{-15} J(E_o) E_o \frac{k_r}{|k_r|} \frac{\omega_p^2}{\omega_c^3} \frac{\omega^2}{\omega_c^2} \frac{1}{(1 - \omega/\omega_c)^5} \left[1 - \frac{\omega_{\max}}{\omega_c} \frac{\omega_c}{\omega} \right] \quad \text{III-38b}$$

and the imaginary part of the frequency becomes

$$\omega_i = -3.25 \times 10^{-4} J(E_o) E_o \frac{\omega_p}{\omega_c^2} \left(\frac{\omega}{\omega_c} \right)^{\frac{5}{2}} \frac{1}{(1 - \omega/\omega_c)^{7/2}} \left[1 - \frac{\omega_{\max}}{\omega_c} \frac{\omega_c}{\omega} \right] \quad \text{III-39}$$

To obtain an estimate of these quantities we evaluate them at the magnetic equator by using $J(E_o) E_o = 4 \times 10^8 \text{ kev/cm}^2\text{-sec}$, $\omega_p^2 = (4\pi N_o e^2)/m = 4.5 \times 10^{13}/L^3$, and $\omega_c^o = 5.5 \times 10^6/L^3$. III-38 and III-39 then become

$$k_i = 5.9 \times 10^{-13} L^6 \frac{y_o^2}{(1 - y_o)^5} \left(1 - \frac{\omega_{\max}}{\omega_c^o} / y_o \right) \quad \text{III-40}$$

$$\omega_i = -2.9 \times 10^{-2} L^{\frac{9}{2}} \frac{y_o^{5/2}}{(1 - y_o)^{7/2}} \left(1 - \frac{\omega_{\max}}{\omega_c^o} / y_o \right) \quad \text{III-41}$$

where $y_o = \omega/\omega_c^o$. In figures 7 and 8, $-k_i/5.9 \times 10^{-13} L^6$ and $\omega_i/2.9 \times 10^{-2} L^{4.5}$, respectively, are plotted as functions of y_o for $y_o < \omega_{\max}/\omega_c^o$ for various representative values of ω_{\max}/ω_c^o . Also plotted as dashed lines are the functions $y_o(\omega_{\max}/\omega_c^o)$ and $y_o^{3/2}(\omega_{\max}/\omega_c^o)$, which are the asymptotic limits which k_i and ω_i respectively approach as $y_o \rightarrow 0$. For frequencies $y_o > \omega_{\max}/\omega_c^o$, both k_i and ω_i show very strong damping because of their inverse dependence on $(1 - y_o)$.

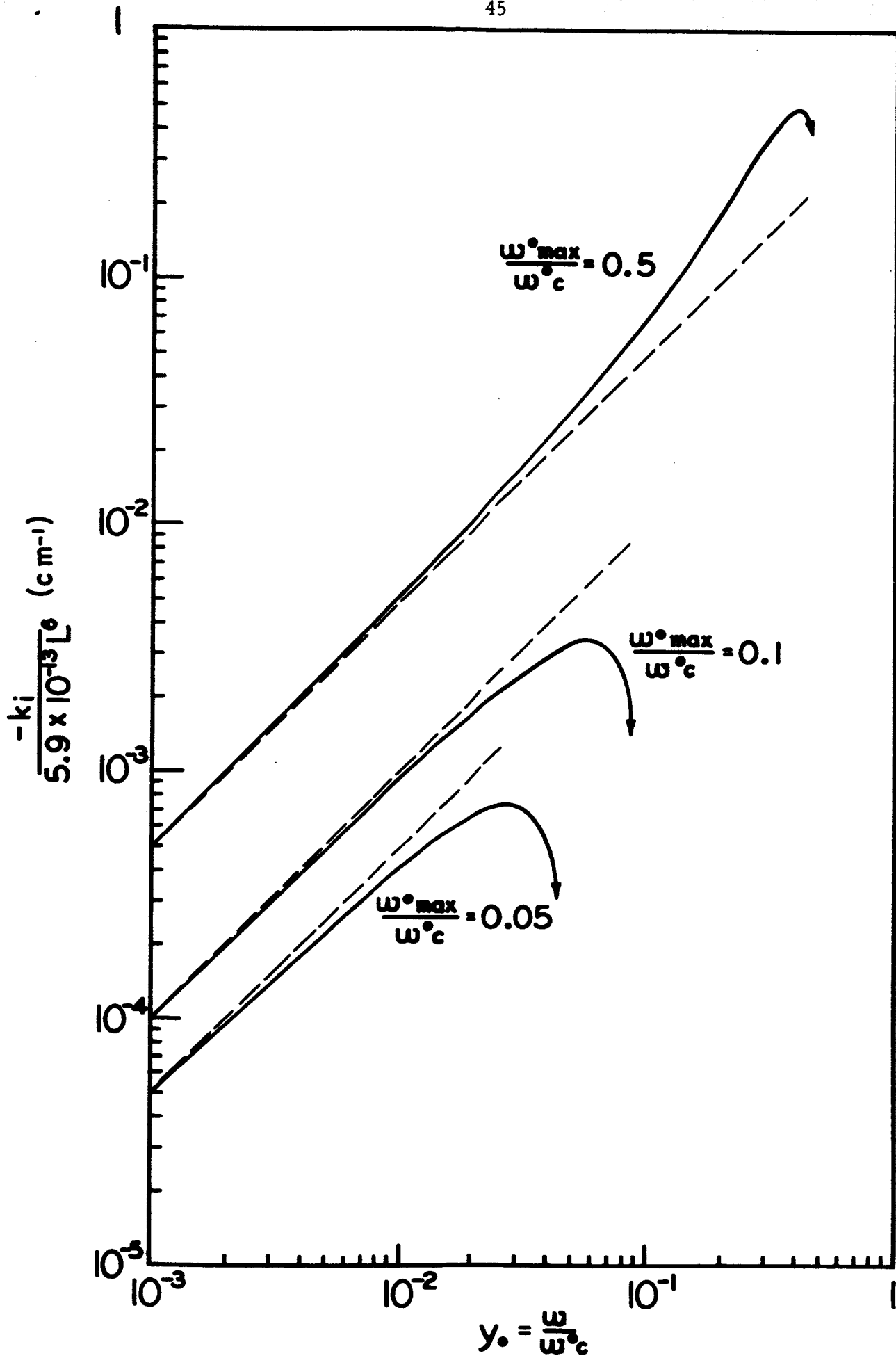


Figure 7. The imaginary part of the complex wave number plotted as a function of the wave frequency.

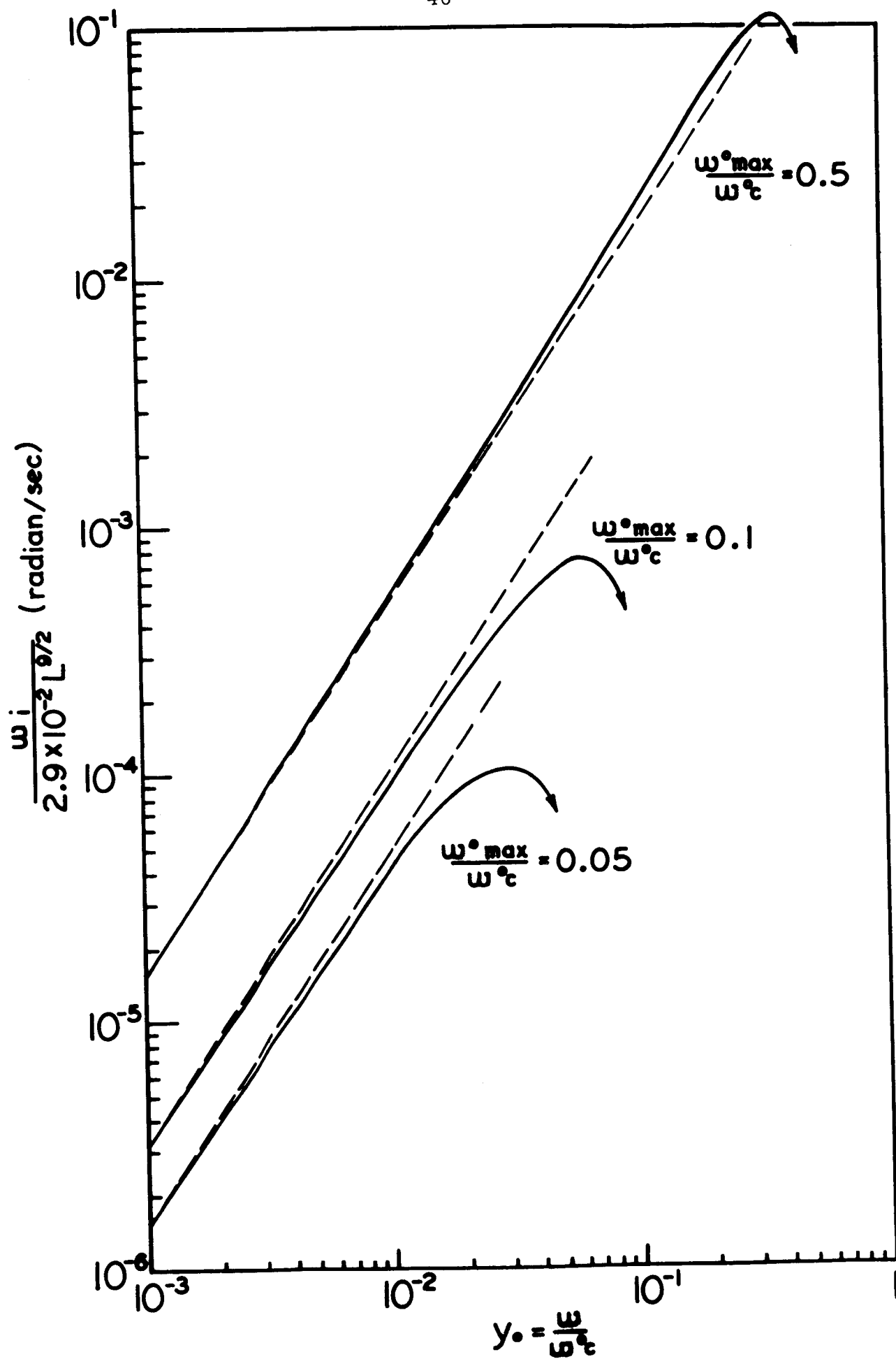


Figure 8. The imaginary part of the complex wave frequency plotted as a function of the real part of the wave frequency.

Using II-27, the velocity of the gyroresonant particles can be expressed as

$$\begin{aligned}
 v_z^2 &= \frac{(\omega_c - \omega)^2}{k^2} c^2 \\
 &= \frac{(\omega_c - \omega)^3}{\omega_p^2 \omega} c^2 \\
 &= (\omega_c / \omega) (1 - \omega / \omega_c)^3 (\omega_c^2 / \omega_p^2) c^2
 \end{aligned}
 \tag{III-42}$$

and their parallel energy E_z^0 at the equator as

$$E_z^0 = \frac{1.70 \times 10^2}{L^3} (\omega_c^0 / \omega) (1 - \omega / \omega_c^0)^3 \text{ kev}
 \tag{III-43}$$

In figure 9, the resonant energy E_z^0 is plotted vs. $y_0 = \omega / \omega_c^0$ for L values of 4, 6 and 8. Also plotted is the energy $E_{z \min}^0$, the equatorial gyroresonant particle energy corresponding to $(\omega_{\max} / \omega_c^0)$ as given by III-37b and figure 6. Despite the strong dependence of E_z^0 on L and ω , $E_{z \min}^0$ is seen to be about 5 kev, relatively independent of L.

For E_z greater than 100 kev, relativistic corrections and effects become important, but these can be neglected in the energy range of 1 - 50 kev with which we shall be primarily concerned.

From figures 7 and 8, it is readily noted that the wave growth is largest at those frequencies just below the maximum allowed frequency for instability. That this should be so follows from III-43, which shows that the energies of the particles gyroresonating with the unstable electron cyclotron waves and therefore responsible for their growth are smallest at these high frequencies close to ω_{\max} . Since the electron velocity

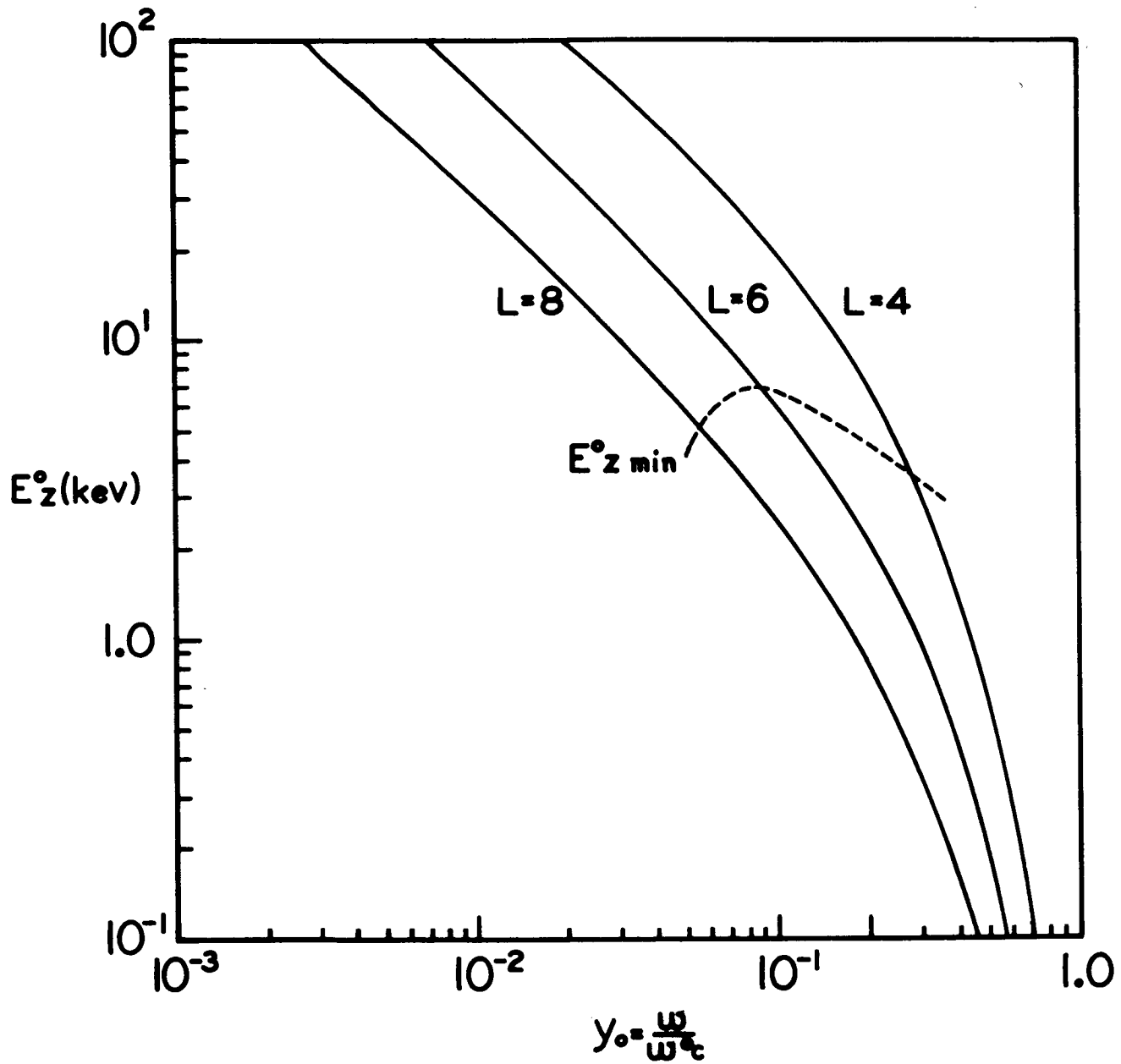


Figure 9. The frequency dependence of the gyroresonant particle energy at L values of 4, 6 and 8. $E_z^0 \text{ min}$ is the electron energy corresponding to $\omega^0 \text{ max}$ as given in Figure 6.

distribution has been assumed to be monotonically decreasing as a function of energy, this means that the number of particles available to gyroresonate with a given wave increases with decreasing gyroresonant energy and increasing wave frequency. The wave growth (or damping) is thus seen to be almost directly proportional to the number of available gyroresonant electrons.

In order to determine the growth or damping that a wave packet undergoes in travelling through the magnetosphere, we must consider the value of k_i for a fixed wave frequency ω that the wave encounters at each point of its path through the magnetosphere. The change in wave amplitude will then be given by

$$e^{-\int k_i(z) dz}$$

III-44

From the study of whistlers, electron cyclotron waves are known to be roughly channelled along magnetic field lines and reflected at some upper ionospheric level back into the magnetosphere with little amplitude loss. The integral in III-42 is therefore to be taken along a magnetic field line. Anticipating that the major contribution to $\int k_i(z) dz$ will come from the region about the magnetic equator, at which point ω/ω_c is largest and therefore the number of gyroresonant particles greatest, we will consider k_i to be of the form III-38b, neglect the logarithmic B dependence of $Z(L, B)$, and assume $\omega_p^2/\omega_c = 8.2 \times 10^6$, independent of L and the magnetic latitude along a given field line. We again take $J(E_0)E_0 = 4 \times 10^8 \text{ kev/cm}^2\text{-sec}$ and now consider ω_c as an explicit function of the magnetic latitude λ . It must also be noted that $\omega_{\text{max}}/\omega_c$ as given by III-37a is a function of B and hence of the magnetic latitude. ω_c is

well known as a function of λ to be given by

$$\omega_c = \omega_c^0 \frac{(1 + 3 \sin^2 \lambda)^{1/2}}{\cos^6 \lambda} \quad \text{III-45}$$

where ω_c^0 as before denotes the equatorial electron gyrofrequency, numerically equal to $(5.5 \times 10^6)/L^3$. k_i is then given by

$$k_i = 5.9 \times 10^{-13} L^6 \left(\frac{\cos^6 \lambda}{(1 + 3 \sin^2 \lambda)^{1/2}} \right)^2 \frac{y^2}{(1-y)^5} \left(1 - \frac{0.4a}{L^3 y} \frac{(1 + 3 \sin^2 \lambda)^{1/2}}{\cos^6 \lambda} \right) \quad \text{III-46}$$

where $y = \omega/\omega_c = \omega/\omega_c(\lambda)$.

In figure 10, k_i is plotted vs λ for $L = 6$ and $\omega/\omega_c^0 = .4a/L^2 = 0.082$, $\omega/\omega_c^0 = .05, .01$. In general, the major contribution to k_i comes from within 10° of the magnetic equator and so

$$\begin{aligned} \int k_i(z) dz &\approx \frac{2 \times 10^0}{180^\circ} \pi L R_e k_i(\lambda = 0^\circ) \approx \frac{L R_e}{3} k_i(\lambda = 0^\circ) \\ &= 1.3 \times 10^{-4} L^7 \frac{y_0^2}{(1-y_0)^5} \left[1 - \frac{0.4a}{L^2 y} \right] \quad \text{III-47} \end{aligned}$$

for each transit of an electron cyclotron wave between the magnetic poles.

The anomalous appearing behavior at $\omega/\omega_c^0 = .4a/L^3 = \omega_{\max}^0/\omega_c^0$ results simply from the fact that the growth rate for this wave component goes to zero at the equator and only as this wave moves away from the equator does its frequency drop below the local ω_{\max} .

Waves with frequencies greater than ω_{\max}^0 , though generated away from the equator, will be heavily damped when they pass through the equatorial plane. The equatorial damping will generally exceed the growth that occurs away from the equator, since the gyroresonant particles a given wave encounters at the equator are of lower energy and greater

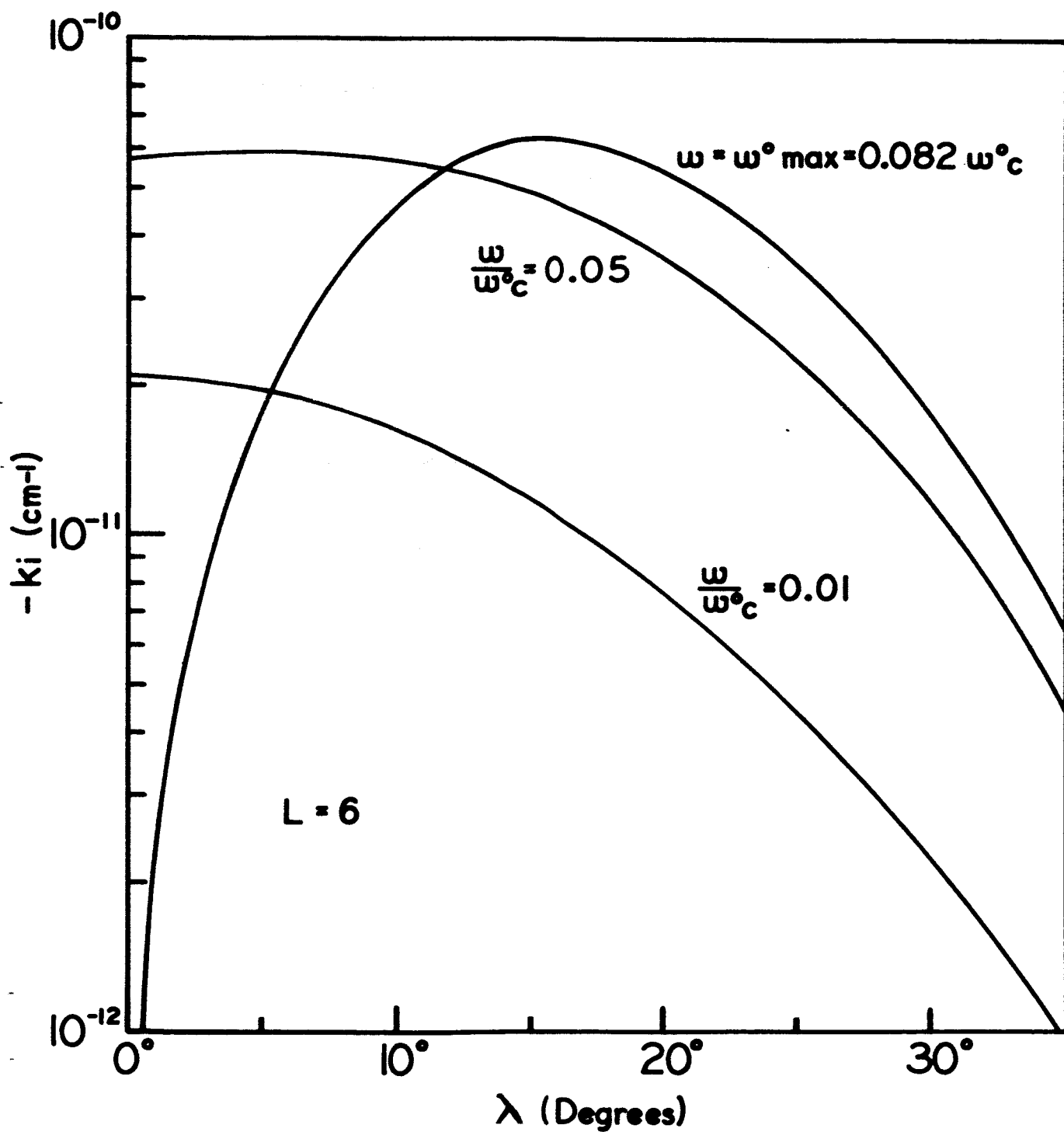


Figure 10. The geomagnetic latitude dependence of the imaginary part of the complex wave number for various values of the wave frequency and $L = 6$.

relative number density. In general, therefore, the maximum wave frequency that undergoes net growth on a given field line will be given by ω_{\max}^0 .

If rather than the form III-30 for $f'_0(v_z, v_\perp)$, we had used

$$f_0(v, \sin^2 \theta/B) = \frac{4(1.6 \times 10^{-9})^2}{\pi m^2} \frac{J(E_0)E_0^2}{N_0} e^{-aB/\sin^2 \theta} \left(\frac{B_{\max}}{B} \sin^2 \theta \right) \quad \text{III-48}$$

which corresponds to a spectral parameter $a = 2$ in III-2, such as would apply for energies greater than 40 keV and $L > 6$, the only basic change in the above relations other than factors of order unity would be an additional multiplicative factor $E_0/(mv_z^2/2) \propto k^2/(\omega_c - \omega)^2 \propto y/(1-y)^3$.

For a given $J(E_0)$ and a wave frequency such that the gyroresonant particle energy is E_0 , the results obtained from III-30 and III-48 will be within a factor of order unity.

Referring to figure 7, which gives the y dependence of III-47 for various assumed values of $\omega_{\max}^0/\omega_c^0$, it is readily estimated that the maximum value for $\int k_i(z)dz$ over the unstable wave spectrum is approximately 0.1, essentially independent of L , the L^7 factor being counterbalanced by the fact that $\omega_{\max}^0/\omega_c^0$ is largest for small L and so there are proportionately more gyroresonant particles able to enhance the wave growth at these larger allowed values for y_0 at small L . Just what the implications of this small but by no means negligible wave growth are will be spelled out in the next section.

In summary, we have used the available experimental information about the properties of energetic electron fluxes in the magnetosphere to

put together a reasonable and consistent model for the electron velocity distribution function. Using this model, we have solved for the properties of electron cyclotron wave growth resulting from the instability derived in Section II and have found this growth to be small but not negligible.

IV. ELECTROMAGNETIC TURBULENCE AND ELECTRON VELOCITY DIFFUSION

The net result of the fact that the electron velocity distribution in the magnetosphere is unstable with respect to the growth of electron cyclotron waves will be the setting up in the magnetosphere of a low level of electromagnetic turbulence. This turbulence, interacting with the electrons themselves which generated it, will act to diffuse the electrons in pitch angle until a marginally stable state is set up, namely one in which the further growth of the wave spectrum is exactly counterbalanced by the further diffusion in electron pitch angle which this turbulence would produce, so tending to destroy the anisotropy in electron velocity which was responsible for the original wave growth. Needless to say, it would be extremely difficult to solve for the exact spectrum of the wave turbulence. Kodomtsev and Petviashvili (1962) have developed a formalism which, by averaging over the statistical ensemble of fluctuating turbulent field states, is able to give a dispersion relation modified from that given in II-18 by including the effects of mode coupling and wave-particle diffusion. The solution of this non-linear equation, however, is extremely complex and beyond the scope of this paper. Nonetheless, one important result is derived which we will be able to use, namely that a weakly turbulent plasma can be represented by an ensemble of waves with magnetic field vectors which obey the equation

$$\sum_{\beta=1}^3 (k^2 \delta_{\alpha\beta} - \frac{\omega^2}{c^2} \tilde{\epsilon}_{\alpha\beta}(\omega, k) - k_{\alpha} k_{\beta}) B_{\alpha}(\omega, k) = 0 \quad \text{IV-1}$$

where α, β denote the three position-space vector components, $\tilde{\epsilon}(\omega, k)$ is

the modified dielectric tensor for the plasma, with the non-linear effects of mode coupling and particle diffusion included, and $\delta_{\alpha\beta}$ is the Kronecker delta.

In the case of the transverse electron cyclotron wave propagating along the zero order magnetic field direction, this equation can be simplified to the scalar relation

$$\left(k^2 - \frac{\omega^2}{c^2} \tilde{\epsilon}(\omega, k)\right) B(\omega, k) = 0 \quad \text{IV-2}$$

For the linear theory of Section II, the dielectric tensor $\epsilon(\omega, k)$ is given by

$$\epsilon(\omega, k) = 1 + \frac{\omega_p^2 \pi}{\omega^2 c^2} \int \frac{\left[(\omega - kv_z) \frac{\partial f_0}{\partial v_{\perp}} + kv_{\perp} \frac{\partial f_0}{\partial v_z} \right]}{\omega - kv_z - \omega_c} v_{\perp}^2 dv_{\perp} dv_z \quad \text{IV-3}$$

The turbulent electron cyclotron wave field, according to IV-2, can only exist for a given wave vector k at a frequency $\omega(k)$ determined by the solution of the dispersion relation

$$k^2 - \frac{\omega^2}{c^2} \tilde{\epsilon}(\omega, k) = 0 \quad \text{IV-4}$$

We shall assume that the plasma has attained marginal stability, so that the imaginary part of the dispersion relation IV-4 vanishes. The real part of the dispersion relation given by Eq. II-24 is seen to depend to first approximation only on the total electron density and so the non-linear terms in $\tilde{\epsilon}(\omega, k)$, which can to lowest order alter only the relative values of T_z and T_{\perp} , will affect primarily the imaginary part of the dispersion relation, which is the part responsible for wave growth and damping. Accordingly, ω will be closely approximated by the real part of the frequency $\omega(k)$ which is the solution to the dispersion relation II-18, which relation can be rewritten in terms of IV-3 as

$$k^2 - \frac{\omega^2}{c^2} \epsilon(\omega, \mathbf{k}) = 0$$

IV-5

In the following, we shall express the diffusion coefficients which represent the effects of this turbulent wave spectrum on the original electron velocity distribution in terms of the turbulent magnetic field autocorrelation function, $\langle B(\omega, \mathbf{k}) B^*(\omega', \mathbf{k}') \rangle$, which Kodomtsev and Petviashvili have shown can be written in the form

$$\langle B(\omega, \mathbf{k}) B^*(\omega', \mathbf{k}') \rangle = I(\mathbf{k}) \delta(\mathbf{k} - \mathbf{k}') \delta(\omega - \omega') \delta(\omega - \tilde{\omega})$$

IV-6

where the asterisk denotes the complex conjugate of a quantity, the brackets denote the average over the statistical ensemble of turbulent field states, $\tilde{\omega}$ is the root of the dispersion relation IV-4, closely approximated by the real part of the root of the dispersion relation IV-5, and $I(\mathbf{k})$ essentially gives the spectral shape of the turbulent wave spectrum.

Although the solution for $I(\mathbf{k})$ remains theoretically undetermined, we shall nonetheless in the following be able to make general arguments for its \mathbf{k} dependence and overall magnitude. These approximations will turn out to be sufficient for our present purposes, especially since the electron velocity distribution in the magnetosphere is both time dependent and not well enough known to warrant further accuracy in $I(\mathbf{k})$.

We now solve the force equation for the interaction of an individual electron with the turbulent wave field denoted by its electric and magnetic field vectors $\underline{E}(\underline{r}, t)$ and $\underline{B}(\underline{r}, t)$, respectively, assumed transverse to and travelling along the zero order magnetic field. The force equations are

$$\frac{dv_x}{dt} = -\frac{e}{m} \frac{v_y}{c} B_0 + \frac{e}{m} \frac{v_z}{c} B_y(\underline{r}, t) - \frac{e}{m} E_x(\underline{r}, t) \quad \text{IV-7a}$$

$$\frac{dv_y}{dt} = \frac{e}{m} \frac{v_x}{c} B_0 - \frac{e}{m} \frac{v_z}{c} B_x(\underline{r}, t) - \frac{e}{m} E_y(\underline{r}, t) \quad \text{IV-7b}$$

$$\frac{dv_z}{dt} = -\frac{e}{m} \frac{v_x}{c} B_y(\underline{r}, t) + \frac{e}{m} \frac{v_y}{c} B_x(\underline{r}, t) \quad \text{IV-7c}$$

where B_0 is the zero order magnitude field, assumed constant and in the z direction. To facilitate a solution, we define the quantities

$$v_x = A e^{i\omega_c t} + A^* e^{-i\omega_c t} = V(t) \cos(\omega_c t + \alpha(t)) \quad \text{IV-8a}$$

$$v_y = -i(A e^{i\omega_c t} - A^* e^{-i\omega_c t}) = V(t) \sin(\omega_c t + \alpha(t)) \quad \text{IV-8b}$$

$$A = V(t) / 2 e^{i\alpha(t)} \quad \text{IV-8c}$$

$$B_{\pm}(\underline{r}, t) = B_x(\underline{r}, t) \pm i B_y(\underline{r}, t), \quad B_-(\underline{r}, t) = B_+^*(\underline{r}, t) \quad \text{IV-8d}$$

$$E_{\pm}(\underline{r}, t) = E_x(\underline{r}, t) \pm i E_y(\underline{r}, t), \quad E_-(\underline{r}, t) = E_+^*(\underline{r}, t) \quad \text{IV-8e}$$

$$v_{\pm} = v_x \pm i v_y = V(t) e^{\pm i(\omega_c t + \alpha(t))} \quad \text{IV-8f}$$

Equations IV-7a-c then become

$$\frac{dV}{dt} \cos(\omega_c t + \alpha) - \frac{d\alpha}{dt} V \sin(\omega_c t + \alpha) = -\omega_c V \sin(\omega_c t + \alpha) + \frac{ev_z}{mc} B_y(\underline{r}, t) - \frac{e}{m} E_x(\underline{r}, t) \quad \text{IV-9a}$$

$$\frac{dV}{dt} \sin(\omega_c t + \alpha) + \frac{d\alpha}{dt} V \cos(\omega_c t + \alpha) = \omega_c V \cos(\omega_c t + \alpha) - \frac{ev_z}{mc} B_x(\underline{r}, t) - \frac{e}{m} E_y(\underline{r}, t) \quad \text{IV-9b}$$

$$\frac{dv_z}{dt} = -\frac{ie}{2mc} \left[v_+ B_- (\underline{r}, t) - v_- B_+ (\underline{r}, t) \right] \quad \text{IV-9c}$$

Equations IV-9a and b can be solved for V and α to obtain

$$\begin{aligned} \frac{dV}{dt} = & -\frac{iev_z}{2mc} \left[B_+ (\underline{r}, t) e^{-i(\omega_c t + \alpha)} - B_- (\underline{r}, t) e^{i(\omega_c t + \alpha)} \right] \\ & - \frac{e}{2m} \left[E_+ (\underline{r}, t) e^{-i(\omega_c t + \alpha)} + E_- (\underline{r}, t) e^{i(\omega_c t + \alpha)} \right] \end{aligned} \quad \text{IV-10a}$$

$$\begin{aligned} V \frac{d\alpha}{dt} = & -\frac{ev_z}{2mc} \left[B_+ (\underline{r}, t) e^{-i(\omega_c t + \alpha)} + B_- (\underline{r}, t) e^{i(\omega_c t + \alpha)} \right] \\ & + \frac{ie}{2m} \left[E_+ (\underline{r}, t) e^{-i(\omega_c t + \alpha)} - E_- (\underline{r}, t) e^{i(\omega_c t + \alpha)} \right] \end{aligned} \quad \text{IV-10b}$$

If $B_{\pm}(\underline{r}, t)$ and $E_{\pm}(\underline{r}, t)$ are neglected in IV-9c, IV-10a and b, these equations then show v_z , V and α all to be constant, which simply describes a particle travelling in a helical path about the zero order magnetic field. Since the ensemble averages or mean values of $E_{\pm}(\underline{r}, t)$ and $B_{\pm}(\underline{r}, t)$ are zero for a turbulent fluctuation field, the lowest order dependence of v_z , V and α on the turbulent wave field will involve terms going as the square of these fields. This essentially means that the first order solution to Eqs. IV-9c, IV-10a and b vanishes and so these equations must be solved to second order in the wave fields.

These equations can be formally solved by performing the integration over time. It must be remembered, however, that this integration is to be carried out over the as yet undetermined trajectory of the electrons,

which in general will involve non-linear terms. In zero order, however, the trajectory is given by $z = z_0 + V_{z_0}(t-t_0)$, where z_0 is the position of the particle at some reference time t_0 and V_{z_0} is its unperturbed original velocity in the z direction. In this approximation, which shall fortunately prove to be sufficient for our purposes, the equations for V , v_z and a then become

$$\begin{aligned}
 V = V_0 - \frac{ie}{2mc} \int_{t_0}^t dt v_z(z_0 + V_{z_0}(t-t_0), t) & \left[B_+(z_0 + V_{z_0}(t-t_0), t) e^{-i(\omega_c t + a)} \right. \\
 - B_-(z_0 + V_{z_0}(t-t_0), t) e^{i(\omega_c t + a)} & \left. \right] - \frac{e}{2m} \int_{t_0}^t dt \left[E_+(z_0 + V_{z_0}(t-t_0), t) e^{-i(\omega_c t + a)} \right. \\
 + E_-(z_0 + V_{z_0}(t-t_0), t) e^{i(\omega_c t + a)} & \left. \right]
 \end{aligned} \tag{IV-11a}$$

$$\begin{aligned}
 a = a_0 - \frac{e}{2mcV_0} \int_{t_0}^t dt v_z \left[B_+ e^{-i(\omega_c t + a)} + B_- e^{i(\omega_c t + a)} \right] \\
 + \frac{ie}{2mV_0} \int_{t_0}^t dt \left[E_+ e^{-i(\omega_c t + a)} - E_- e^{i(\omega_c t + a)} \right]
 \end{aligned} \tag{IV-11b}$$

$$v_z = V_{z_0} - \frac{ie}{2mc} \int_{t_0}^t dt \left[v_+ B_- - v_- B_+ \right] \tag{IV-11c}$$

Using IV-11a and b and neglecting terms of higher order than the square of the fluctuation fields, the equation for v_z becomes

$$\begin{aligned}
v_z = & V_{z_0} - \frac{ieV_{z_0}}{2mc} \int_{t_0}^t dt_1 B_-(t_1) e^{i(\omega_c t_1 + a_0)} \left[1 - \frac{ieV_{z_0}}{2mcV_0} \int_{t_0}^{t_1} dt_2 B_+(t_2) e^{-i(\omega_c t_2 + a_0)} \right. \\
& - \frac{e}{2mV_0} \int_{t_0}^{t_1} dt_2 E_+(t_2) e^{-i(\omega_c t_2 + a_0)} \left. \right] - \frac{e^2 V_{z_0}}{4m^2 c^2} \int_{t_0}^t dt_1 B_-(t_1) \int_{t_0}^{t_1} dt_2 B_+(t_2) e^{i\omega_c(t_1 - t_2)} \\
& + \frac{ie^2}{4m^2 c^2} \int_{t_0}^t dt_1 B_-(t_1) \int_{t_0}^{t_1} dt_2 E_+(t_2) e^{i\omega_c(t_1 - t_2)} + \{ \text{complex conjugate} \} \quad \text{IV-12}
\end{aligned}$$

We have simplified Eq. IV-12 by anticipating, as shall soon be proven, that the correlations $\langle B_{\pm} B_{\pm} \rangle$, $\langle E_{\pm} E_{\pm} \rangle$ and $\langle B_{\pm} E_{\pm} \rangle$ vanish.

The diffusion coefficient $\langle\langle v_z \rangle\rangle$ is defined to be the change in v_z per unit time interval Δt averaged over the statistical ensemble of turbulent field states. Since $\langle B_- \rangle = \langle B_+ \rangle = 0$, we can write for $\langle\langle v_z \rangle\rangle$

$$\begin{aligned}
\langle\langle v_z \rangle\rangle = & - \frac{2e^2 V_{z_0}}{4m^2 c^2} \frac{1}{\Delta t} \int_{t_0}^{t_0 + \Delta t} dt_1 \int_{t_0}^{t_1} dt_2 \langle B_-(t_1) B_+(t_2) \rangle e^{i\omega_c(t_1 - t_2)} \\
& + \frac{2ie^2 V_{z_0}}{4m^2 c^2} \frac{1}{\Delta t} \int_{t_0}^{t_0 + \Delta t} dt_1 \int_{t_0}^{t_1} dt_2 \langle B_-(t_1) E_+(t_2) \rangle e^{i\omega_c(t_1 - t_2)} \\
& + \{ \text{complex conjugate} \} \quad \text{IV-13}
\end{aligned}$$

Integrals of the form

$$\frac{1}{\Delta t} \int_{t_0}^{t_0+\Delta t} dt_1 \int_{t_0}^{t_1} dt_2 \langle B_-(z_0 + V_{z_0}(t_1 - t_0), t_1) B_+(z_0 + V_{z_0}(t_2 - t_0), t_2) \rangle e^{i\omega_c(t_1 - t_2)} \quad \text{IV-14}$$

shall be encountered in solving for all the diffusion coefficients, so we shall consider it below in great detail. We first transform it into the form

$$\frac{1}{\Delta t} \int_0^{\Delta t} dt_1 \int_0^{t_1} dt_2 \langle B_-(z_0 + V_{z_0} t_1, t_0 + t_1) B_+(z_0 + V_{z_0} t_2, t_0 + t_2) \rangle e^{i\omega_c(t_1 - t_2)} \quad \text{IV-15}$$

Correlations between B_- and B_+ will only exist for a time τ_c on the order of an electron gyroperiod. Δt is taken to be greater than this correlation time, so that if as in figure 11a the region of integration of IV-15 is shown in the (t_1, t_2) plane, contributions to the integral will only occur over the crosshatched region. If the limit on the t_2 integration were extended to Δt , then the region of integration would become the crosshatched region in figure 11b, and the value of the integral would be twice that of figure 11a. We shall henceforth deal with this symmetric integral which, by introducing the variable $\tau = t_1 - t_2$, can be transformed into the form

$$\begin{aligned} & \frac{1}{\Delta t} \int_0^{\Delta t} dt_1 \int_0^{\Delta t} dt_2 \langle B_-(z_0 + V_{z_0} t_1, t_0 + t_1) B_+(z_0 + V_{z_0} t_2, t_0 + t_2) \rangle e^{i\omega_c(t_1 - t_2)} \\ &= \frac{1}{\Delta t} \int_0^{\Delta t} dt_1 \int_{-\infty}^{\infty} d\tau \langle B_-(z_0 + V_{z_0} t_1, t_0 + t_1) B_+(z_0 + V_{z_0}(t_1 + \tau), t_0 + t_1 + \tau) \rangle e^{i\omega_c \tau} \quad \text{IV-16} \end{aligned}$$

Since, as shown in figure 11c, the major contribution to the τ integral comes from a region within $\tau_c \ll \Delta t$ of $\tau = 0$ and so is independent of the

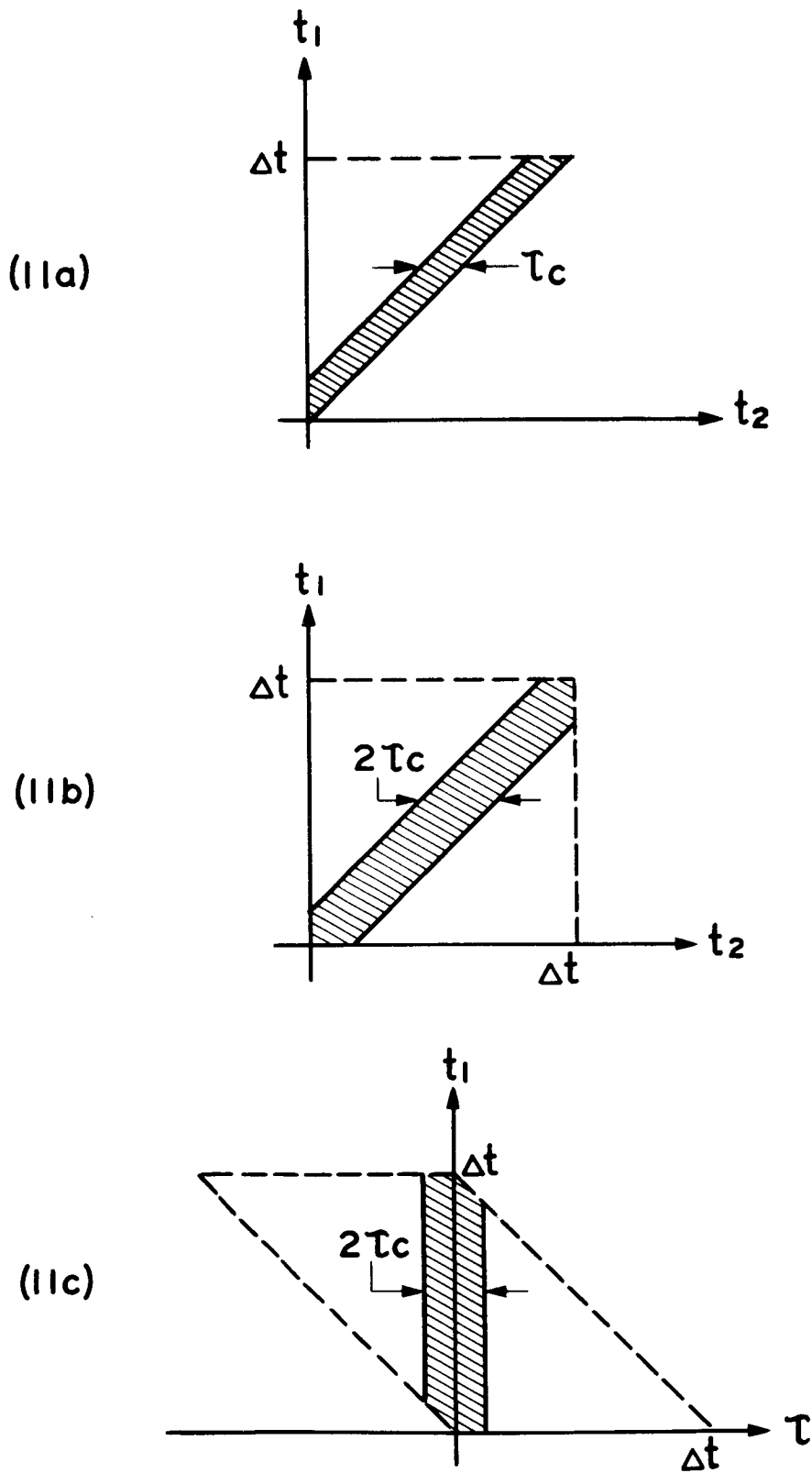


Figure 11. Regions of integration for the autocorrelation integral, Eq. IV-14.

limits on τ , we can for convenience consider these limits to be at $\pm\infty$.

Under the assumption of temporal and spatial uniformity for the turbulence field, the value of the autocorrelation function is independent of t_1 , and so the t_1 integration can be trivially performed and will just cancel the $1/\Delta t$ factor in front of the integral. The diffusion coefficient $\langle\langle v_z \rangle\rangle$ then becomes

$$\begin{aligned} \langle\langle v_z \rangle\rangle = & -\frac{e^2 V_{z_0}}{2m^2 c^2} \int_{-\infty}^{\infty} d\tau \langle B_-(z'_0, t'_0) B_+(z'_0 + V_{z_0} \tau, t'_0 + \tau) \rangle e^{i\omega_c \tau} \\ & + \frac{ie^2}{2m^2 c} \int_{-\infty}^{\infty} d\tau \langle B_-(z'_0, t'_0) E_+(z'_0 + V_{z_0} \tau, t'_0 + \tau) \rangle e^{i\omega_c \tau} \end{aligned} \quad \text{IV-17}$$

If we consider the Fourier transform of the wave field in space and time, then

$$\begin{aligned} & \langle B_-(z'_0, t'_0) B_+(z'_0 + V_{z_0} \tau, t'_0 + \tau) \rangle = \\ & = \int \frac{dkd\omega}{(2\pi)^2} e^{ikz'_0 - i\omega t'_0} \int \frac{dk'd\omega'}{(2\pi)^2} e^{-ik'(z'_0 + V_{z_0} \tau) + i\omega'(t'_0 + \tau)} \langle B_-(\omega, k) B_+(\omega', k') \rangle \\ & = \int \frac{dkdk'd\omega d\omega'}{(2\pi)^4} \langle B_-(\omega, k) B_+(\omega', k') \rangle e^{i(k-k')z'_0 - i(\omega-\omega')t'_0 - ikV_{z_0} \tau + i\omega' \tau} \end{aligned} \quad \text{IV-18}$$

We can now again take advantage of the assumed spatial and temporal uniformity of the autocorrelation and average $\langle B_- B_+ \rangle$ over t'_0 and z'_0 to obtain

$$\begin{aligned}
V = V_0 - \frac{ie}{2mc} \int_{t_0}^t dt_1 B_+(t_1) e^{-i(\omega_c t_1 + a_0)} & \left[V_{z_0} \left(1 + \frac{ieV_{z_0}}{2mcV_0} \int_{t_0}^{t_1} dt_2 B_-(t_2) e^{i(\omega_c t_2 + a_0)} \right) \right. \\
& - \frac{e}{2mV_0} \int_{t_0}^{t_1} dt_2 E_-(t_2) e^{i(\omega_c t_2 + a_0)} - \frac{ieV_0}{2mc} \int_{t_0}^{t_1} dt_2 B_-(t_2) e^{i(\omega_c t_2 + a_0)} \left. \right] \\
& - \frac{e}{2m} \int_{t_0}^t dt_1 E_+(t_1) e^{-i(\omega_c t_1 + a_0)} \left[1 + \frac{ieV_{z_0}}{2mcV_0} \int_{t_0}^{t_1} dt_2 B_-(t_2) e^{i(\omega_c t_2 + a_0)} \right. \\
& \left. - \frac{e}{2mV_0} \int_{t_0}^{t_1} dt_2 E_-(t_2) e^{i(\omega_c t_2 + a_0)} \right] \\
& + \{ \text{complex conjugate} \}
\end{aligned}$$

IV-22

It then follows that to lowest order

$$\begin{aligned}
\langle\langle V \rangle\rangle = & -\frac{e^2 V_0}{4m^2 c^2} \left(1 - \frac{V_{z_0}^2}{V_0^2} \right) \int_{t_0}^{t_0 + \Delta t} dt_1 \int_{t_0}^{t_1} dt_2 \langle B_+(t_1) B_-(t_2) \rangle e^{-i\omega_c(t_1 - t_2)} \\
& + \frac{2ie^2}{4m^2 c} \frac{V_{z_0}}{V_0} \int_{t_0}^{t_0 + \Delta t} dt_1 \int_{t_0}^{t_1} dt_2 \langle B_+(t_1) E_-(t_2) \rangle e^{-i\omega_c(t_1 - t_2)} \\
& + \frac{e^2}{4m^2 V_0} \int_{t_0}^{t_0 + \Delta t} dt_1 \int_{t_0}^{t_1} dt_2 \langle E_+(t_1) E_-(t_2) \rangle e^{-i\omega_c(t_1 - t_2)} \\
& + \{ \text{complex conjugate} \}
\end{aligned}$$

$$\begin{aligned}
&= -\frac{e^2 V_o}{4m^2 c^2} \left(1 - \frac{V_{z_o}^2}{V_o^2}\right) \frac{1}{ZT} \int \frac{dkd\omega}{(2\pi)} \langle B_-(\omega, k) B_+(\omega, k) \rangle \delta(\omega_c - \omega + kV_{z_o}) \\
&+ \frac{ie^2}{2m^2 c} \frac{V_{z_o}}{V_o} \frac{1}{ZT} \int \frac{dkd\omega}{(2\pi)} \langle B_+(\omega, k) E_-(\omega, k) \rangle \delta(\omega_c - \omega + kV_{z_o}) \\
&+ \frac{e^2}{4m^2 V_o} \frac{1}{ZT} \int \frac{dkd\omega}{(2\pi)} \langle E_-(\omega, k) E_+(\omega, k) \rangle \delta(\omega_c - \omega + kV_{z_o}) \tag{IV-23}
\end{aligned}$$

For the diffusion coefficient $\langle\langle V^2 \rangle\rangle$ for V^2 , it follows from Eq. IV-22

that

$$\begin{aligned}
\langle\langle V^2 \rangle\rangle &= \frac{e^2 V_{z_o}^2}{4m^2 c^2} \int_0^{\Delta t} dt_1 \int_0^{\Delta t} dt_2 \langle B_+(t_1) B_-(t_2) \rangle e^{-i\omega_c(t_1-t_2)} \\
&+ \frac{e^2}{4m^2} \int_0^{\Delta t} dt_1 \int_0^{\Delta t} dt_2 \langle E_+(t_1) E_-(t_2) \rangle e^{-i\omega_c(t_1-t_2)} \\
&+ \frac{2ie^2}{4m^2 c} \int_0^{\Delta t} dt_1 \int_0^{\Delta t} dt_2 \langle B_+(t_1) E_-(t_2) \rangle e^{-i\omega_c(t_1-t_2)} \\
&\quad + \{ \text{complex conjugate} \} \\
&= \frac{e^2 V_{z_o}^2}{2m^2 c^2} \frac{1}{ZT} \int \frac{dkd\omega}{(2\pi)} \langle B_-(\omega, k) B_+(\omega, k) \rangle \delta(\omega_c - \omega + kV_{z_o}) \\
&+ \frac{e^2}{2m^2} \frac{1}{ZT} \int \frac{dkd\omega}{(2\pi)} \langle E_-(\omega, k) E_+(\omega, k) \rangle \delta(\omega_c - \omega + kV_{z_o}) \\
&+ \frac{ie^2}{m^2 c} \frac{1}{ZT} \int \frac{dkd\omega}{(2\pi)} \langle B_+(\omega, k) E_-(\omega, k) \rangle \delta(\omega_c - \omega + kV_{z_o}) \tag{IV-24}
\end{aligned}$$

Lastly, the diffusion coefficient $\langle\langle v_z V \rangle\rangle$ is given by

$$\begin{aligned}
\langle\langle v_z V \rangle\rangle &= -\frac{e^2 V_o V_{z_o}}{4m^2 c^2} \int_0^{\Delta t} dt_1 \int_0^{\Delta t} dt_2 \langle B_+(t_1) B_-(t_2) \rangle e^{-i\omega_c(t_1-t_2)} \\
&+ \frac{ie^2 V_o}{4m^2 c} \int_0^{\Delta t} dt_1 \int_0^{\Delta t} dt_2 \langle B_-(t_1) E_+(t_2) \rangle e^{-i\omega_c(t_1-t_2)} \\
&+ \{ \text{complex conjugate} \} \\
&= -\frac{e^2 V_o V_{z_o}}{2m^2 c^2} \frac{1}{ZT} \int \frac{dkd\omega}{(2\pi)} \langle B_-(\omega, k) B_+(\omega, k) \rangle \delta(\omega_c - \omega + kV_{z_o}) \\
&+ \frac{ie^2 V_o}{2m^2 c} \frac{1}{ZT} \int \frac{dkd\omega}{(2\pi)} \langle B_-(\omega, k) E_+(\omega, k) \rangle \delta(\omega_c - \omega + kV_{z_o})
\end{aligned} \tag{IV-25}$$

The correlation terms involving $\langle B_{\pm}(t_1) B_{\pm}(t_2) \rangle$, $\langle E_{\pm}(t_1) E_{\pm}(t_2) \rangle$ and $\langle B_{\pm}(t_1) E_{\pm}(t_2) \rangle$ can be easily shown to be zero, since for terms as these the t_1 integration in IV-16 involves an additional factor $e^{\pm 2i\omega_c t_1}$.

The t_1 integration then becomes

$$\begin{aligned}
\frac{1}{\Delta t} \int_0^{\Delta t} dt_1 e^{\pm 2i\omega_c t_1} &= \pm \frac{1}{2i\omega_c} \left[\frac{e^{2i\omega_c \Delta t} - 1}{\Delta t} \right] \\
&= \pm \frac{e^{i\omega_c \Delta t} \sin \omega_c \Delta t}{\omega_c \Delta t}
\end{aligned} \tag{IV-26}$$

and this averages to zero for $\Delta t \gg \omega_c^{-1} \approx \tau_c$.

From Maxwell's equation II-2 it follows that

$$E_{\pm}(\omega, k) = \mp \frac{i\omega}{kc} B_{\pm}(\omega, k) \tag{IV-27}$$

Correlations involving $E_{\pm}(\omega, k)$ will therefore involve terms as

$$\int \frac{dkd\omega}{(2\pi)} \langle B_{\mp}(\omega, k) E_{\pm}(\omega, k) \rangle \delta(\omega_c - \omega + kV_{z_0})$$

$$= \mp i \int \frac{dkd\omega}{(2\pi)} \frac{\omega}{kc} \langle B_{-}(\omega, k) B_{+}(\omega, k) \rangle \delta(\omega_c - \omega + kV_{z_0}) \quad \text{IV-28a}$$

$$\int \frac{dkd\omega}{(2\pi)} \langle E_{\mp}(\omega, k) E_{\pm}(\omega, k) \rangle \delta(\omega_c - \omega + kV_{z_0})$$

$$= \int \frac{dkd\omega}{(2\pi)} \left(\frac{\omega}{kc}\right)^2 \langle B_{-}(\omega, k) B_{+}(\omega, k) \rangle \delta(\omega_c - \omega + kV_{z_0}) \quad \text{IV-28b}$$

We may therefore summarize the diffusion coefficients in the form

$$\langle\langle v_z \rangle\rangle = \frac{-e^2}{2m^2 c^2} \frac{1}{ZT} \int \frac{dkd\omega}{(2\pi)} (V_{z_0} - \frac{\omega}{k}) \langle B_{-}(\omega, k) B_{+}(\omega, k) \rangle \delta(\omega_c - \omega + kV_{z_0}) \quad \text{IV-29a}$$

$$\langle\langle v_z^2 \rangle\rangle = \frac{e^2 V_0^2}{2m^2 c^2} \frac{1}{ZT} \int \frac{dkd\omega}{(2\pi)} \langle B_{-}(\omega, k) B_{+}(\omega, k) \rangle \delta(\omega_c - \omega + kV_{z_0}) \quad \text{IV-29b}$$

$$\langle\langle V \rangle\rangle = \frac{-e^2}{4m^2 c^2 V_0} \frac{1}{ZT} \int \frac{dkd\omega}{(2\pi)} [V_0^2 - (V_{z_0} - \omega/k)^2] \langle B_{-}(\omega, k) B_{+}(\omega, k) \rangle \delta(\omega_c - \omega + kV_{z_0}) \quad \text{IV-29c}$$

$$\langle\langle V^2 \rangle\rangle = \frac{e^2}{2m^2 c^2} \frac{1}{ZT} \int \frac{dkd\omega}{(2\pi)} (V_{z_0} - \frac{\omega}{k})^2 \langle B_{-}(\omega, k) B_{+}(\omega, k) \rangle \delta(\omega_c - \omega + kV_{z_0}) \quad \text{IV-29d}$$

$$\langle\langle v_z \rangle\rangle = \frac{-e^2 V_0}{2m^2 c^2} \frac{1}{ZT} \int \frac{dkd\omega}{(2\pi)} (V_{z_0} - \frac{\omega}{k})^2 \langle B_{-}(\omega, k) B_{+}(\omega, k) \rangle \delta(\omega_c - \omega + kV_{z_0}) \quad \text{IV-29e}$$

The diffusion coefficients reflect the fact that only the waves in gyroresonance with a given electron are able to affect its motion significantly when averaged over a period of time longer than an electron gyroperiod. This result is, of course, to be expected, since only changes that occur on the time scale of an electron gyroperiod ($\omega - kV_{z_0} = \omega_c$) are able to

interact coherently with a rotating electron and so are able to break down the adiabatic invariance of the electron's magnetic moment.

From the diffusion coefficients given in Eq. IV-29 we are able to calculate the diffusion coefficients for the electron energy and pitch angle. The energy of the electron is given by

$$E = \frac{1}{2} m (V(t)^2 + v_z(t)^2) \quad \text{IV-30}$$

so that the diffusion coefficient or change in this energy per unit time interval Δt averaged over the statistical ensemble of turbulent field states is given by

$$\begin{aligned} \langle\langle E \rangle\rangle &= \frac{m}{2} (2V_o \langle\langle V \rangle\rangle + \langle\langle V^2 \rangle\rangle + 2V_{z_o} \langle\langle v_z \rangle\rangle + \langle\langle v_z^2 \rangle\rangle) \\ &= \frac{e^2}{4mc^2} \frac{1}{ZT} \int \frac{dkd\omega}{(2\pi)} \left[-(V_o^2 - (V_{z_o} - \frac{\omega}{k})^2) + (V_{z_o} - \frac{\omega}{k})^2 \right. \\ &\quad \left. - 2V_{z_o} (V_{z_o} - \frac{\omega}{k}) + V_o^2 \right] \langle B_-(\omega, k) B_+(\omega, k) \rangle \delta(\omega_c - \omega + kV_{z_o}) \\ &= -\frac{e^2}{2mc^2} \frac{1}{ZT} \int \frac{dkd\omega}{(2\pi)} \frac{\omega}{k} (V_{z_o} - \frac{\omega}{k}) \langle B_-(\omega, k) B_+(\omega, k) \rangle \delta(\omega_c - \omega + kV_{z_o}) \quad \text{IV-31} \end{aligned}$$

or

$$\langle\langle E \rangle\rangle = m \langle\langle \frac{\omega}{k} v_z \rangle\rangle \quad \text{IV-32}$$

That this final relation should hold follows from the fact that in the frame of reference moving with the phase velocity of the wave, the wave has only a magnetic field and so in this frame the energy of the electron must be rigorously conserved. Therefore we may write

$$\frac{1}{2} m (V^2 + (v_z - \frac{\omega}{k})^2) = \text{constant} \quad \text{IV-33}$$

Equation IV-32 easily follows from Eq. IV-33 upon taking ensemble averages of the change in IV-33 per unit time.

The pitch angle θ is given by

$$\theta = \tan^{-1} \frac{V(t)}{v_z(t)} \quad \text{IV-34}$$

Upon taking ensemble averages of the change in θ per unit time it follows that

$$\begin{aligned} \langle\langle \theta \rangle\rangle &= \frac{1}{V_o^2 + V_{z_o}^2} (V_{z_o} \langle\langle V \rangle\rangle - V_o \langle\langle v_z \rangle\rangle) = \\ &= \frac{e^2}{4m^2 c^2 ZT} \int \frac{dkd\omega}{(2\pi)} \frac{[-V_{z_o} (V_o^2 - (V_{z_o} - \frac{\omega}{k})^2) + 2V_o^2 (V_{z_o} - \frac{\omega}{k})]}{V_o (V_o^2 + V_{z_o}^2)} \langle B_-(\omega, k) B_+(\omega, k) \rangle \delta(\omega_c - \omega + kV_{z_o}) \\ &= \frac{e^2}{4m^2 c^2 ZT} \int \frac{dkd\omega}{(2\pi)} \left[\frac{V_{z_o}}{V_o} - 2 \frac{\frac{\omega}{k}}{V_o} + \frac{(\frac{\omega}{k})^2 V_{z_o}}{(V_o^2 + V_{z_o}^2) V_o} \right] \langle B_-(\omega, k) B_+(\omega, k) \rangle \delta(\omega_c - \omega + kV_{z_o}) \quad \text{IV-35} \end{aligned}$$

The sense of $\langle\langle \theta \rangle\rangle$ is such as to increase the perpendicular electron velocity and decrease V_{z_o} .

For the diffusion coefficient of E^2 , the dominant terms (neglecting terms of higher order than the square of the turbulent field) are given by

$$\begin{aligned} \langle\langle E^2 \rangle\rangle &= \frac{m^2}{4} (4V_o^2 \langle\langle V^2 \rangle\rangle + 8 V_{z_o} V_o \langle\langle V v_z \rangle\rangle + 4V_{z_o}^2 \langle\langle v_z^2 \rangle\rangle) \\ &= \frac{e^2 V_o^2}{2c^2} \cdot \frac{1}{ZT} \int \frac{dkd\omega}{(2\pi)} \left[(V_{z_o} - \frac{\omega}{k})^2 - 2V_{z_o} (V_{z_o} - \frac{\omega}{k}) + V_{z_o}^2 \right] \\ &\quad \cdot \langle B_-(\omega, k) B_+(\omega, k) \rangle \delta(\omega_c - \omega + kV_{z_o}) \end{aligned}$$

$$\begin{aligned}
&= \frac{e^2 V_o^2}{2c^2} \cdot \frac{1}{ZT} \int \frac{dkd\omega}{(2\pi)} \frac{(\omega)^2}{k} \langle B_-(\omega, k) B_+(\omega, k) \rangle \delta(\omega_c - \omega + kV_{z_o}) \\
&= m \langle \langle \left(\frac{\omega}{k} v_z\right)^2 \rangle \rangle
\end{aligned}$$

IV-36

And finally, for the diffusion coefficient of θ^2 we obtain

$$\begin{aligned}
\langle \langle \theta^2 \rangle \rangle &= \frac{1}{(V_o^2 + V_{z_o}^2)^2} (V_{z_o}^2 \langle \langle V^2 \rangle \rangle - 2V_o V_{z_o} \langle \langle V v_z \rangle \rangle + V_o^2 \langle \langle v_z^2 \rangle \rangle) \\
&= \frac{e^2}{2m^2 c^2} \cdot \frac{1}{ZT} \int \frac{dkd\omega}{(2\pi)} \frac{\left[V_{z_o}^2 \left(V_{z_o} - \frac{\omega}{k} \right)^2 + 2V_o^2 V_{z_o} \left(V_{z_o} - \frac{\omega}{k} \right) + V_o^4 \right]}{(V_o^2 + V_{z_o}^2)^2} \\
&\quad \cdot \langle B_-(\omega, k) B_+(\omega, k) \rangle \delta(\omega_c - \omega + kV_{z_o}) \\
&= \frac{e^2}{2m^2 c^2} \cdot \frac{1}{ZT} \int \frac{dkd\omega}{(2\pi)} \frac{\left[(V_o^2 + V_{z_o}^2) \left(V_{z_o} - \frac{\omega}{k} \right) \right]^2}{(V_o^2 + V_{z_o}^2)^2} \\
&\quad \cdot \langle B_-(\omega, k) B_+(\omega, k) \rangle \delta(\omega_c - \omega + kV_{z_o})
\end{aligned}$$

IV-37

From the results of Section III we expect that the spectrum of electromagnetic turbulence in the magnetosphere will cut off at a maximum frequency on the order of $\omega_{\max} \approx 0.1\omega_c$. Thus it follows that

$$|V_{z_o}| = \left| \frac{\omega - \omega_c}{k} \right| \approx \left| \frac{\omega_c}{k} \right| \gg \left| \frac{\omega}{k} \right|$$

Using this inequality, the energy and pitch angle diffusion coefficients can be simplified by neglecting terms of order ω/k compared with V_{z_o} . The coefficients can then be conveniently approximated as

$$\frac{\langle \langle E \rangle \rangle}{E} \approx - \frac{e^2}{m^2 c^2} \frac{1}{ZT} \int \frac{dkd\omega}{(2\pi)} \frac{\omega V_{z_o}}{(V_o^2 + V_{z_o}^2)} \langle B_-(\omega, k) B_+(\omega, k) \rangle \delta(\omega_c - \omega + kV_{z_o}) \quad \text{IV-38a}$$

$$\frac{\langle\langle E^2 \rangle\rangle}{E^2} \approx \frac{2e^2}{m^2 c^2} \cdot \frac{1}{ZT} \int \frac{dkd\omega}{(2\pi)} \frac{(\frac{\omega}{k} V_o)^2}{(V_o^2 + V_{z_o}^2)^2} \langle B_-(\omega, k) B_+(\omega, k) \rangle \delta(\omega_c - \omega + k V_{z_o}) \quad \text{IV-38b}$$

$$\langle\langle \theta \rangle\rangle \approx \frac{e^2}{4m^2 c^2} \cdot \frac{1}{ZT} \frac{V_{z_o}}{V_o} \int \frac{dkd\omega}{(2\pi)} \langle B_-(\omega, k) B_+(\omega, k) \rangle \delta(\omega_c - \omega + k V_{z_o}) \quad \text{IV-38c}$$

$$\langle\langle \theta^2 \rangle\rangle \approx \frac{e^2}{2m^2 c^2} \cdot \frac{1}{ZT} \int \frac{dkd\omega}{(2\pi)} \langle B_-(\omega, k) B_+(\omega, k) \rangle \delta(\omega_c - \omega + k V_{z_o}) \quad \text{IV-38d}$$

In this form, the energy and pitch angle diffusion coefficients can be readily compared:

$$\frac{\langle\langle E \rangle\rangle}{E} \leq \frac{4(\frac{\omega}{k})}{V_{z_o}} \cdot \frac{V_o}{(V_o^2 + V_{z_o}^2)^{1/2}} < 1 \quad \text{IV-39a}$$

$$\frac{\langle\langle E^2 \rangle\rangle}{E^2} \leq \frac{4(\frac{\omega}{k})^2}{V_{z_o}^2} \cdot \frac{V_o^2}{(V_o^2 + V_{z_o}^2)} < 1 \quad \text{IV-39b}$$

Thus it follows that angular diffusion dominates over energy diffusion, especially for pitch angles near the loss cone ($V_{z_o} \gg V_o$). This fact can also readily be surmised from the Maxwell relation given in IV-27. The ($\underline{v} \times \underline{B}$) magnetic force on the electron can only change its pitch angle, and from IV-27 this force is ($V_{z_o} / (\omega/k)$) larger than the electric field term which is responsible for energy diffusion. Thus while some small amount of energy diffusion will result from the interaction of an electron with electromagnetic electron cyclotron turbulence, the major effect of the turbulence will be to diffuse the electron in pitch angle.

With this above assumption that energy diffusion times are much greater than angular diffusion times, an electron will pitch angle diffuse into the atmospheric loss cone before its energy has undergone any significant diffusive change. A Fokker-Planck type of equation can now be written for the diffusion of the electron pitch angle:

$$\frac{\partial [n(\theta, t) \sin \theta]}{\partial t} = - \frac{\partial}{\partial \theta} [n(\theta, t) \sin \theta \langle \langle \theta \rangle \rangle] + \frac{1}{2} \frac{\partial^2}{\partial \theta^2} [n(\theta, t) \sin \theta \langle \langle \theta \rangle \rangle] \quad \text{IV-40}$$

where $n(\theta, t)$ is the density of electrons at time t within unit solid angle of the pitch angle θ .

By making use of Eqs. IV-38c and d this equation can be written

$$\frac{\partial [n(\theta, t) \sin \theta]}{\partial t} = \frac{e^2}{4m^2 c^2 Z} \left[- \frac{\partial}{\partial \theta} [n(\theta, t) \cos \theta \Gamma(\theta)] + \frac{\partial^2}{\partial \theta^2} [n(\theta, t) \sin \theta \Gamma(\theta)] \right] \quad \text{IV-41}$$

where

$$\Gamma(\theta) = \frac{1}{ZT} \int \frac{dkd\omega}{(2\pi)} \langle B_-(\omega, k) B_+(\omega, k) \rangle \delta(\omega_c - \omega + kV_{z_0}) \quad \text{IV-42}$$

$$= \int_{-\infty}^{\infty} d\tau \langle B_-(z_0, t_0) B_+(z_0 + V_{z_0} \tau, t_0 + \tau) \rangle e^{i\omega_c \tau} \quad \text{IV-42}$$

contains the dependence of the diffusion coefficients on the magnetic field autocorrelation function. If use is now made of IV-6 this becomes

$$\Gamma(\theta) = \frac{dkd\omega}{(2\pi)^3} I(k) \delta(\omega - \omega(k)) \delta(\omega_c - \omega + kV_{z_0}) \quad \text{IV-43}$$

since the delta function $\delta(k - k')$ can be interpreted as

$$\lim_{k' \rightarrow k} \delta(k' - k) = \lim_{k' \rightarrow k} \frac{1}{2\pi} \int_{-Z/2}^{Z/2} e^{i(k' - k)z} dz = \frac{Z}{2\pi} \quad \text{IV-44}$$

and similarly for $\delta(\omega - \omega)$.

According to the arguments presented earlier, $\tilde{\omega}(k)$ is assumed to be closely approximated by II-27, so that

$$c^2 k^2 = \tilde{\omega}^2 + \frac{\omega_p^2 \tilde{\omega}}{\omega_c - \tilde{\omega}} \approx \frac{\omega_p^2 \tilde{\omega}}{\omega_c - \tilde{\omega}} \quad \text{IV-45}$$

It is reasonable to expect that the wave energy at a given wave number will be roughly proportional to the imaginary part of the wave number obtained in the linear theory. Wave diffusion of the electron pitch angle, however, will probably slightly reduce the degree of velocity anisotropy and so reduce the value of ω_{\max} predicted in Section III. Referring to Eq. III-40 and figure 7, reasonable assumptions for the form of $I(k)$ can now be made. Since $y \propto k^2$, a reasonable approximation is to take $I(k) \propto k^m$, with $m \approx 2$, for k less than a maximum value, k_{\max} , corresponding to ω_{\max} . For $k > k_{\max}$, $I(k)$ can be effectively considered to be zero, so that there is no turbulent wave energy for $k > k_{\max}$ or $\omega > \omega_{\max}$. $I(k)$ is thus assumed to have the simple form

$$\begin{aligned} I(k) &\propto |k|^m && (|k| < |k_{\max}|) \\ &= 0 && (|k| > |k_{\max}|) \end{aligned} \quad \text{IV-46}$$

where

$$k_{\max}^2 c^2 \approx \frac{\omega_p^2 \omega_{\max}}{\omega_c - \omega_{\max}} \quad \text{IV-47}$$

$\Gamma(\theta)$ then becomes

$$\begin{aligned} \Gamma(\theta) &\propto \int_{-|k_{\max}|}^{|k_{\max}|} \frac{dk}{(2\pi)^3} |k|^m \delta(\omega_c - \tilde{\omega}(k) + kV_{z_0}) \\ &= \int_{-|k_{\max}|}^{|k_{\max}|} \frac{dk}{(2\pi)^3} |k|^m \frac{\delta(k - k_0)}{\left| \frac{d(\tilde{\omega}(k) - kV_{z_0})}{dk} \right|_{k=k_0}} \end{aligned} \quad \text{IV-48}$$

From IV-45 it follows that

$$\tilde{\omega}(k) = \frac{k^2 c^2 \omega_c}{k^2 c^2 + \omega_p^2} = \omega_c \frac{k^2 c^2}{\omega_p^2} \cdot \frac{1}{1 + \frac{k^2 c^2}{\omega_p^2}} \approx \omega_c \frac{k^2 c^2}{\omega_p^2} \quad \text{IV-49a}$$

$$k_0 = -\frac{\omega_c}{V_{z_0}} \cdot \frac{1}{1 + k_0^2 \frac{c^2}{\omega_p^2}} \approx -\frac{\omega_c}{V_{z_0}} \quad \text{IV-49b}$$

$$\frac{d\tilde{\omega}}{dk} = \frac{2kc^2 \omega_c \omega_p^2}{(k^2 c^2 + \omega_p^2)^2} = \frac{2kc^2 \omega_c}{\omega_p^2} \cdot \frac{1}{(1 + k^2 \frac{c^2}{\omega_p^2})^2} \approx \frac{2kc^2 \omega_c}{\omega_p^2} \quad \text{IV-49c}$$

$$\begin{aligned} \left| \frac{d(\tilde{\omega}(k) - kV_{z_0})}{dk} \right|_{k=k_0} &= |V_{z_0}| \left(1 + \frac{2\omega_c^2 c^2}{V_{z_0}^2 \omega_p^2} \cdot \frac{1}{(1 + k_0^2 \frac{c^2}{\omega_p^2})^3} \right) \\ &\approx |V_{z_0}| \end{aligned} \quad \text{IV-49d}$$

so that, provided $\omega/\omega_c \ll 1$, $\Gamma(\theta)$ becomes

$$\begin{aligned} \Gamma(\theta) &\propto \frac{1}{(2\pi)^4} \cdot \left| \frac{\omega_c}{V_{z_0}} \right|^{m+1} \cdot \frac{2\pi}{\omega_c} \quad (|k_0| < |k_{\max}|) \\ &= 0 \quad (|k_0| > |k_{\max}|) \end{aligned} \quad \text{IV-50}$$

We now introduce the mean square electron cyclotron turbulence field
(compare Eq. IV-19)

$$\begin{aligned}
 \langle B^2 \rangle &= \overline{\langle B_-(z, t) B_+(z, t) \rangle} \\
 &= \frac{1}{ZT} \int \frac{dkd\omega}{(2\pi)^2} \langle B_-(\omega, k) B_+(\omega, k) \rangle \\
 &= \int \frac{dkd\omega}{(2\pi)^4} I(k) \delta(\omega - \tilde{\omega}(k)) \\
 &= \int_{-|k_{\max}|}^{|k_{\max}|} \frac{dk}{(2\pi)^4} I(k) \\
 &\propto \frac{1}{(2\pi)^4} \cdot \frac{2}{m+1} |k_{\max}|^{m+1}
 \end{aligned} \tag{IV-51}$$

In terms of this quantity, $\Gamma(\theta)$ can now be expressed as

$$\Gamma(\theta) = \langle B^2 \rangle \left| \frac{\omega_c}{k_{\max} V_{z_0}} \right|^{m+1} \cdot \frac{2\pi}{\omega_c} \cdot \frac{m+1}{2} \tag{IV-52}$$

Comparing this expression with Eq. IV-42, it is seen that the correlation time τ_c is indeed roughly equal to an electron gyroperiod as had been assumed earlier.

From III-42 and IV-47 it follows that

$$\left(\frac{\omega_c}{k_{\max} V_{z_0}} \right)^2 = \frac{\omega_c^2 c^2}{\omega_p^2 (V_o^2 + V_{z_0}^2)} \cdot \frac{(1 - y_{\max})}{y_{\max}} \cdot \frac{1}{\cos^2 \theta} \tag{IV-53}$$

$$\cos^2 \theta \Big|_{k_o = k_{\max}} = \frac{\omega_c^2 c^2}{\omega_p^2 (V_o^2 + V_{z_o}^2)} \cdot \frac{(1 - y_{\max})^3}{y_{\max}} \quad \text{IV-54}$$

where $y_{\max} = \omega_{\max} / \omega_c$. $\Gamma(\theta)$ then becomes

$$\begin{aligned} \Gamma(\theta) &= \langle B^2 \rangle \left[\frac{\omega_c^2 c^2}{\omega_p^2 (V_o^2 + V_{z_o}^2)} \cdot \frac{(1 - y_{\max})^3}{y_{\max}} \right]^{\frac{m+1}{2}} \cdot \frac{\pi(m+1)}{\omega_c} \cdot \frac{1}{\cos^{m+1} \theta} \\ &= \Gamma' \cdot \frac{1}{\cos^{m+1} \theta} \quad \left(\cos^2 \theta > \frac{\omega_c^2 c^2}{\omega_p^2 (V_o^2 + V_{z_o}^2)} \cdot \frac{(1 - y_{\max})^3}{y_{\max}} \right) \\ &= 0 \quad \left(\cos^2 \theta < \frac{\omega_c^2 c^2}{\omega_p^2 (V_o^2 + V_{z_o}^2)} \cdot \frac{(1 - y_{\max})^3}{y_{\max}} \right) \end{aligned} \quad \text{IV-55}$$

where

$$\Gamma' = \langle B^2 \rangle \left[\frac{\omega_c^2 c^2}{\omega_p^2 (V_o^2 + V_{z_o}^2)} \cdot \frac{(1 - y_{\max})^3}{y_{\max}} \right]^{\frac{m+1}{2}} \cdot \frac{\pi(m+1)}{\omega_c} \quad \text{IV-56}$$

From IV-54 it is seen that because of the cutoff of the wave spectrum at k_{\max} there will be no wave energy available to gyroresonate with an electron having an energy less than a minimum energy E_{\min} . This energy is given by (see also Eq. III-43)

$$E_{\min} = \frac{1}{2} mc^2 \cdot \frac{\omega_c^2}{\omega_p^2} \cdot \frac{(1 - y_{\max})^3}{y_{\max}} \quad \text{IV-57a}$$

which becomes, evaluated at the geomagnetic equator,

$$E_{\min}^o = \frac{170}{L^3} \cdot \frac{(1 - y_{\max}^o)^3}{y_{\max}^o} \quad \text{kev} \quad \text{IV-57b}$$

where $y_{\max}^0 = \omega_{\max}^0 / \omega_c^0$. For energies but slightly above this, there will be particle-wave gyroresonance only if the pitch angle of the particle is very near the loss cone ($\approx 0^\circ$ or 180°).

The form given above for $\Gamma(\theta)$ will break down for a number of reasons if $y_{\max} \geq 0.1$: a) the approximations made in IV-49 which greatly simplified the θ dependence of $\Gamma(\theta)$ would no longer hold; b) the energy diffusion terms would have to be reconsidered in the writing of a diffusion equation as IV-40 since they are typically of order ω/ω_c with respect to the angular diffusion terms. In addition, there will be less energy in the wave spectrum for $\omega_{\max}/2 < \omega < \omega_{\max}$ than that predicted by our model for $I(k)$ given in Eq. IV-46, which has a sharp discontinuity at ω_{\max} rather than the more complicated sharp but continuous transition which would be inferred from figure 7. In solving the diffusion equation IV-41 based on $\Gamma(\theta)$ as given by Eq. IV-55, account must be taken of these above considerations. Such a diffusion equation will therefore be expected to hold only for values of $\omega_{\max}/\omega_c < 0.1$, and only for values of θ in the vicinity of the loss cone. In addition, the angular diffusion will be overestimated for particles with energies just above the minimum gyroresonance energy, E_{\min} .

$\Gamma(\theta)$ as given by Eq. IV-55 must be also modified for an electron travelling along a magnetic field line, since it is a function of the position of the electron through the magnetic latitude dependence of ω_c , ω_p , y_{\max} , $\cos \theta$ and even $\langle B^2 \rangle$.

The latitude dependence of ω_c was given by Eq. III-45. In the vicinity of the geomagnetic equator, we assume that ω_p^2/ω_c is independent

of the geomagnetic latitude and has the value 8.2×10^6 /sec. From III-19, it follows that

$$\cos^2 \theta = 1 - \frac{\omega_c}{\omega_c^0} (1 - \cos^2 \theta_0) \quad \text{IV-58}$$

Since equatorial wave damping or growth was shown in Section III to dominate over the overall damping or growth that a wave undergoes in passing through the magnetosphere, the maximum allowed frequency in the turbulence spectrum on a given field line will be roughly given by the maximum allowed frequency for wave growth at the equator, so that

$$y_{\max} = \frac{\omega_{\max}}{\omega_c} \approx y_{\max}^0 \frac{\omega_c^0}{\omega_c} \quad \text{IV-59}$$

The latitude dependence of the mean square turbulence field, $\langle B^2 \rangle$, is the most difficult quantity to estimate, since there are a number of competing factors which must be considered. If we consider the ideal case of strictly longitudinal waves generated in the vicinity of the equator and travelling away from it along the zero order field lines, then the latitude dependence can be estimated by the following argument. The one-way energy flux, \underline{S} , of the turbulence field is given by

$$|\underline{S}| = \frac{c}{4\pi} |\langle \underline{E}_- \times \underline{B}_+ \rangle| = \frac{1}{4\pi} \left| \langle \frac{\omega}{k} B_- B_+ \rangle \right| \quad \text{IV-60}$$

where

$$\begin{aligned} \langle \frac{\omega}{k} B_- B_+ \rangle &= \frac{1}{ZT} \int \frac{dk d\omega}{(2\pi)^2} \frac{\omega}{k} \langle B_-(\omega, k) B_+(\omega, k) \rangle \\ &\approx \int \frac{dk}{(2\pi)^4} I(k, \lambda) \frac{\omega_c k c^2}{\omega^2 p} \end{aligned} \quad \text{IV-61}$$

and we have included in $I(k)$ the hitherto suppressed latitude dependence of the turbulence field. Since in the vicinity of the geomagnetic equator ω_p^2/ω_c can be considered independent of the magnetic latitude, \underline{S} will have the same latitude dependence as the turbulence field $\langle B^2 \rangle$. Since the turbulence waves are assumed to be travelling along the magnetic field lines and since further the cross sectional area of a flux tube is inversely proportional to the magnetic field, only if \underline{S} and therefore $\langle B^2 \rangle$ vary proportionally to the magnetic field will the flow of wave energy along a field line be divergenceless. A divergenceless flow field is necessary for a steady state situation, and so it follows that under the assumption of strictly longitudinal waves, $\langle B^2 \rangle \propto \omega_c$.

Turbulent waves, however, will be also generated travelling at an angle to the magnetic field. We have not solved for these non-longitudinal waves because of the great complexity involved in their dispersion relation resulting from non-diagonal terms, and the added difficulty in considering ray paths crossing a non-uniform zero order magnetic field. Nonetheless, these waves will certainly be generated through gyroresonance with the anisotropic electron distribution. These waves will be reflected and refracted as they cross magnetic field lines. Such turbulence field components should result in a more uniform background of turbulence throughout the magnetosphere and along a given field line than that predicted by $\langle B^2 \rangle \propto \omega_c$.

The turbulence field will therefore have a weaker dependence on magnetic latitude than that given for the strictly longitudinal case, and we represent this dependence by $\langle B^2 \rangle \propto \omega_c^n$, where $n \leq 1$. In addition,

if $I(k)$ as given by Eq. IV-46 is assumed to have an angular dependence to account for non-longitudinal wave components generated within a cone of pitch angles about the magnetic field, and to take account of this a three dimensional space-wave number Fourier transformation is used in the derivation of the diffusion coefficients, then it can be readily shown that the relations IV-52 and IV-55 still hold, where $\langle B^2 \rangle$ now includes the non-longitudinal field components.

Using all the above dependencies and approximations, $\Gamma(\theta)$ can be written

$$\Gamma(\theta, \lambda) \approx \Gamma'(\lambda = 0^\circ) \cdot \frac{\left[\frac{(1 + 3 \sin^2 \lambda)^{1/2}}{\cos^6 \lambda} \right]^{m+n}}{\left[1 - \frac{(1 + 3 \sin^2 \lambda)^{1/2}}{\cos^6 \lambda} (1 - \cos^2 \theta_0) \right]^{m+1/2}} \quad \text{IV-62a}$$

where

$$\Gamma'(\lambda = 0^\circ) = \left[\frac{170}{EL^3} \cdot \frac{1 - y_{\max}^0}{y_{\max}^0} \right]^{m+1/2} \cdot \frac{\pi(m+1)}{\omega_c^0} \langle B^2(\lambda = 0^\circ) \rangle \quad \text{IV-62b}$$

The path of the electron can now be taken into account by suitably averaging $\Gamma(\theta, \lambda)$ along a magnetic field line.

$$\overline{\Gamma(\theta, \lambda)} = \Gamma'(\lambda = 0^\circ) \int_0^{t(\lambda_{\max})} \frac{\left[\frac{(1 + 3 \sin^2 \lambda)^{1/2}}{\cos^6 \lambda} \right]^{m+n}}{\left[1 - \frac{(1 + 3 \sin^2 \lambda)^{1/2}}{\cos^6 \lambda} (1 - \cos^2 \theta_0) \right]^{m+1/2}} \frac{dt}{\tau_B/4} \quad \text{IV-63}$$

where

$$dt = \frac{dz}{V_z} = \frac{dz}{(V_o^2 + V_{z_o}^2)^{1/2} \cos \theta} \quad \text{IV-64}$$

and

$$dz = [(dr)^2 + (rd\lambda)^2]^{1/2} = [1 + 3 \sin^2 \lambda]^{1/2} (LR_e) \cos \lambda d\lambda \quad \text{IV-65}$$

is the differential distance along a magnetic field line, the equation of which is given by

$$r = (LR_e) \cos^2 \lambda \quad \text{IV-66}$$

With τ_B given by III-15, the integral for $\overline{\Gamma(\theta, \lambda)}$ becomes

$$\begin{aligned} & \int_0^{\lambda_{\max}} \frac{\left[\frac{(1 + 3 \sin^2 \lambda)^{1/2}}{\cos^6 \lambda} \right]^{m+n} dt}{\left[1 - \frac{(1 + 3 \sin^2 \lambda)^{1/2}}{\cos^6 \lambda} (1 - \cos^2 \theta_0) \right]^{\frac{m+1}{2}} \tau_B^{1/4}} \\ &= \int_0^{\lambda_{\max}} d\lambda \frac{(1 + 3 \sin^2 \lambda)^{\frac{m+n+1}{2}}}{(\cos \lambda)^{6(m+n)-1}} \left/ \left[1 - \frac{(1 + 3 \sin^2 \lambda)^{1/2}}{\cos^6 \lambda} (1 - \cos^2 \theta_0) \right]^{\frac{m+2}{2}} \right. \end{aligned} \quad \text{IV-67}$$

where λ_{\max} is determined from the condition

$$E \geq E_{\min} = \frac{170}{L^3} \frac{(1 - y_{\max}^0)^3}{y_{\max}^0} \frac{(1 + 3 \sin^2 \lambda)}{\cos^{12} \lambda} \frac{1}{\cos^2 \theta} \quad \text{IV-68}$$

which puts an upper bound on λ for a given particle energy E and equatorial pitch angle θ_0 . Since $\cos \theta$ decreases as λ increases from 0° , $E_{\min} > E_{\min}^0$ and the minimum energy condition is more stringent as an electron moves away from the equator. The condition IV-68 finally becomes

$$\frac{\cos^{12} \lambda_{\max}}{(1+3 \sin^2 \lambda_{\max})} = \frac{\frac{170}{EL^3} \cdot \frac{(1-y_{\max}^o)^3}{y_{\max}^o}}{1 - \frac{(1+3 \sin^2 \lambda_{\max})^{1/2}}{\cos^6 \lambda_{\max}} (1 - \cos^2 \theta_o)} \quad \text{IV-69}$$

Equation IV-69 can be graphically solved for λ_{\max} , and the integral

$$\int_0^{\lambda_{\max}} d\lambda \frac{(1+3 \sin^2 \lambda)^{\frac{m+n+1}{2}}}{(\cos \lambda)^{6(m+n)-1}} \quad \text{IV-70}$$

can be solved explicitly for $(m+n)$ odd. Dividing this result by $\cos^{(m+2)/2} \theta(\lambda_{\max})$ then gives a close upper bound to IV-67 when $\theta_o \neq 0$.

$\overline{\Gamma}(\theta, \lambda)$ can finally be expressed as

$$\overline{\Gamma}(\theta, \lambda) = \langle B^2(\lambda = 0^o) \rangle \cdot \frac{2\pi}{\omega_c} Q(E, L, m, n, y_{\max}^o, \theta_o) \quad \text{IV-71}$$

where

$$Q(E, L, m, n, y_{\max}^o, \theta_o) = \left[\frac{170}{EL^3} \frac{(1-y_{\max}^o)}{y_{\max}^o} \right]^{\frac{m+1}{2}} \cdot \frac{m+1}{2} \int_0^{\lambda_{\max}} d\lambda \frac{(1+3 \sin^2 \lambda)^{\frac{m+n+1}{2}}}{(\cos \lambda)^{6(m+n)-1}} \left/ \left[1 - \frac{(1+3 \sin^2 \lambda)^{\frac{1}{2}}}{\cos^6 \lambda} (1 - \cos^2 \theta_o) \right]^{\frac{m+2}{2}} \right. \quad \text{IV-72}$$

In figure 12, Q is plotted vs.

$$Y = \frac{170}{EL^3} \cdot \frac{1-y_{\max}^o}{y_{\max}^o} \approx \frac{E_{\min}^o}{E} \quad \text{IV-73}$$

for various representative values of m , n and θ_o .

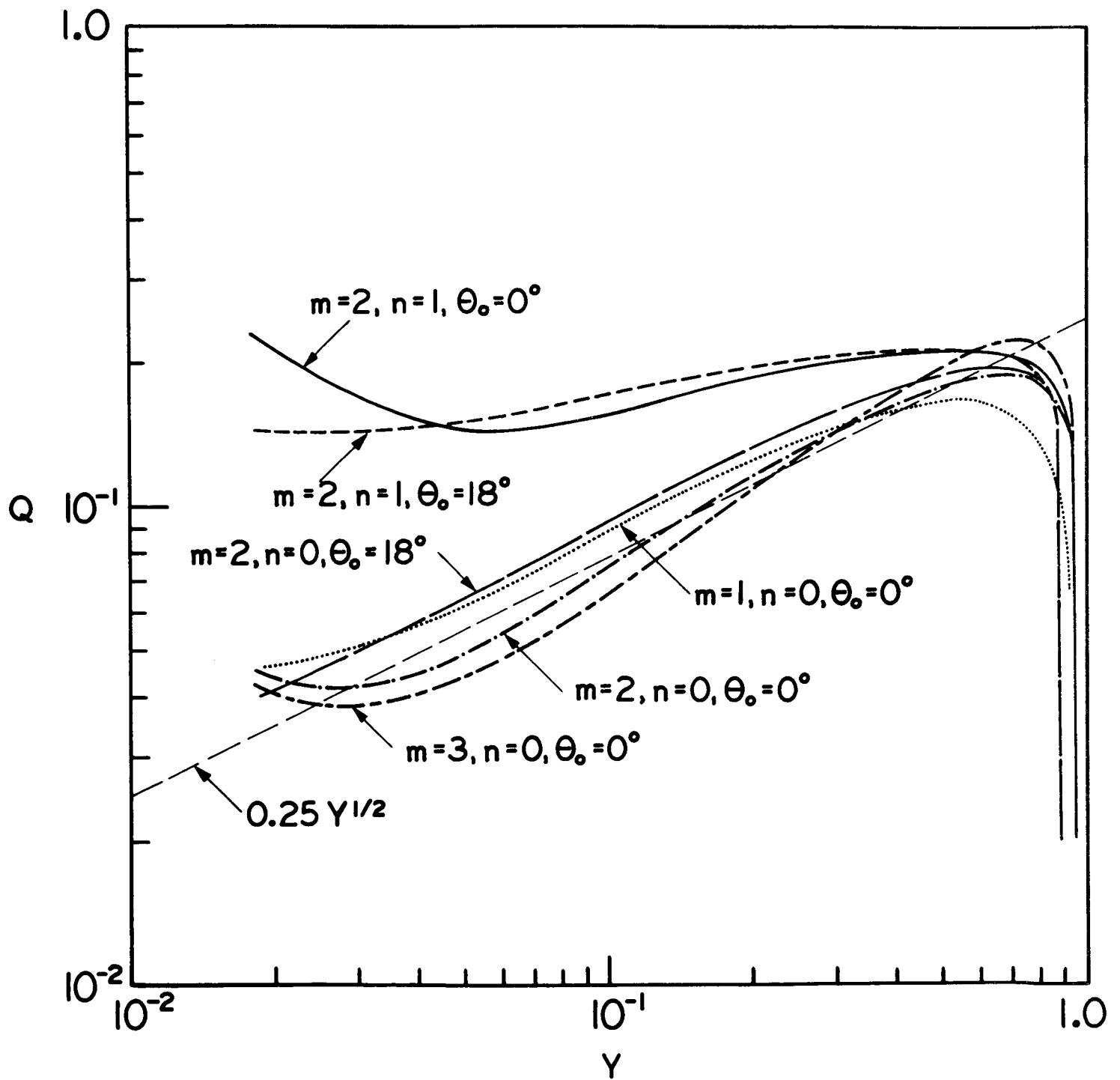


Figure 12. The various dependencies of the electron angular diffusion coefficient averaged over the changing conditions encountered by an electron along its path through the magnetosphere.

Q is generally seen to be relatively independent of θ_0 and m , and for $n = 0$ can be well approximated by

$$\begin{aligned} Q &= 0.25 Y^{1/2} && (Y < \cos^2 \theta_0) \\ &= 0 && (Y > \cos^2 \theta_0) \end{aligned} \quad \text{IV-74}$$

for θ_0 in the vicinity of the loss cone. For $Y > 0.2$, Q is depressed below the equatorial value of $\frac{m+1}{2} Y^{(m+1)/2}$ which would apply if the electron never moved from the equator. For lower Y , however, Q tends to be greater than the equatorial value. These results reflect the fact that particles gyroresonate with higher frequency wave components away from the equator, so that particles with energies close to E_{\min}^0 quickly move into a region where their energy is below the local E_{\min} , while particles with energies $E \gg E_{\min}^0$ gyroresonate with the higher frequency more intense part of the turbulence spectrum only upon moving away from the equator. The net result is that the strong dependence of $\Gamma(\theta)$ as given by Eq. IV-55 upon $Y^{(m+1)/2}$ and $1/(\cos^{m+1} \theta)$ is levelled out, the major wave-particle interaction taking place not at the equator, but at that magnetic latitude at which $E \cos^2 \theta \gtrsim E_{\min}$ and the electron is interacting with the most intense part of the turbulence spectrum.

With all the above restrictions and considerations, the diffusion equation IV-41 becomes

$$\frac{\partial}{\partial t} [n(\theta_0, t) \sin \theta_0] = \frac{e^2 \overline{\Gamma'}}{4m^2 c^2} \left[-\frac{\partial}{\partial \theta_0} [n(\theta_0, t) \cos \theta_0] + \frac{\partial^2}{\partial \theta_0^2} [n(\theta_0, t) \sin \theta_0] \right] \quad \text{IV-75}$$

where

$$\begin{aligned} \overline{\Gamma} &= \langle B^2(\lambda=0^0) \rangle \cdot \frac{2\pi}{\omega_c} Q(Y, \theta_0, m, n) \\ &\approx \langle B^2(\lambda=0^0) \rangle \cdot \frac{2\pi}{\omega_c} \cdot 0.25Y^{1/2} \quad (Y < \cos^2 \theta_0) \\ &= 0 \quad (Y > \cos^2 \theta_0) \end{aligned} \quad \text{IV-76}$$

If a solution of the form

$$n(\theta_0, t) = N(t) M(\theta_0) \quad \text{IV-77}$$

is assumed, then Eq. IV-75 can be separated into the two equations

$$\frac{\partial N(t)}{\partial t} = -K \frac{e^{2\overline{\Gamma}}}{4m^2 c^2} N(t) \quad \text{IV-78}$$

$$\frac{\partial^2 M(\theta_0)}{\partial \theta_0^2} + \frac{\cos \theta_0}{\sin \theta_0} \frac{\partial M(\theta_0)}{\partial \theta_0} + KM(\theta_0) = 0 \quad \text{IV-79}$$

where K is a separation constant which will be determined by the boundary conditions on $M(\theta_0)$ near the loss cone.

The solution to IV-78 is simply an exponential decay given by

$$N(t) \propto e^{-t/KT_D} \quad \text{IV-80}$$

where

$$\begin{aligned} T_D &= \frac{4m^2 c^2}{e^{2\overline{\Gamma}}} = \frac{B_0^2}{\langle B^2(\lambda=0^0) \rangle} \cdot \frac{2}{\pi \omega_c} \cdot \frac{1}{Q} \\ &\approx \frac{B_0^2}{\langle B^2(\lambda=0^0) \rangle} \cdot \frac{8}{\pi \omega_c Y^{1/2}} \quad (Y < \cos^2 \theta_0) \\ &= \infty \quad (Y > \cos^2 \theta_0) \end{aligned} \quad \text{IV-81}$$

A solution to IV-79 is obtained in Appendix II. K is determined by the condition that $M(\theta_0)$ go to zero at the loss cone angle $\theta = B_0/B_{\max}$ and is found to be of order unity and have a weak logarithmic dependence on L .

Equation IV-75 thus describes the diffusion of particles into the loss cone and predicts a $1/e$ folding time of $KT_D \approx T_D$ for the decay of the electron density by means of this diffusion. The lifetime T of a magnetospheric electron of energy $E > E_{\min}^0$ interacting with the spectrum of electromagnetic electron cyclotron turbulence can thus be given by

$$T = KT_D = \frac{B_0^2}{\langle B^2(\lambda=0^0) \rangle} \cdot \frac{2}{\pi \omega_c^0} \cdot \frac{K}{Q}$$

$$\approx \frac{B_0^2}{\langle B^2(\lambda=0^0) \rangle} \cdot \frac{8}{\pi \omega_c^0 Y^{1/2}}$$

IV-82

This equation states the obvious conclusion that an electron diffuses into the loss cone in the mean time it takes for the electron pitch angle to diffuse about a radian. A definitive solution of the electron diffusion equation would have to take additional account of the unknown source function of electrons injected or accelerated into trapped particle orbits and the steady state equilibrium which is reached between this injection of particles, the turbulence resulting from the steady-state pitch angle distribution, and finally the loss of electrons from the diffusion induced by this turbulence. Because of the complexity of this task, we have attempted to solve the simpler diffusion Eq. IV-41 in order to obtain a rough estimate of the electron lifetime.

The pitch angle distribution which follows from Eq. IV-79 is derived in Appendix II and can be written in the compact form

$$M(\theta_0) = 1 + \frac{K}{2} \log_e \sin^2 \theta_0 \quad \text{IV-83}$$

Because of the restrictions placed on $\cos^2 \theta_0$ in IV-76, in the vicinity of $\theta_0 \approx \pi/2$ there is no diffusion and Eq. IV-79 will no longer hold.

The density at $\theta_0 \approx \pi/2$ will be determined by the unknown injection spectrum and limited by the fact that if the density at $\theta_0 \approx \pi/2$ increases too greatly without being drained off by diffusion, a sufficiently large value of $\partial f_0 / \partial \theta$ will result until, according to Eq. II-43, instability will develop at a low enough frequency to diffuse these electrons into the loss cone. In figure 13 $M(\theta_0)$, properly normalized and with $K = 0.33$, is plotted for comparison with j_0 (40 keV, θ_0) at $L = 6$ obtained from figure 4. The agreement is reasonably good in the vicinity of the loss cone where it would be hoped that Eq. IV-79 would apply, but at larger pitch angles j_0 is flatter than M , inferring reduced diffusion near $\theta \approx \pi/2$ which will tend to reduce the electron velocity anisotropy produced by diffusion into the loss cone and so limit the growth of the wave turbulence. In all, the two curves are in reasonable agreement and IV-82 should give a fair estimate of the lifetime of an electron in the magnetosphere under quasi-equilibrium conditions.

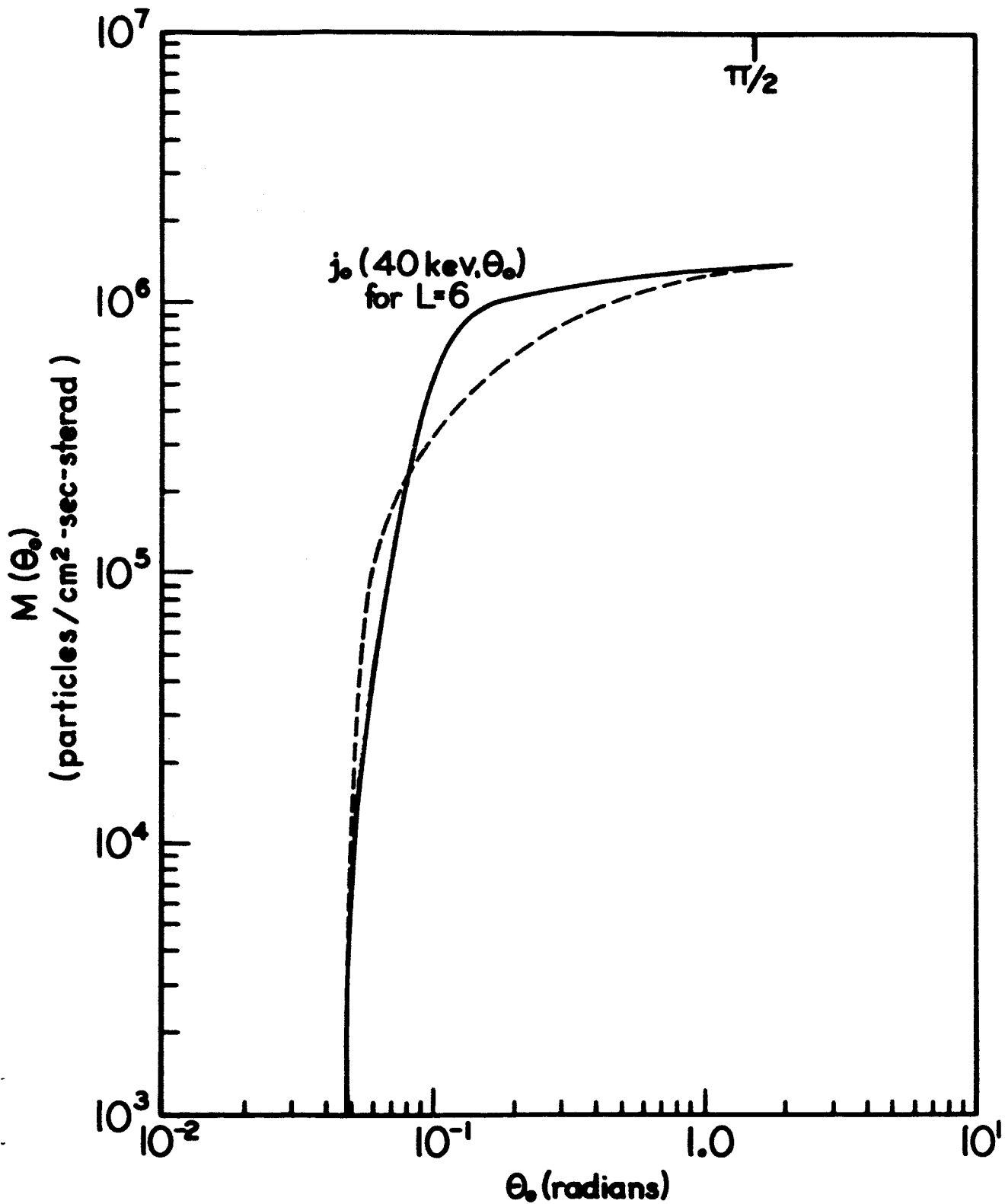


Figure 13. The equatorial electron pitch angle distribution at $L = 6$ obtained from solving the diffusion equation, Eq. IV-75. The distribution is normalized to agree with $j_0(40 \text{ keV}, \theta_0)$ at $L = 6$ as given in Figure 4, which is also plotted for comparison.

V. APPLICATION TO OBSERVED PHENOMENA

A significant amount of information exists concerning the characteristics of electron precipitation in the magnetosphere. Results from the polar orbital satellites Injun I and III (O'Brien (1962), (1964)) have comprehensively covered the characteristics of electrons with energy greater than 40 kev both precipitated and trapped at low altitudes (≈ 1000 km). Two distinct phenomena are observed in time studies of the precipitated and trapped electron fluxes at low altitudes. The first is a relatively low level of electron precipitation, on the order of 10^3 particles/cm²-sec-sterad. or less, which provides a constant background of precipitation unvarying over a time scale on the order of minutes. This phenomenon is commonly termed "drizzle." The second is a sporadic higher level of precipitation termed "splash" lasting on the order of seconds and superimposed upon the lower level drizzle. In the splashes, the precipitated flux approaches equality with the trapped flux at the satellite altitude, which is on the order of 10^5 particles/cm²-sec-sterad. These phenomena can readily be seen in figures 14 and 15, taken from O'Brien (1964).

The average intensity of precipitated particles, \bar{J}_p , observed on Injun I and III can be roughly approximated by

$$\begin{aligned} \bar{J}_p &\approx 10^2 L^4 \quad / \text{cm}^2\text{-sec-sterad.} & (2 < L < 6) \\ &\approx 10^5 \quad / \text{cm}^2\text{-sec-sterad.} & (6 < L < 15) \end{aligned} \quad \text{V-1}$$

where L is here best interpreted as referring to the invariant latitude Λ (Eq. III-1), which is essentially equal to the magnetic latitude, λ , at which

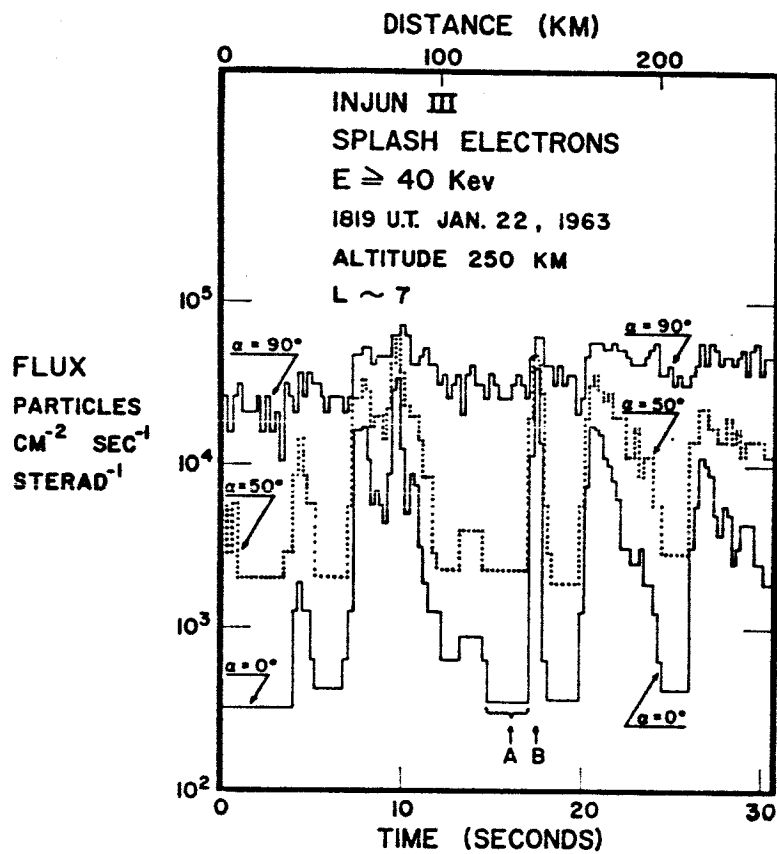


Fig. 14 Samples of several splashes detected by three Geiger tubes viewing trapped particles (at $\alpha \sim 90^\circ$) and precipitated particles (at $\alpha \sim 50^\circ$ and $\alpha \sim 0^\circ$). Trapping persists between splashes, and the precipitated flux varies by a greater proportional amount than does the trapped flux, in such a manner as to approach isotropy. Nominal $B/B_0 \sim 700-500$.

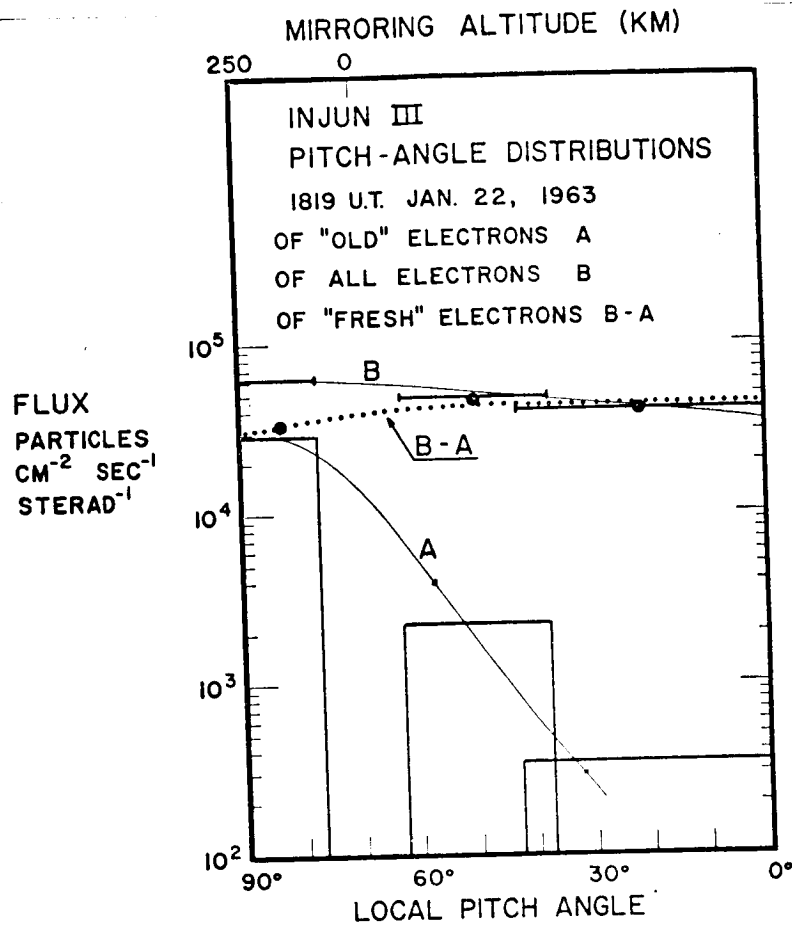


Fig. 15 Pitch-angle distributions derived from measurements at *A* and *B* of Figure 7. For simplicity it is assumed that each detector sees particles with uniform cross section over the range of pitch angles shown as a block. They actually have conical fields of view (see Table 2). Nominal $B/B_0 \sim 600$.

the satellite observation was made. These averages reflect the fact that while drizzle is a more common steady state occurrence than splash, the splashes that do occur are of sufficiently great intensity that the lower level drizzle rates have almost no effect on the average precipitation rates and thus on the effective electron lifetime. In addition, simultaneous auroral light and energy precipitation measurements made on Injun III (O'Brien and Taylor (1964)) show that auroral light generation, presumably caused by electron precipitation in the 1 - 10 keV range (McIlwain (1960)), is strongly correlated with the enhanced precipitation of 40 keV electrons that occurs during splash events.

The electron lifetime given by Eq. IV-82 is one that would apply in a quasi-equilibrium situation such as applies during drizzle. Indeed, the pitch angle distribution shown in figure 15 is just what would be expected from equatorial pitch angle distributions as those given in figure 13.

To determine the electron drizzle lifetime we must consider the number of particles in the radiation belt above a square centimeter of area at the satellite altitude and the rate at which these particles are drained off by the drizzle precipitation rate measured at the satellite. The number of electrons in a flux tube is obtained from equatorial measurements of the electron flux. From the conservation of magnetic flux, it follows that the cross sectional area A of a flux tube varies as

$$\frac{A_o}{A_s} = \frac{B_s}{B_o} \approx L^3$$

where the subscript s refers to the satellite, o as usual to the equator. Thus if there are J_o particles/cm²-sec passing through the equatorial plane, there are $J_o A_o / A_s \approx J_o L^3$ particles/cm²-sec passing through the equatorial plane above a square centimeter of area at the satellite altitude.

The bounce period for a particle of energy E(kev) was given in section III as

$$\tau_B \approx 1.35 \frac{L}{E^{1/2}} \text{ sec} \quad \text{III-15}$$

Since each bounce period a given particle will cross the equator twice, there are

$$\eta = J_o(E) L^3 \frac{\tau_B}{2} \approx 0.68 J_o(E) \frac{L^4}{E^{1/2}} \text{ particles/cm}^2 \quad \text{V-3}$$

in the radiation belt above one square centimeter at the satellite altitude of approximately 1000 km. The dumping cone at 1000 km is about 55° wide, so that the belt is being emptied at a rate

$$\frac{d\eta}{dt} = 4\pi(1 - \cos 55^\circ) j_p(E) \quad \text{V-4}$$

by an average precipitation intensity in the loss cone of $j_p(E)$ particles/cm²-sec-sterad.

The electron lifetime is thus given by

$$T(E) = \frac{\eta}{\frac{d\eta}{dt}} = 0.1 \frac{J_o(E)}{j_p(E)} \cdot \frac{L^4}{E^{1/2}} \text{ sec} \quad \text{V-5}$$

For $E = 40$ kev, $J_o(40 \text{ kev}) = 10^7 / \text{cm}^2\text{-sec}$, and a drizzle precipitation

rate $j_p^d(E) = 10^3 / \text{cm}^2\text{-sec-sterad}$

$$T^d(40 \text{ kev}) = 2.1 \times 10^5 \left(\frac{L}{6}\right)^4 \text{ sec} \quad \text{V-6}$$

If T^d as given by V-6 is equated to the diffusion loss time as given by IV-82, it follows that

$$\begin{aligned} \langle B^2(\lambda = 0^\circ) \rangle^d &\approx \frac{2K}{\pi} \cdot \frac{1}{2.1 \times 10^5 \left(\frac{L}{6}\right)^4} \cdot \frac{B_o^2}{\omega_c^o Q} \\ &\approx \frac{2.7 \times 10^{-10}}{L^7} \left(\frac{E}{E_{\min}^o}\right)^{1/2} \\ &\approx 1.6 \times 10^{-15} \left(\frac{6}{L}\right)^7 (\text{gauss})^2 \end{aligned} \quad \text{V-7}$$

for a typical $E_{\min}^o = 15 \text{ kev}$. Thus drizzle lifetimes at 40 kev require a root mean square turbulence field at the equator of magnitude

$$\sqrt{\langle B^2 \rangle^d} \approx 4.0 \times 10^{-3} \left(\frac{6}{L}\right)^{3.5} \gamma \quad \text{V-8}$$

where $\gamma = 10^{-5} \text{ gauss}$. The implications and observability of this turbulence field will be considered in the following.

Splashes can be considered as a sporadic and short lived tendency towards isotropization of the local pitch angle. This can be caused by a sudden compression of the geomagnetic field which, by increasing adiabatically the perpendicular electron velocity and hence the amount of electron velocity anisotropy triggers a burst of electron cyclotron waves from the marginally stable electron pitch angle-electromagnetic

turbulence quasi-equilibrium. To effect local pitch angle isotropization, the turbulence burst must be able to diffuse an electron passing once through the equatorial plane through the range of pitch angle observed at the satellite altitude of 1000 km, typically an equatorial pitch angle spread of about $(1/L^3)^{1/2}$ radians. Using IV-37, this condition becomes

$$\begin{aligned} \frac{1}{L^3} &\approx 2 \langle \theta^2 \rangle \tau_B / 2 \\ &\approx \frac{e^2 \langle B^2 \rangle^s}{m^2 c^2} \cdot \frac{2\pi}{\omega_c^0} Q \cdot (0.68 \frac{L}{E^{1/2}}) \end{aligned} \quad \text{V-9}$$

which gives

$$\begin{aligned} \langle B^2 \rangle^s &\approx \frac{4.1 \times 10^{-9}}{L^7} \cdot \frac{E^{1/2}}{Q} \\ &\approx \frac{1.6 \times 10^{-8}}{L^7} \left(\frac{E}{E_{\min}^0} \right)^{1/2} \\ &\approx 10^{-12} \left(\frac{6}{L} \right)^7 (\text{gauss})^2 \end{aligned} \quad \text{V-10}$$

for $E = 40$ kev, $E_{\min}^0 = 5$ kev. Thus splashes of 40 kev electrons require a root mean square equatorial turbulence field of magnitude

$$\sqrt{\langle B^2 \rangle^s} = 0.1 \left(\frac{6}{L} \right)^{3.5} \gamma \quad \text{V-11}$$

which is an order of magnitude or so greater than the drizzle field V-8.

VLF turbulence has been observed on Injun III to occur concurrently with electron precipitation (Gurnett and O'Brien (1964)). The receiver used on Injun III, however, had a low frequency cutoff below 1 kcps. In

figure 16 f_{\max} is plotted vs L , where f_{\max} is the maximum turbulence frequency as obtained from Eq. IV-57b corresponding to minimum precipitation energies of 1, 5, 10 and 20 kev. In the limit $y_{\max}^0 = (2\pi f_{\max})/\omega_c^0 \ll 1$, f_{\max} is given by

$$f_{\max} = \frac{3.2 \times 10^3}{E_{\min}^0} \left(\frac{6}{L}\right)^6 \text{ cps} \quad \text{V-12}$$

From figure 16 and the above equation it is seen that for $E_{\min}^0 = 10$ kev, which will be shown in the following to be a typical minimum precipitation energy, $f_{\max} < 1$ kcps for $L > 4.5$, so that the electromagnetic turbulence generated by electrons in the outer radiation belt will for the most part be below the effective frequency range of the Injun III VLF receiver. Nonetheless, Gurnett and O'Brien state that "Hiss having frequencies less than 1 kcps and chorus are the electromagnetic emissions most commonly observed at the satellite" and that this "ELF (extra low frequency) hiss is often characterized by a sharply defined upper frequency limit." In addition, Gurnett and O'Brien also find that VLF activity is generally enhanced during splash precipitation events, with the root mean square signal strength in the range 0.5 - 7 kcps on the order of 10^{-2} γ during splashes. This observed level for $f > 0.5$ kcps is roughly one order of magnitude less than that given by Eq. V-11, which gives the root mean square turbulence field at the equator required to account for splash events. Since the maximum frequency in this splash field is itself on the order of 0.5 kcps, and since the response of the Injun III receiver is down by about 15 db at this frequency, the observed splash signal

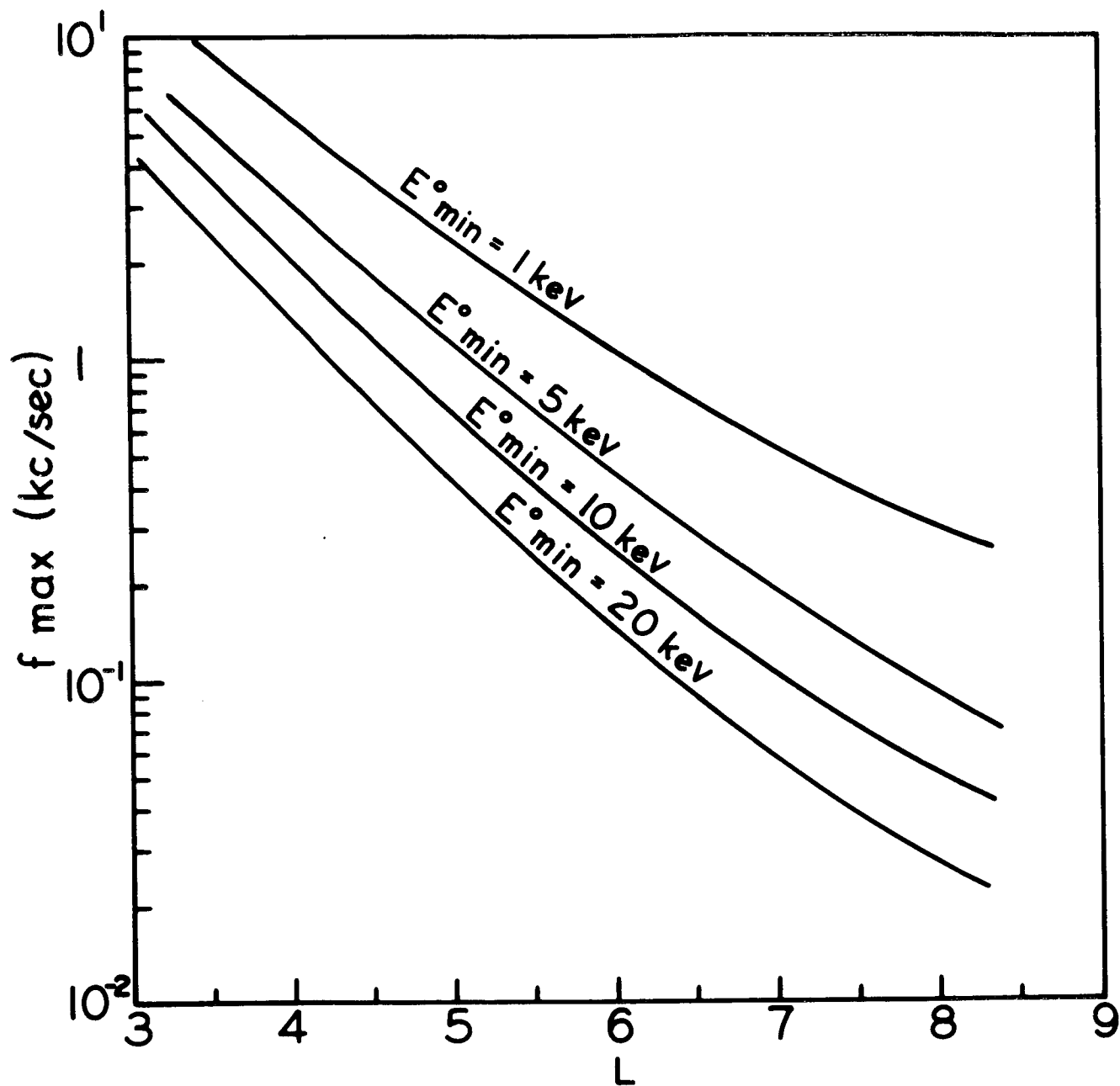


Figure 16. The L dependence of the maximum turbulence frequency for various representative values of the minimum electron precipitation energy.

strength is consistent with the turbulence field predicted on the basis of the above diffusion theory. During normal or drizzle conditions, the wide band VLF signal level is below the 10^{-3} γ noise level of the receiver. This again is consistent with the equatorial drizzle field on the order of 4×10^{-3} γ predicted by Eq. V-8, when the receiver response is once more taken into account.

Thus drizzle is consistent with a low level of electromagnetic turbulence always present in the magnetosphere, while splashes are consistent with the triggering of a burst of electron cyclotron turbulence by a geomagnetic compression which leads to local isotropization of the pitch angle and enhanced diffusion into the loss cone. Furthermore, the increase in y_{\max}^0 during the compression resulting from the increased electron velocity anisotropy will permit the lower energy electrons responsible for visual auroral effects to precipitate into the atmosphere.

Figure 9 showed E_{\min}^0 corresponding to ω_{\max} as given in figure 6 and derived from the observed electron pitch angle distribution at Injun III altitudes. E_{\min}^0 so derived is seen to be about 5 kev, roughly independent of L. E_{\min}^0 will actually be slightly greater than this both because of non-linear effects leading to the marginal stability of the turbulence spectrum and also the fact that α as appears in Eq. III-37 for ω_{\max} is most likely less than the assumed value given in Table 1, so tending to decrease ω_{\max} by a factor of about two. In addition, our model for the turbulence spectrum tended to overestimate the diffusion of particles with energies close to E_{\min}^0 , so that in all a more realistic estimate for the effective E_{\min}^0 under quasi-equilibrium drizzle

conditions is upwards of 10 kev, say 15 - 20 kev as assumed in obtaining the drizzle field V-8.

During splashes, however, the effective y_{\max}° will increase as the marginally stable turbulence spectrum is triggered and lower energy electrons in the 1 - 15 kev range will be able to interact with the turbulence spectrum and diffuse in pitch angle into the loss cone. It is just these electrons which are known to cause auroras and carry the major part of the precipitated energy flux in splash events. In figure 17, the relation IV-57b is plotted vs L for various representative values of y_{\max}° . Steady low level drizzle of 40 kev electrons is consistent with a y_{\max}° of less than 0.1, while splashes and auroral phenomena involving precipitated electrons as low as 1 kev in energy infer an increase in the effective value of y_{\max}° to greater than 0.1.

In a magnetic compression, the parallel electron velocity will remain constant but the perpendicular velocity will be changed by the induced Faraday field created by the changing magnetic flux linked by the electron orbit. Since the magnetic moment v_{\perp}^2 / B_0 will be conserved by compressions occurring on a time scale longer than an electron gyroperiod ($1.14 \times 10^{-6} L^3$ sec), the fractional change in the mean perpendicular electron velocity will be given by

$$\frac{\overline{\Delta(v_{\perp}^2)}}{\overline{v_{\perp}^2}} = \frac{\Delta B_0}{B_0}$$

V-13

In part II, y_{\max} was seen to be effectively given by

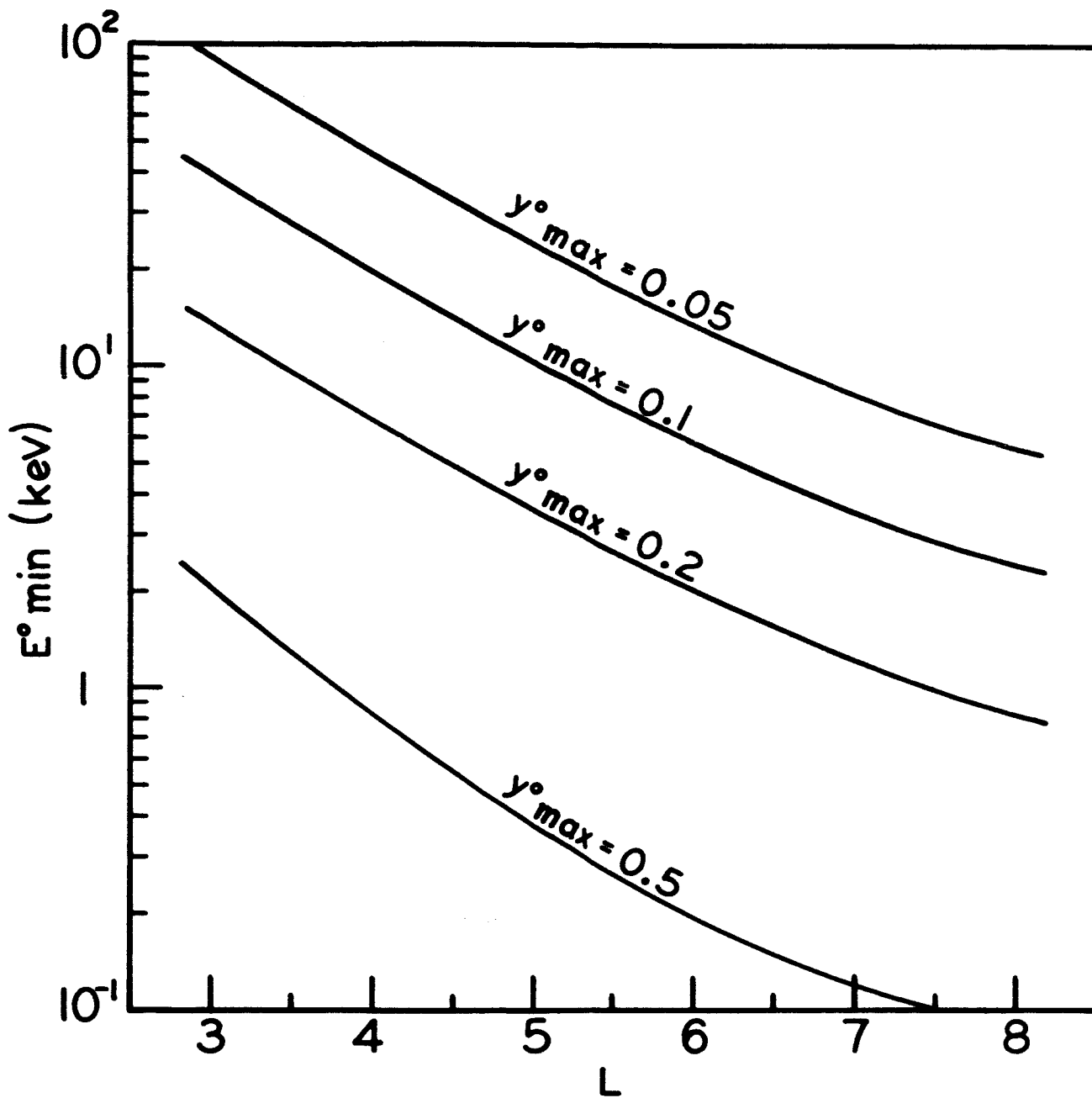


Figure 17. The L dependence of the minimum electron precipitation energy for various representative values of $y^\circ \text{ max}$.

$$y_{\max} \approx \frac{T_{\perp} - T_z}{T_{\perp}} \approx \frac{\sqrt{v_{\perp}^2} - \sqrt{v_z^2}}{\sqrt{v_{\perp}^2}} \quad \text{V-14}$$

so that a change Δy_{\max}° in y_{\max}° will involve a change

$$\frac{\Delta B_o}{B_o} = \Delta y_{\max}^{\circ} \quad \text{V-15}$$

in the magnetic field.

From Eq. IV-57b we can by neglecting the slowly varying $(1 - y_{\max}^{\circ})^3$ factor obtain the relations

$$\Delta E_{\min}^{\circ} \approx - E_{\min}^{\circ} \frac{\Delta y_{\max}^{\circ}}{y_{\max}^{\circ}} \quad \text{V-16a}$$

$$\frac{\Delta E_{\min}^{\circ}}{E_{\min}^{\circ}} \approx - \frac{E_{\min}^{\circ} L^3}{170} \Delta y_{\max}^{\circ} = - \frac{E_{\min}^{\circ} L^3}{170} \cdot \frac{\Delta B_o}{B_o} \quad \text{V-16b}$$

Since B_o itself goes as $1/L^3$, it follows that

$$\frac{\Delta E_{\min}^{\circ}}{E_{\min}^{\circ}} \approx - \frac{E_{\min}^{\circ} L^6}{50} \Delta B_o \quad \text{V-17}$$

and for a typical drizzle value $E_{\min}^{\circ} = 15$ kev and a compression ΔB_o of magnitude 1γ

$$\Delta E_{\min}^{\circ} = 2 \left(\frac{L}{6} \right)^6 \text{ kev/gamma} \quad \text{V-18}$$

Thus for a given minimum drizzle energy experimentally inferred to be roughly independent of L , a given magnetic compression will have a much greater effect at high L values than at low L values in precipitating out low energy electrons. Small magnetic compressions on the order

of γ 's in the steady state geomagnetic equatorial field will thus readily precipitate low energy electrons in the 1 - 10 kev range at higher L values near the boundary of the magnetosphere, but these same compressions should have little or no effect at $L = 4$ and observable but not quite as great an effect at $L = 6$.

Auroral electron precipitation and splashes tend to occur in the range $6 < L < 12$, corresponding to an invariant magnetic latitude range of $65^\circ < \Lambda < 73^\circ$. For $L > 8$, the electron fluxes on the night side of the magnetosphere decrease greatly in magnitude and become significantly time varying, but on the day side of the earth the magnetosphere is compressed so that while the magnetosphere boundary is encountered at a radial distance of about 10 - 12 earth radii, the corresponding L values are 14 - 16 or $\Lambda \approx 75^\circ$ (see figure 1).

Thus precipitation events observed on the night side of the earth at L values greater than 8 ($\Lambda > 69^\circ$) will correspond to the direct injection of electrons into the magnetosphere, probably from the neutral sheet in the magnetospheric tail. These events have been frequently observed on the Alouette satellite (McDiarmid and Burrows (1965)) and characteristically involve much more intense fluxes than the trapped electron fluxes that exist for $\Lambda < 69^\circ$. These events most probably correspond to the extremely intense events occasionally observed on balloon experiments (see, for example, Winckler et al, (1962)) and cannot be explained on the basis of the above diffusion theory. These extremely intense precipitation events are observed on Alouette to occur only on the night side of the magnetosphere and at L values greater than 8. For

$L < 8$ on the night side of the earth and $L < 15$ on the day side, the geomagnetic field will be well ordered and precipitation events will be driven by turbulence diffusion. It is with events occurring in this region, which corresponds to Zone 1 in the terminology of Piddington (1965), that this paper is concerned.

We shall now consider whether triggered wave growth rates are consistent with order of magnitude increases in the turbulence field level occurring on a time scale of seconds as required to effect splashes. For $L > 6$ the electron distribution in the 1 - 40 keV range that we are primarily concerned with is given more appropriately by III-48 rather than by III-30. Properly interpolating from Eq. III-41 for the wave growth rate, it follows that for $y < y_{\max}^0 \ll 1$,

$$\omega_i \approx -3 \times 10^{-2} L^{4.5} y_1^{3/2} y_{\max}^0 \left(\frac{y}{y_1} \right)^{5/2} \quad \text{V-19}$$

where $y_1 \approx 170/40L^3$ is the value of y at a given L corresponding to the normalization energy $E_0 = 40$ keV, and a normalization flux $J(40 \text{ keV}) = 10^7/\text{cm}^2\text{-sec}$ has been assumed. For a compression such that y_{\max}^0 is increased so that particles of energy E are precipitated, i. e., such that

$$y_{\max}^0 \approx \frac{170}{EL^3} \quad \text{V-20}$$

it follows that

$$\begin{aligned} \omega_i &\approx -3 \times 10^{-2} \left(\frac{170}{40} \right)^{3/2} \left(\frac{170}{EL^3} \right) \left(\frac{y}{y_1} \right)^{5/2} \\ &= \frac{45}{EL^3} \left(\frac{y}{y_1} \right)^{5/2} \end{aligned} \quad \text{V-21}$$

The maximum wave growth rate at $y < y_{\max}^0$ is thus roughly given by

$$\omega_i^{\max} \approx \frac{4.5 \times 10^5}{E^{3.5} L^3}$$

$$\approx 1 \quad \text{for } L = 6, E = 10 \text{ kev}$$

V-22

Thus wave growth rates are such that if magnetic compressions at a given L value are strong enough to increase E_{\min}^0 significantly from its drizzle value of about 15 kev, then the wave growth rates resulting from these compressions are sufficiently large that the order of magnitude growth in the turbulence field required to effect splashes can take place on a time scale of seconds consistent with splash lifetimes. The inverse dependence of ω_i^{\max} on L^3 for a given E is in agreement with the strong inverse dependence on L of the turbulence fields given in V-8 and 11 as required for drizzle and splash.

The energy dependence of the precipitated electron flux is experimentally known to show a number of interesting characteristics (O'Brien (1964)). During splashes, tenfold increases in the precipitated flux with $E > 40$ kev are accompanied by significantly smaller increases, on the order of a factor of two or less in the precipitated flux with $E > 250$ kev, while the precipitated flux with $E > 1$ mev shows no experimentally significant ($> 10\%$) variation. Integral energy measurements of the flux of electrons with $E > 1$ kev lead to the equivalence relation that at Injun altitudes and midlatitudes a directional number flux of magnitude $j(40 \text{ kev}) \approx 10^5 / \text{cm}^2 \text{-sec-sterad.}$ corresponds to a directional integral energy flux of particles with $E > 1$ kev of magnitude $1 \text{ erg/cm}^2 \text{-sec-sterad.}$ This

equivalence, based on particle energy flux measurements (O'Brien (1962)) is in agreement with measurements made on Injun III of auroral light intensity (O'Brien and Taylor (1964)) if this intensity is assumed to result from collisional excitation of ionospheric constituents by electrons in the 1 - 10 keV range. Using III-8, the above flux-energy equivalence can easily be shown to infer that the effective spectral parameter a in the range $1 < E < 40$ keV must be at least 2 and probably about 2.5 in the measured low altitude flux of precipitated electrons.

The precipitated energy spectrum in the auroral zone is thus extremely soft at low energies, $E < 40$ keV, having a spectral parameter if anything slightly greater than the value of 2 which Frank (1965) observed at $L \approx 7$ in the equatorial plane. This overall spectral picture is in agreement with diffusion lifetimes as follow from Eqs. IV-82, V-5 and 10, namely

$$T = \frac{0.1 J_o(E)}{j_p(E)} \cdot \frac{L^4}{E^{1/2}} \approx T_D = \left(\frac{B_o^2}{\langle B^2(\lambda = 0^\circ) \rangle} \right) \frac{2}{\pi \omega_i^o Q} \quad V-23$$

where $\langle B^2(\lambda = 0^\circ) \rangle$ is now meant to represent an average turbulence field as results from both splash and drizzle. Since $Q \propto 1/E^{1/2}$, the average precipitated particle number flux goes as

$$j_p(E) \propto \frac{J_o(E)}{E} \propto \frac{1}{E^{a+1}} \quad V-24$$

where a is the equatorial value of the spectral parameter, namely approximately 1 at $L = 4$ rising to approximately 2 at $L = 7$. This predicted behavior is in agreement with the observed very soft precipitation spectrum in the range $1 < E < 40$ keV and predicts a precipitated spectrum for energies greater than 40 keV which has the proper fall off observed at higher energies.

It also predicts a softer precipitated spectrum at higher L values, again in agreement with Injun III observations (O'Brien and Taylor (1964)).

Recent measurements by Sharp et al (1965) on a polar orbited satellite have directly observed the precipitated electron spectrum in the auroral zone down to 180 ev. Their results are consistent with a spectral parameter of about 2 and a minimum precipitation energy of no less than 1 kev. The existence of a minimum energy cutoff and the observed spectral shape of the precipitated electron flux are thus both in agreement with the predictions of the turbulence diffusion theory.

It is instructive to compare the electromagnetic energy in the turbulence field with the energy of those electrons in the radiation belt able to interact with this turbulence. Using III-7 for the total particle energy density of electrons with $E > E_1$, the ratio, r, of turbulence field energy to particle energy is given by

$$r = \frac{\langle B^2 \rangle / 4\pi}{8.5 \times 10^{-19} \frac{J(E_0) E_0^a}{1 - \frac{1}{2a}} \cdot \frac{1}{E_1^{a-1/2}}} \quad \text{V-25}$$

First considering the drizzle field given by V-7 and taking $E_0 = 40$ kev, $J(40) = 10^7 / \text{cm}^2\text{-sec}$, $E_1 = E_{\min}^0$, we have that

$$\begin{aligned} r^d &= \frac{16}{L^7} \frac{(1 - \frac{1}{2a})}{(40)^a} E_{\min}^0{}^{a-1} \\ &= 7.2 \times 10^{-7} \left(\frac{6}{L} \right)^7 \quad (a = 1) \\ &= 1.07 \times 10^{-6} \left(\frac{6}{L} \right)^7 \left(\frac{E_{\min}^0}{40} \right) \quad (a = 2) \end{aligned} \quad \text{V-26}$$

For the splash field of Eq. V-10 it follows that

$$r^S = 2.7 \times 10^{-4} \left(\frac{6}{L} \right)^7 \quad (a = 1)$$

$$= 4.1 \times 10^{-4} \left(\frac{6}{L} \right)^7 \left(\frac{E_{\min}^0}{40} \right) \quad (a = 2) \quad \text{V-27}$$

Thus the turbulent field energy is but a small fraction of the energy in the gyroresonant particles which are diffused and eventually precipitated by the turbulence. There is no contradiction in this fact, however, since just as coulomb collisions involve but a small amount of energy in the electric fields through which two charged particles interact, so the electron-turbulence interaction is really but the intermediate stage in an electron-electron collision taking place by means of a low level of electron cyclotron turbulence, which essentially provides the action at a distance force which effects electron-electron scattering. The turbulence, whose level depends on the degree of electron velocity anisotropy, actually itself sustains the anisotropy by diffusing electrons into the loss cone. A low level of particle precipitation or drizzle is therefore intrinsic to any magnetically confined loss cone type of distribution.

Higher levels of enhanced precipitation are generated by increasing the amount of electron velocity anisotropy. A geomagnetic compression driven by the fluctuating solar wind, as described above, is one way of effecting this. Note, however, that a geomagnetic decompression reduces the degree of velocity anisotropy and will therefore decrease the precipitation level. Geomagnetic fluctuations can therefore act as a net effective acceleration mechanism, since compressions involving the

increase of electron energy lead to the precipitation of these energized electrons, while decompressions, although leading to deenergizations, do not lead to precipitation and are therefore essentially reversible.

Pulsating electron precipitation events observed by balloon auroral-zone X-ray and ground based auroral absorption measurements (Brown et al (1965)) might well be due to micropulsations of the geomagnetic field modulating the electron velocity anisotropy and hence the electromagnetic turbulence level in the outer belt, and so in turn modulating the electron diffusion and precipitation rates.

Another possible energization mechanism has been given by Hones (1963) and is driven by the drift of electrons in the asymmetric magnetosphere, distorted by the pressure of the solar wind. Particle drifts in the magnetosphere are of two basic types: a) the gradient and curvature drifts resulting from the fact that the magnetospheric field is not uniform in magnitude and direction; b) the imposed rotation of magnetic flux tubes tied by means of the ionospheric Hall current to the earth's rotation.

The drift motions resulting from a) can be further subdivided by considering separately particles confined to the equatorial plane ($\theta \approx 90^\circ$) and those near the loss cone ($\theta \approx 0^\circ$ or 180°). In the former case, the drift of the electrons is such as to conserve the first adiabatic invariant, $v_\perp^2/B_0 \approx v^2/B_0$ and so particles with $\theta \approx 90^\circ$ will tend to drift under a) so as to move around the earth on an equatorial geomagnetic equipotential. These paths are shown as the dotted lines in figure 18, reproduced from Hones (1963). Particles not confined to the equatorial

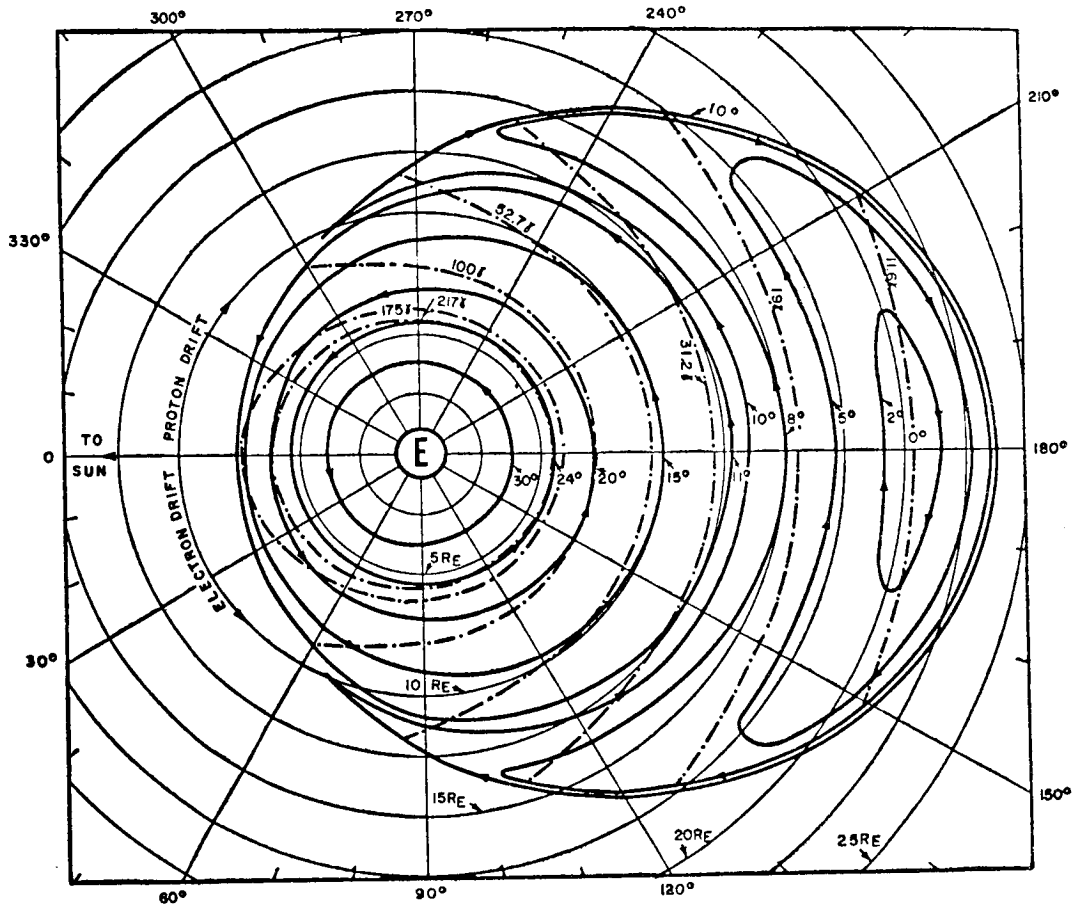


Fig. 18 Equatorial plane of the model magnetosphere. The heavy solid lines are the paths followed by the equatorial intersections of lines of force as the earth rotates. The geomagnetic colatitude at which each line intersects the earth is indicated. The dot-dash lines are the field gradient-induced drift paths of particles whose motion is confined to the equatorial plane. The drift paths are those for *nonrotating* magnetosphere or, approximately, for high-energy particles in a rotating magnetosphere. Both electrons and protons (or other positive ions) drift along the same paths, electrons to the east and positive ions to the west. The drift velocity of a particle is proportional to the particle's kinetic energy and, for singly charged particles, is $\sim 10W_{\perp}$ to $\sim 70W_{\perp}$ cm/sec, where W_{\perp} is in electron volts.

plane will tend to rotate so as to conserve the second or longitudinal invariant

$$I = \oint v_z dz \propto \oint \left(1 - \frac{B(z)}{B_m}\right)^{1/2} dz \quad \text{V-28}$$

where B_m is the field strength at which the particle mirrors and z denotes distance along the field line. The equatorial intersection of drift paths preserving I for various values of I are shown in figure 19, also reproduced from Hones (1963).

The drift paths resulting from b) are given by the solid lines in both figures. The rotational speed of the earth is 4.6×10^4 cm/sec, and so at an equatorial distance LR_e the rotational drift velocity v_R resulting from b) will be

$$v_R = 4.6 \times 10^4 L \text{ cm/sec} \quad \text{V-29}$$

The curvature-gradient driven velocity from a) has been numerically computed by Hamlin et al (1961) and can be written

$$v_D = 3 \times 10^3 E L^2 f(\theta) \text{ cm/sec} \quad \text{V-30}$$

where $f(\theta) = .35 + .15 \sin \theta$ and E is in kev. For $L = 6$, a particle with $E \approx 6$ kev will have equal drift velocities from a) and b).

From figures 18 and 19 it is readily seen that electrons drifting under the combined influence of a) and b) will be energized on the dawn side of the earth as they drift eastward from the midnight to the noon meridian, and will be deenergized as they drift on the dusk side of the earth. Further, particles whose motion is confined to the equatorial plane will

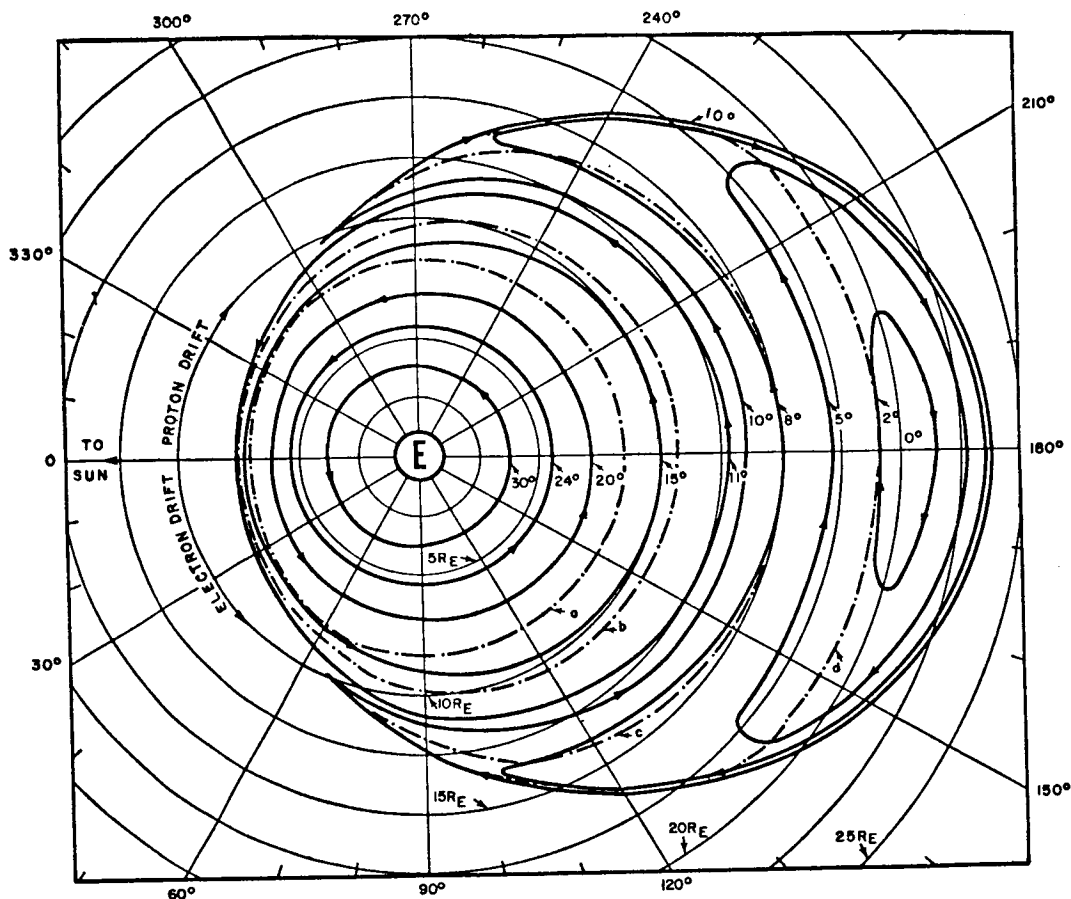


Fig. 19 Equatorial plane of the model magnetosphere. The paths of equatorial intersections of various lines are the same as in Figure 2. The dot-dash curves are the equatorial intersections of surfaces of constant integral invariant for particles mirroring at a field strength of 50,000 gammas. Values of the quantity

$$I' = \oint \left(1 - \frac{H}{H_m}\right)^{1/2} dS$$

for the four curves are: $I_a' = 44.0R_e$; $I_b' = 58.8R_e$; $I_c' = 91.2R_e$; $I_d' = 124R_e$.

not undergo as great an energy change as those mirroring away from the equatorial plane, and low energy electrons with $v_R > v_D$ will experience greater percentage energy changes than those with higher energy and $v_D > v_R$. Referring to figures 18 and 19 again, it is seen that for $L > 5$, drift motions of particles driven by the earth's rotation into regions of increased field strength on the dawn side of the earth can have their perpendicular energy increased by factors on the order of 4 or 5.

Unfortunately, even these apparently large energizations are still insufficient by several orders of magnitude to account for the observed energy precipitation rate of about $1 - 5 \text{ ergs/cm}^2\text{-sec}$ for electrons of energy greater than 1 kev, as can be arrived at by comparing the daily increase in the energy of particles in the magnetosphere with energy $E > 1 \text{ kev}$ as they drift into the dawn meridians with the average energy required to sustain auroras and high-latitude precipitation as observed on Injun III.

Drift electron energization, however, should produce velocity anisotropies leading to enhanced diffusion and precipitation preferentially on the dawn side of the earth. This is in agreement with the observed local time variation of the four major types of precipitation phenomena observed in that region of the auroral zone that connects with the trapped electrons in the outer belt: a) the precipitated flux of electrons with energy greater than 40 kev, which shows a maximum at about 11:00 local time (Frank et al. (1964)); b) mantle auroras, which have a maximum incidence near dawn

and a minimum in the afternoon (Sandford (1964)); c) auroral-zone X-ray events resulting from the bremsstrahlung produced by precipitated electrons slowing down in the upper atmosphere, which also has a maximum frequency of occurrence in the dawn meridians (R. R. Brown, private communication); and d) auroral absorption of cosmic radio noise resulting from the increased ionospheric ionization caused by precipitated electrons, which shows an almost one-to-one correspondence with X-ray events and a maximum incidence in the dawn meridians (Hartz et al (1963)). Auroral-zone X-ray and absorption events also indicate similar and simultaneous precipitation patterns occurring near the conjugate points at either end of a given geomagnetic field line, a result obviously consistent with the picture of turbulence diffusion occurring in the vicinity of the geomagnetic equator and equally affecting electrons travelling both north and south along a given field line.

VI. DISCUSSION

Electron cyclotron turbulence diffusion is thus able reasonably to explain the major characteristics of the phenomena associated with the precipitation of outer belt electrons. "Drizzle" precipitation is readily accounted for by a low level background of electromagnetic turbulence always present in the magnetosphere, while "splashes" are consistent with sporadic order of magnitude increases in the turbulence field level triggered or driven by small geomagnetic compressions which result from both fluctuations in the magnitude of the solar wind and particle drifts in the asymmetrical magnetosphere. The magnitude of the required "drizzle" field ($4 \times 10^{-3} \left(\frac{6}{L}\right)^{3.5}$ gamma for a precipitation flux of 10^3 particles/cm²-sec-sterad.) and the enhanced level of this field during "splashes" are both consistent with VLF measurements made on Injun III (Gurnett and O'Brien (1964)).

The observed diurnal asymmetry in outer belt precipitation phenomena is also naturally explained on the basis of the turbulence diffusion theory. Electron drifts in the solar wind deformed magnetosphere adiabatically increase the component of the electron velocity transverse to the geomagnetic field as electrons drift eastward into the dawn meridians. The resulting enhancement of the transverse-parallel electron velocity anisotropy leads to a corresponding enhancement of the turbulence field magnitude and hence of the diffusion driven precipitation rate, thus producing the maximization of electron precipitation phenomena observed to occur between the dawn and noon meridians.

Other observed precipitation characteristics, such as the shape of the precipitated electron spectra and its low energy cutoff, the isotropization of the electron pitch angle during "splashes", and the conjugate point symmetry in precipitation events, are all readily explained on the basis of turbulence diffusion. Accordingly, it is proposed that electron cyclotron turbulence diffusion provides the dominant scattering mechanism for outer belt electrons and determines their precipitation characteristics and lifetimes.

Aspects of the turbulence generation and diffusion problem which bear further investigation are the generation of electron cyclotron waves travelling at an angle to the geomagnetic field, the channelling of waves along a field line, and the exact nature of the marginally stable turbulence field state. Unlike the situation in a uniform infinite medium problem, the turbulence is generated primarily in a small region about the geomagnetic equator and the turbulence energy is constantly being convected away from this region into the ionosphere where it is absorbed and reflected. The quasilinear solution to the electron cyclotron instability problem in the case of a uniform infinite medium results in a small fraction of the electron particle energy going over into the turbulence field with an ensuing cessation of wave generation (Engel (1965)). In the less ideal magnetospheric problem waves are constantly being generated and then convected away and the resulting equilibrium is more of a dynamic than static nature.

The means by which electrons are injected into trapped particle orbits and then provided with sufficient energy to account for worldwide precipitation phenomena also remains to be solved, since the primary effect

of turbulence diffusion is to scatter electrons in pitch angle, with negligible energy change and no diffusion across field lines. Lacking the solution to these basic problems, the understanding of electron precipitation is necessarily incomplete. Electron cyclotron turbulence diffusion, however, must remain a major factor in the explanation of outer belt electron precipitation phenomena.

APPENDIX I

In order to solve the dispersion equation II-18 for complex k , we must formally consider the boundary value problem in the semi-infinite space $z > 0$. To this end we introduce a Laplace transform in space and a Fourier transform in time, namely

$$P(\omega, k) = \int_{-\infty}^{\infty} dt \int_0^{\infty} dz e^{-i(kz - \omega t)} P(t, z) \quad \text{AI-1a}$$

$$P(t, z) = \frac{1}{(2\pi)^2} \int_{-\infty}^{\infty} d\omega \int_K dk e^{i(kz - \omega t)} P(\omega, k) \quad \text{AI-1b}$$

where the contour K is chosen in the lower half k plane, below any possible singularities of $P(\omega, k)$. This insures that $P(\omega, k)$ exists and that $P(t, z) = 0$ for $z < 0$. To solve for $z < 0$, an analogous transformation can be defined in terms of a consistent set of boundary value conditions at the $z = 0^-$ half plane, where the contour K is now in the upper half K plane above any singularities in $P(\omega, k)$.

For the complex ω case, Eq. II-19 essentially gave the proper definition to the integrals appearing in the dispersion equation, II-18. If we now attempt to define the dispersion integrals in the case of the $z > 0$ boundary value problem by assuming k to have a small negative imaginary part, analogous to the small positive imaginary part assumed in section II for ω , we obtain

$$\frac{1}{\omega - \omega_c - kv_z} = -\frac{1}{k_r} P \frac{1}{v_z + \frac{\omega_c - \omega}{k_r}} - \frac{i\pi}{k_r} \delta \left(v_z + \frac{\omega_c - \omega}{k_r} \right) \text{sgn}(\omega - \omega_c) \quad \text{AI-2}$$

where k_r is the real part of $k = k_r + ik_i$. In the case $k_r > 0$ and $\omega < \omega_c$, using AI-2 in II-18 and solving for k_i will give a damped wave at large z where Eq. II-25 predicts a growing wave at large t . A similar inconsistency arises in the case $k_r < 0$ and $\omega > \omega_c$. AI-2 will therefore lead to incorrect results for k_i under these conditions.

The proper definition for the dispersion integrals must be obtained by considering causality, the boundary conditions at infinity and the symmetry of space, which will give

$$\frac{1}{\omega - \omega_c - kv_z} = -\frac{1}{k_r} P \frac{1}{v_z + \frac{\omega_c - \omega}{k_r}} - \frac{i\pi}{|k_r|} \delta\left(v_z + \frac{\omega_c - \omega}{k_r}\right) \quad \text{AI-3}$$

for the definition of the v_z integrations appearing in the dispersion relation. This prescription, which is the same as the Landau prescription II-19 for the initial value problem, can be formally obtained by defining the sense of the v_z integrations with ω assumed to have a large positive imaginary part and then analytically continuing the v_z integrals so defined to real ω .

The k_r factor in AI-3 will introduce a branch cut in the complex k plane, since it leads to two distinct and not analytically connected results for the velocity space integration when $k_r > 0$ and $k_r < 0$. This branch cut in the complex k plane can then introduce a possible contribution to the spatial dependence of the final solution for the wave fields when the inverse k transformation AI-1b is performed. To explicitly show this, we shall consider the Cauchy velocity distribution function II-33 with $a = 1$.

The integrals appearing in the dispersion relation, Eq. II-18, can be explicitly solved in the case of a Cauchy velocity distribution.

Taking the proper v_z and v_\perp derivations and performing the v_\perp integration, II-18 can be written

$$\frac{c^2 k^2}{\omega^2} = 1 - \frac{2\Delta^3 \omega_p^2}{\pi(1-x)^{1/2} \omega} \cdot \int_{-\infty}^{\infty} dv_z \frac{(1 + \frac{x}{1-x} \frac{kv_z}{\omega})}{(\omega - \omega_c - kv_z) (\frac{v_z}{1-x} + \Delta^2)^2} \quad \text{AI-4}$$

The v_z integration can be done by the method of residues by writing

$$\left(\frac{v_z}{1-x} + \Delta^2 \right) = \left(\frac{v_z}{(1-x)^{1/2}} + i\Delta \right) \left(\frac{v_z}{(1-x)^{1/2}} - i\Delta \right) \quad \text{AI-5}$$

and, as mentioned above, assuming ω to have a large positive imaginary part. The $(\omega - \omega_c - kv_z)$ factor will then give a pole contribution in the upper half v_z plane when $k_r > 0$, and in the lower half v_z plane when $k_r < 0$. The v_z integration can then be closed at infinity in either the lower or upper half plane so as not to pick up this pole contribution from the resonance denominator factor. The result can then be written

$$\frac{c^2 k^2}{\omega^2} = 1 + \frac{\omega_p^2}{\omega} \left\{ \frac{(\omega_c - \omega)_{\mp} - 2ik\Delta' - \frac{x}{1-x} \frac{(k\Delta')^2}{\omega}}{(\omega_c - \omega_{\mp} - ik\Delta')^2} \right\} \quad \text{AI-6}$$

where $\Delta' = \Delta(1-x)^{1/2}$ and the upper sign holds when $k_r > 0$, the lower sign when $k_r < 0$.

The index of refraction will thus have two analytically distinct definitions in the left and right half complex k plane, namely

$$\frac{c^2 k^2}{\omega^2} = n_-^2(\omega, k) = 1 + \frac{\omega_p^2}{\omega} \left\{ \frac{(\omega_c - \omega) + 2ik\Delta' - \frac{x}{1-x} \frac{(k\Delta')^2}{\omega}}{(\omega_c - \omega + ik\Delta')^2} \right\} \quad \text{AI-7a}$$

($k_r < 0$)

$$\frac{c^2 k^2}{\omega^2} = n_+^2(\omega, k) = 1 + \frac{\omega_p^2}{\omega} \left\{ \frac{(\omega_c - \omega) - 2ik\Delta' - \frac{x}{1-x} \frac{(k\Delta')^2}{\omega}}{(\omega_c - \omega - ik\Delta')^2} \right\} \quad \text{AI-7b}$$

($k_r > 0$)

The spatial dependence of the wave field is determined by the inverse transformation

$$B_-(\omega, z) = \int_K \frac{\{\text{Boundary Terms}\}}{-k^2 + \frac{\omega^2}{c^2} n^2(\omega, k)} e^{i(kz - \omega t)} dk \quad \text{AI-8}$$

where the contour K is to go below all the roots of AI-7a in the left half plane and below all the roots of AI-7b in the right half plane. Since

$$n_-^2(\omega, -k) = n_+^2(\omega, k) \quad \text{AI-9}$$

if k_1 is a root of AI-7a, then $-k_1$ is a root of AI-7b. Thus for every wave travelling in the $+z$ direction, there is an identical wave travelling in the $-z$ direction as required by considerations of spatial symmetry.

A representative set of contours for evaluating AI-8 is shown in figure 20. Since the contours at infinity give no contribution, we have that

$$K = K_- + K_+ \quad \text{AI-10a}$$

$$K_- + C_-^\infty + C_-^b = \sum \text{Res}(-) \quad \text{AI-10b}$$

$$K_+ + C_+^\infty + C_+^b = \sum \text{Res}(+) \quad \text{AI-10c}$$

$$K = \sum \text{Res}(-) + \sum \text{Res}(+) - C_-^b - C_+^b \quad \text{AI-10d}$$

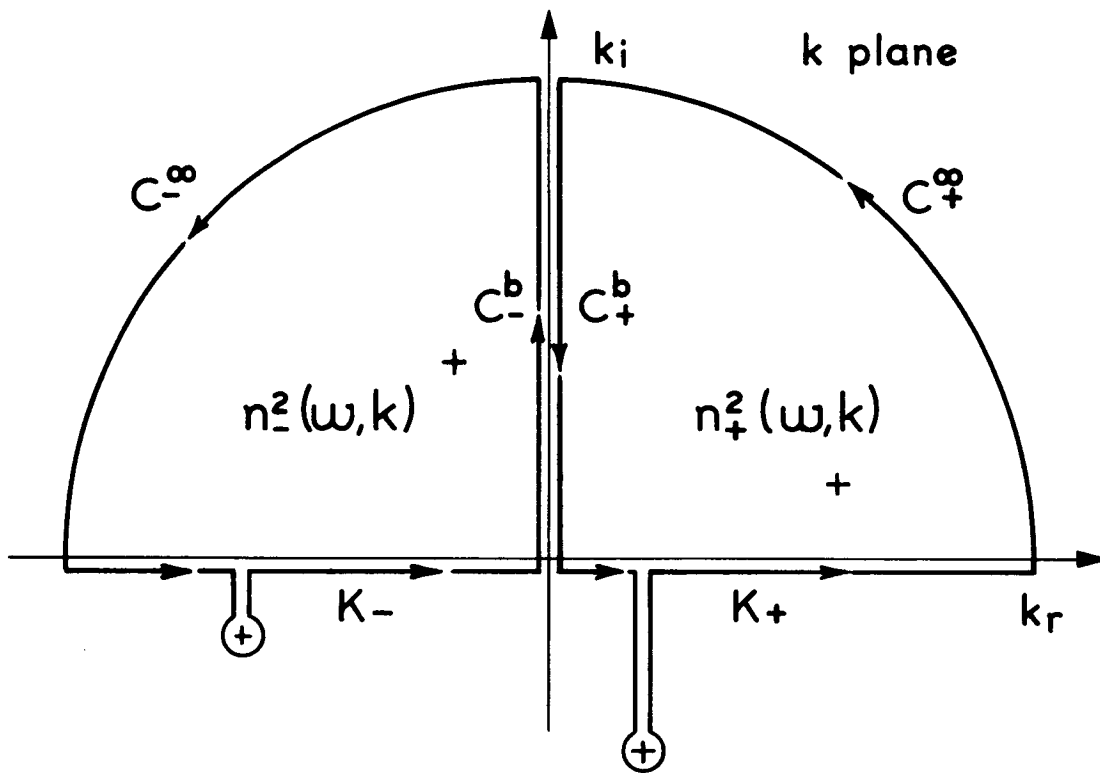


Figure 20. Typical contours for the evaluation of integrals as Eq. AI-8 arising from the solution of the boundary value problem for complex k . The crosses represent poles of the dispersion relation AI-7 and are symmetrically located about the origin.

The contribution from C_-^b and C_+^b can be expressed in terms of a branch cut integral

$$C_-^b + C_+^b \propto \int_0^{i\infty} dk e^{ikz} \left(\frac{1}{k^2 - \frac{\omega^2}{c^2} n_-^2(\omega, k)} - \frac{1}{k^2 - \frac{\omega^2}{c^2} n_+^2(\omega, k)} \right) \quad \text{AI-11}$$

where the boundary terms have been assumed to have only a weak dependence on k . Using AI-7, AI-11 becomes

$$\begin{aligned} C_-^b + C_+^b &\propto \int_0^{i\infty} dk e^{ikz} \frac{\frac{\omega^2}{c^2} (n_-^2(\omega, k) - n_+^2(\omega, k))}{(k^2 - \frac{\omega^2}{c^2} n_-^2(\omega, k))(k^2 - \frac{\omega^2}{c^2} n_+^2(\omega, k))} \\ &= -4i\Delta^3(1-x)^{\frac{1}{2}} \left(1 - x \frac{\omega_c}{\omega}\right) \frac{\omega_p^2 \omega}{c^2} \int_0^{i\infty} dk e^{ikz} \frac{k^3}{[(\omega_c - \omega)^2 + (k\Delta')^2]^2 (k^2 - \frac{\omega^2}{c^2} n_-^2)(k^2 - \frac{\omega^2}{c^2} n_+^2)} \end{aligned}$$

AI-12

For z we take $R_e = 6.4 \times 10^8$ cm, a typical magnetospheric scale size. The e^{ikz} factor will then act as an exponential cutoff for $k > 1/R_e > 10^{-9}$ cm $^{-1}$. The denominator in AI-12 can accordingly be greatly simplified, and AI-12 becomes

$$\begin{aligned} C_-^b + C_+^b &\propto - \frac{4i\Delta^3(1-x)^{1/2} \left(1 - x \frac{\omega_c}{\omega}\right) c^2}{\omega_p^2 \omega (\omega_c - \omega)^2} \int_0^{i\infty} dk k^3 e^{ikz} \\ &= - \frac{24i\Delta^3(1-x)^{1/2} \left(1 - x \frac{\omega_c}{\omega}\right) c^2}{z^4 \omega_p^2 \omega (\omega_c - \omega)^2} \end{aligned} \quad \text{AI-13}$$

The residue or pole contributions to AI-8 will give terms as

$$\sum \text{Res} \propto \frac{2\pi i e^{ikz}}{(k+k_0)(k-k_0)} \cdot (k-k_0) \Big|_{k=k_0}$$

$$= \frac{\pi i e^{ik_0 z}}{k_0}$$
AI-14

where k_0 is the root of the dispersion relation AI-7, given by

$$c^2 k_{or}^2 = \omega^2 + \frac{\omega_p^2 \omega}{(\omega_c - \omega)} \left(1 + \frac{k_{or}^2 \Delta^2}{(\omega_c - \omega)^2} \left(1 - x \frac{\omega_c}{\omega} \right) \right)$$

$$\approx \frac{\omega_p^2 \omega}{\omega_c - \omega}$$
AI-15a

$$k_{oi} = \pm \frac{\omega_p^2 \omega k_{or}^2 \Delta^3 (1-x)^{1/2}}{c^2 (\omega_c - \omega)^4} \left(1 - x \frac{\omega_c}{\omega} \right)$$

$$\approx \pm \frac{\omega_p^4 \omega^2 \Delta^3 (1-x)^{1/2}}{(\omega_c - \omega)^5 c^4} \left(1 - x \frac{\omega_c}{\omega} \right)$$
AI-15b

(+ for $k_{or} > 0$, - for $k_{or} < 0$)

The branch cut and pole contributions can now be compared and we obtain

$$\frac{C_-^b + C_+^b}{\sum \text{Res}} \approx \frac{24}{\pi} \frac{\Delta^3 c (1-x)^{1/2} \left(1 - x \frac{\omega_c}{\omega} \right)}{z^4 e^{ik_0 z} \omega_p \omega^{1/2} (\omega_c - \omega)^{5/2}}$$
AI-16

The branch cut terms will only be important if either $\omega \approx \omega_c$, in which case $e^{ik_0 z}$ will also show strong damping and, by reducing the magnitude

of the pole term, further tend to enhance the effect of the branch cut, or if z is very small, i. e. , if one looks very close to the boundary at $z = 0$. The branch cut will thus essentially represent the effects of the boundary at $z = 0$.

In the magnetosphere, this boundary would correspond to the beginning of a region in passing through which the electron cyclotron wave AI-15 experiences significant growth or damping. From the results of Section III, this region of enhanced growth or damping is centered about the geomagnetic equator and is of dimension $LR_e/3$. If other typical magnetospheric values and parameters are used in evaluating AI-16, it is readily seen that the branch cut contribution is many orders of magnitude less than the pole contribution for $\omega \lesssim x\omega_c$. If the dispersion equation II-18 is then solved for complex k by using AI-3, the results for k_i are well approximated by II-29 and the effects of the branch cut can be completely neglected in calculating the net damping or growth that a wave encounters in passing through the magnetosphere.

APPENDIX II

To solve the diffusion equation IV-41, we consider $\Gamma(\theta)$ to be given in the general form

$$\Gamma(\theta) = \frac{\Gamma'}{\cos^p \theta} \quad (p \geq 0, \text{ integer}) \quad \text{AII-1}$$

The diffusion equation then becomes

$$\begin{aligned} \frac{\partial}{\partial t} [n(\theta, t) \sin \theta] = \frac{e^2 \Gamma'}{4m^2 c^2} \left\{ \frac{\sin \theta}{\cos^p \theta} \frac{\partial^2 n(\theta, t)}{\partial \theta^2} \right. \\ \left. + \frac{1}{\cos^{p-1} \theta} \left(1 + \frac{2p(1-\cos^2 \theta)}{\cos^2 \theta} \right) \frac{\partial n(\theta, t)}{\partial \theta} + \frac{\sin \theta}{\cos^p \theta} \left(2p + \frac{p(p+1)(1-\cos^2 \theta)}{\cos^2 \theta} \right) n(\theta, t) \right\} \end{aligned} \quad \text{AII-2}$$

Assuming a separated solution of the form

$$n(\theta, t) = N(t) M(\theta) \quad \text{AII-3}$$

AII-2 leads to the two equations

$$\frac{\partial N(t)}{\partial t} = -K \frac{e^2 \Gamma'}{4m^2 c^2} N(t) \quad \text{AII-4}$$

$$\begin{aligned} \cos^2 \theta \frac{\partial^2 M(\theta)}{\partial \theta^2} + \frac{\cos \theta}{\sin \theta} (2p + (1-2p) \cos^2 \theta) \frac{\partial M(\theta)}{\partial \theta} \\ + (p(p+1) - p(p-1) \cos^2 \theta + K \cos^{p+2} \theta) M(\theta) = 0 \end{aligned} \quad \text{AII-5}$$

The solution to AII-4 has already been considered in Section IV. To solve AII-5, we introduce the variable $\mu = \cos \theta$, in terms of which AII-5 becomes

$$\mu^{2(1-\mu^2)} \frac{\partial^2 M}{\partial \mu^2} - \mu(2p + 2(1-p)\mu^2) \frac{\partial M}{\partial \mu} + (p(p+1) - p(p-1)\mu^2 + K\mu^{p+2}) M = 0 \quad \text{AII-6}$$

If a series solution of the form

$$M(\mu) = \sum_{n=0}^{\infty} a_n \mu^{n+s} \quad \text{AII-7}$$

is substituted into AII-6, then for p even a solution can be found involving only even or only odd powers of μ . The even solution requires $s = p$ and has the recurrence relation

$$a_n = a_{n-2} \frac{(n-2)}{n} - K \frac{a_{n-p-2}}{n(n-1)} \quad \text{AII-8}$$

Retaining only terms linear in K , the solution for $M(\mu)$ can be written in the compact form

$$M^e(\mu) = \mu^p \left\{ 1 + \frac{K}{2(p+1)} \left[\log_e(1-\mu^2) + \sum_{q=1}^{p/2} \frac{\mu^{2q}}{q} \right] \right\} \quad \text{AII-9}$$

The odd solution for p even requires $s = p + 1$ and has the recurrence relation

$$a_n = a_{n-2} \frac{(n-1)}{(n+1)} - K \frac{a_{n-p-2}}{n(n+1)} \quad \text{AII-10}$$

Again retaining only terms linear in K , the solution for $M(\mu)$ can be written in the compact form

$$M^o(\mu) = \mu^p \left\{ \tanh^{-1} \mu - \frac{K}{(p+2)} \left[\tanh^{-1} \mu - \sum_{q=0}^{p/2} \frac{\mu^{2q+1}}{2q+1} \right] \right\} \quad \text{AII-11}$$

The separation constant K is determined by requiring $M(\mu)$ to go to zero at the loss cone angle $\mu_c \approx 1 - 1/(4L^3)$. K is relatively insensitive to the exact value of L and in Table 2 is given for various values of p in the case $L = 6$. In general, K is of order unity.

In figure 13, $M^e(\mu)$ is plotted vs. θ for $p = 0$. In figure 21, $M^e(\mu)$ is plotted vs. θ for $p = 2$ and 4, and $M^o(\mu)$ is plotted vs. θ for $p = 0$. All these functions are normalized in the vicinity of $\theta \approx \pi/2$ to agree with $j_o(40 \text{ kev}, \theta_o)$ at $L = 6$ as given in figure 4 and plotted again here for comparison. In general, the shape of all these plotted functions is quite similar in the vicinity of the loss cone. Near $\theta \approx \pi/2$, however, there is some disparity and only $M^e(\mu)$ for $p = 0$ does not go to zero at $\theta = \pi/2$. Because, however, of the restrictions placed on the diffusion coefficient $\Gamma(\theta)$ in the vicinity of $\theta \approx \pi/2$ (see Eq. IV-55), the diffusion equation AII-5 no longer holds in this region and the shape of the angular distribution function near $\theta \approx \pi/2$ is determined rather by considerations involving the unknown electron source function and turbulence diffusion, as discussed at the end of Section IV. Thus it follows that the overall shape of the angular distribution function is relatively insensitive to p .

p	K	
	Even solution	Odd solution
0	0.33	2.75
2	1.16	6.20
4	2.22	10.20
6	3.30	14.40

TABLE 2

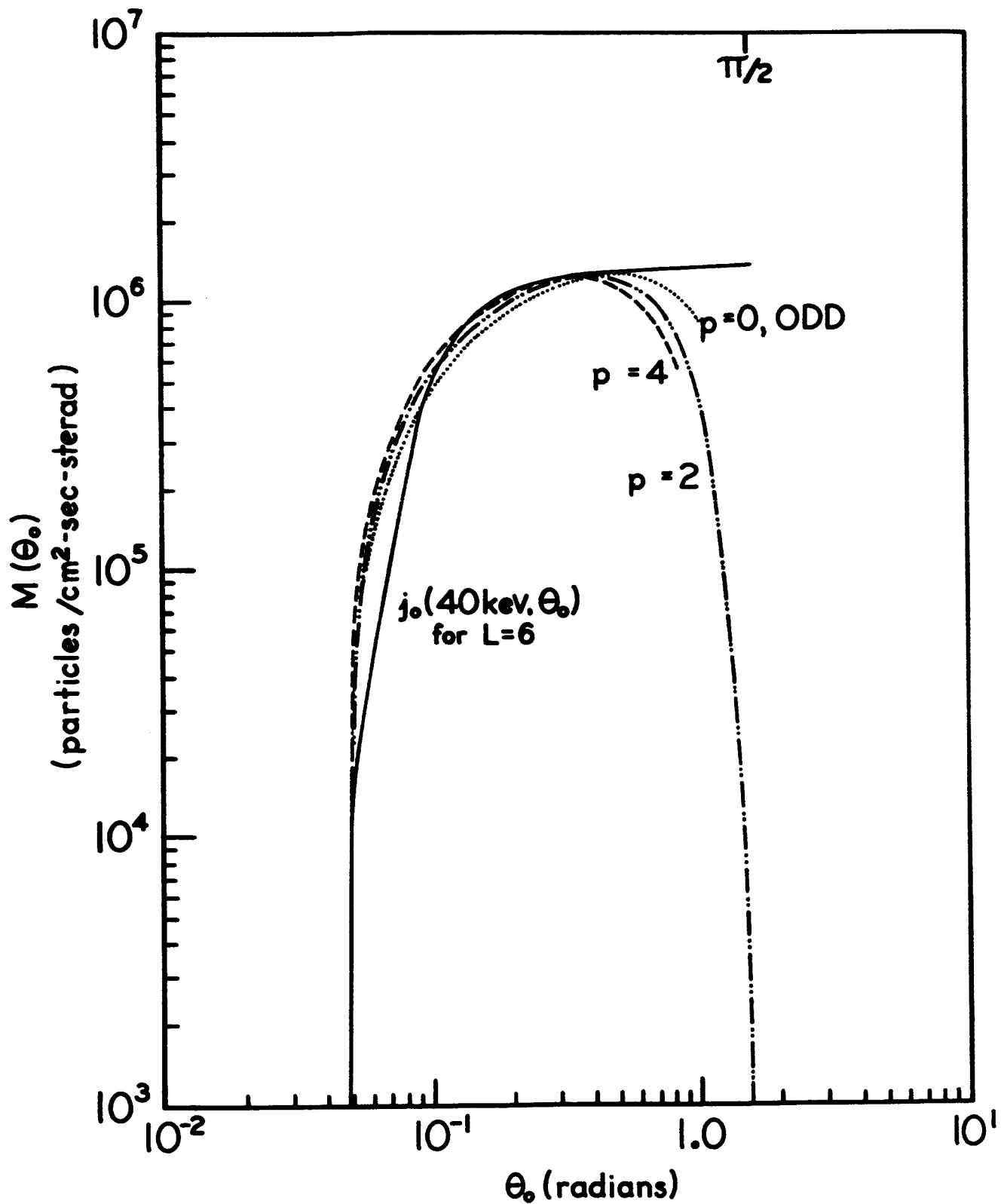


Figure 21. The equatorial electron pitch angle distribution at $L = 6$ obtained from solving the diffusion equation, Eq. AII-1. The distributions are given for various values of the parameter p and are normalized to agree with $j_0(40 \text{ keV}, \theta_0)$ at $L = 6$ as given in Figure 4, which is also plotted for comparison.

REFERENCES

- ANDERSON, K. A., H. K. HARRIS, and R. J. PAOLI: 1965,
J. Geophys. Res. 70, 1039.
- ARMSTRONG, T.: 1965, J. Geophys. Res. 70, 2077.
- BELL, T. F., and O. BUNEMAN: 1964, Phys. Rev. 133, A1300.
- BRICE, N.: 1963, J. Geophys. Res. 68, 4626.
- BROWN, R. R., K. A. ANDERSON, C. D. ANGER, and D. S. EVANS:
1963, J. Geophys. Res. 68, 2677.
- BROWN, R. R., J. R. BARCUS, J. REID, and N. R. PARSONS:
1965, J. Geophys. Res. 70, 1246.
- CORNWALL, J. M.: 1964, J. Geophys. Res. 69, 1251.
- CORNWALL, J. M.: 1965, J. Geophys. Res. 70, 61.
- DRAGT, A. J.: 1961, J. Geophys. Res. 66, 1641.
- DUNGEY, J. W.: 1963a, J. Fluid Mechs. 15, 74.
- DUNGEY, J. W.: 1963b, Plan. Space Sci. 11, 591.
- ENGEL, R. D.: 1965, Phys. Fluids 8, 939.
- FRANK, L. A.: 1965, J. Geophys. Res. 70, 1593.
- FRANK, L. A., J. A. VAN ALLEN, and J. D. CRAVEN: 1964,
J. Geophys. Res. 69, 3155.
- FRANK, L. A., J. A. VAN ALLEN, and H. K. HILLS: 1964,
J. Geophys. Res. 69, 2171.
- FURTH, H. P.: 1963, Phys. Fluids 6, 48.
- GURNETT, D. A. and B. J. O'BRIEN: 1964, J. Geophys. Res. 69, 65.
- HAMLIN, D. A., R. KARPLUS, R. C. VIK, and K. M. WATSON: 1961,
J. Geophys. Res. 66, 1.
- HARRIS, E. G.: 1961, J. Nucl. Energy, Part C 2, 138.

REFERENCES (Cont.)

- HARTZ, T. R., L. E. MONTBRIAND, and E. L. VOGAN: 1963, Can. J. Phys. 41, 581.
- HELLIWELL, R. A.: 1965, Whistlers and Related Ionospheric Phenomena, Stanford University Press, Stanford.
- HONES, E. W., JR.: 1963, J. Geophys. Res. 68, 1209.
- KADOMTSEV, B. B. and V. I. PETVIASHVILI: 1962, Zhur. Eksp. i. Teoret. Fiz. 43, 2234. (English transl.: Soviet Phys. J.E.T.P. 16, 1578 (1963)).
- LANDAU, L. D.: 1946, J. Phys. (U.S.S.R.) 10, 25.
- LIEMOHN, H. B. and F. L. SCARF: 1964, J. Geophys. Res. 69, 883.
- McDIARMID, I. B. and J. R. BURROWS: 1965, J. Geophys. Res. 70, 3031.
- McILWAIN, C. E.: 1960, Space Research, Proc. Intern. Space Sci. Symp., 1st, Nice, 1960, edited by H. K. Kallmann-Bijl, North-Holland Publishing Company, Amsterdam, pp. 715-720.
- McILWAIN, C. E.: 1961, J. Geophys. Res. 66, 3681.
- NOERDLINGER, P. D.: 1963, Ann. Phys. (N.Y.) 22, 12.
- O'BRIEN, B. J.: 1962, J. Geophys. Res. 67, 3687.
- O'BRIEN, B. J.: 1963, J. Geophys. Res. 68, 989.
- O'BRIEN, B. J.: 1964, J. Geophys. Res. 69, 13.
- O'BRIEN, B. J. and H. TAYLOR: 1964, J. Geophys. Res. 69, 45.
- OLBERT, S.: 1965, paper presented at Conference on Shock Waves in Collision-Free Plasmas, NASA-Ames Research Center, March 1-3, 1965.
- PIDDINGTON, J. H.: 1965, Planet. Space Sci. 13, 565.
- SANDFORD, B. J.: 1964, J. Atmos. Terr. Phys. 26, 749.
- SCARF, F. L.: 1962, Phys. Fluids 5, 6.

REFERENCES (Cont.)

SHARP, R. D., J. B. REAGAN, S. R. SALISBURY, and L. F. SMITH:
1965, J. Geophys. Res. 70, 2119.

SPITZER, L., JR.: 1962, Physics of Fully Ionized Gases, Interscience
Publishers, Inc., New York.

SUDAN, R. N.: 1963, Phys. Fluids 6, 57.

WENTZEL, D. G.: 1961a, J. Geophys. Res. 66, 359.

WENTZEL, D. G.: 1961b, J. Geophys. Res. 66, 363.

WINCKLER, J. R., P. D. BHAVSAR, and K. A. ANDERSON: 1962,
J. Geophys. Res. 67, 3717.